6-16-1963

Whole-Field Methods in the Measurement of Post-Elastic Surface Strains

Siew Poh Chan

POST-
ELASTIC
SURFACE
STRAINS

CHAN

IMPORTANT!

Special care should be taken to prevent loss or damage of this volume. If lost or damaged, it must be paid for at the current rate of typing.

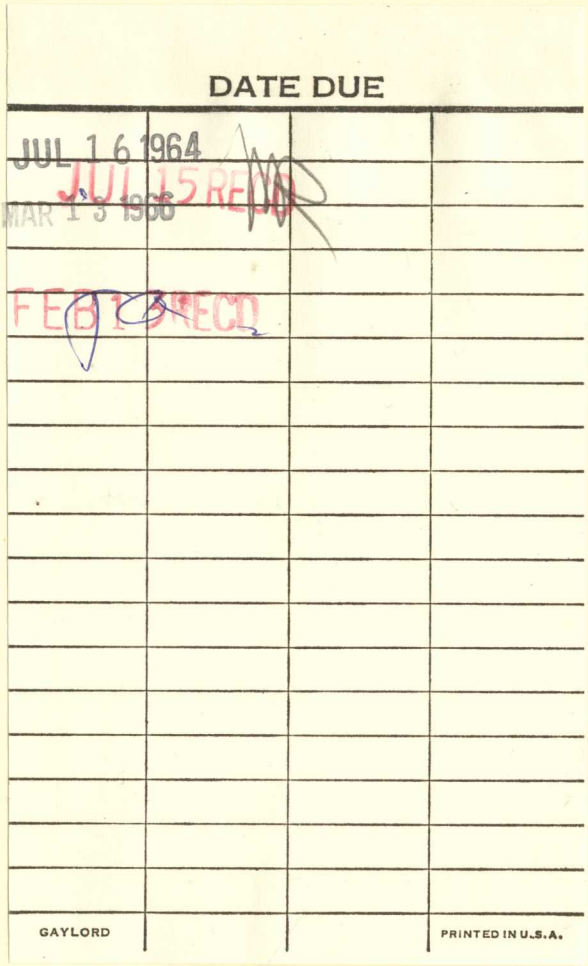

WHOLE-FIELD METHODS IN THE MEASUREMENT OF POST-ELASTIC SURFACE STRAINS

By
Siew Poh Chan

A Thesis
Submitted in Partial Fulfillment of the
Requirement for the Degree of
Master of Science in Mechanical Engineering

The University of New Mexico
1963

This thesis, directed and approved by the candidate's committee, has been accepted by the Graduate Committee of the University of New Mexico in partial fulfillment of the requirements for the degree of

MASTER OF SCIENCE

W. J. Parish

Dean

June 26, 1963

Date

Thesis committee

Frederick R. Lee

Chairman

R. C. Dove

James P. Gas

ABSTRACT

Several whole-field methods were studied and a new technique was developed for the purpose of measuring post-elastic surface strains in metals. Critical evaluation was given to the following experimental techniques: the moiré effect and the birefringent coating.

In both methods, the principal experimental model designed for the study of the techniques was a simple tension plate with a central, circular hole as a stress raiser. Fringe patterns developed in both methods were recorded by photography.

The range of strain to be measured is from the elastic limit to the rupture point of the metal. Measurement of strains at or near the fracture in the metal has been emphasized. The moiré method is found to be a better method than the birefringent coating method for measuring post-elastic surface strains. The advantages of the moiré method compared to the birefringent coating method are outlined as follows:

1. The moiré screen does not reinforce the specimen; while the birefringent coating has a significant reinforcing effect on the metal in the post-elastic range.

2. The moiré method does not require any calibration procedure. Calibration is necessary for the birefringent coating method to check the strain optical sensitivity constant.

3. The experimental apparatus of the moiré method is much more easily arranged than that of the birefringent coating method.

The combination whole-field method was developed to enable a direct determination of individual values of the principal strains. This method utilizes the characteristics of the moiré and birefringent coating methods.

ACKNOWLEDGEMENT

The author would like to express his sincere appreciation to Dr. F. D. Ju and Dr. R. C. Dove of the Mechanical Engineering Department for their advice and guidance throughout this work.

Thanks must also be given to Mr. W. M. Derr for his help in instrumentation and obtaining data.

NOMENCLATURE

a	Pitch of screen lines
d	Fringe spacing due to normal strain
e	Elongation
h	Fringe spacing due to rotation of model screen
n	Fringe order
n_1, n_2	Principal indices of refraction of birefringent plastic
p	Master grid pitch
t	Thickness
u, w	Displacement components
C	Stress optical coefficient
E	Modulus of elasticity
F, G, C	Correction factors
$J_o(pr), J_1(pr)$	Bessel functions
K	Strain sensitivity constant
Q	Strain optical coeffecient
W, U	Constants
α	Angle of rotation
δ	Fringe spacing
δ_n	Relative retardation
ε	Average strain
$\varepsilon_1, \varepsilon_2$	Principal strains in Cartesian coordinates
$\varepsilon_{xx}, \varepsilon_{yy}, \varepsilon_{zz}$	Strain components in Cartesian coordinates
$\varepsilon_{rr}, \varepsilon_{\theta\theta}$	Strain components in Cylindrical coordinates
ε_d	Strain produced by pure deformation
ε_m	Fictitious strain corresponding to pitch mismatch
λ	Relative retardation per fringe order
ν	Poisson's ratio
$\sigma_{xx}, \sigma_{yy}, \sigma_{zz}$	Stress components in Cartesian coordinates

TABLE OF CONTENTS

1.0 INTRODUCTION

In the fields of experimental mechanics and design there is a continuing need for knowledge about post-elastic strain distribution in metals. The purpose of this investigation is to evaluate some experimental techniques for the measurement of post-elastic surface strains in metal plates. This investigation is restricted to the evaluation of two whole-field experimental methods. One of the two whole-field methods involves using a mechanical interferometer. This is generally referred to as the moiré method. The other is the birefringent or photoelastic coating method. The theories of these two methods will be explained fully in later sections. The accuracy of the birefringent coating method was checked by the use of variable resistant strain gages.

The range of post-elastic strain to be measured is from the elastic limit up to the rupture point of the metal. Although strain gages can be used to measure post-elastic strains, each gage can measure strain at one point only. If the critical point in a structure is known, for example, from its geometrical shape, the use of strain gage will be suitable. However, when the critical point in a structure is not known, it is much better to use the whole-field method, for which strain at all points in the specimen are available from one data record. The present investigation will emphasize the application of two whole-field methods for measuring post-elastic strains in metals, especially their application in measurement of strains in the neighborhood of a crack. Previous investigators studied and

published results on the reinforcing effect of the birefringent coating on the elastic metal plate. This effect was overlooked by investigators who have used the birefringent coating to measure post-elastic strains. It has been found by this author that the coating has a significant reinforcing effect in the post-elastic range of the metals. A detailed discussion of this effect can be found in later sections.

Both the moiré and birefringent coating methods are based on optical phenomena. The states of strain are interpreted from fringe patterns due to optical interference. The fringe patterns are recorded by photography with both a Fastax high-speed camera and a Polaroid still camera. The analysis of experimental data was based primarily on Polaroid pictures because a much better resolution was obtained in the Polaroid pictures, and because the self-developing feature of the Polaroid film enables the photographed picture to be checked on the spot for resolution. The experimental work included the investigation of the best arrangement of the apparatus in order to obtain the best resolution from both methods, especially illumination and positioning of apparatus. Since the data must be recorded by means of a camera, the design of light sources for both the methods are very important and critical. Its light intensity must enable the pictures to be photographed with near instant exposure; the illumination must be uniform for the whole specimen. Since the camera for taking pictures of the birefringent fringes must be placed behind the analyzer, the camera cannot be placed close enough to the specimen, special arrangement of the reflection polariscope was to be designed.

Due to the fact that strains in two orthogonal directions can be easily obtained by the moiré method and that the principal strain difference can be obtained by the birefringent coating method, an attempt was made to obtain the individual, principal strains (thus the state of strains) by combining the results of both methods. The principle can be briefly verified as follows:

By definition, the summation of normal strains at a point is invariant, therefore

$$\varepsilon_1 + \varepsilon_2 = \varepsilon_{xx} + \varepsilon_{yy} ;$$

where ε_{xx} and ε_{yy} can be obtained by the moiré method. From the birefringent fringes the value $|\varepsilon_1 - \varepsilon_2|$ is obtained. Hence, the individual values of ε_1 and ε_2 can be obtained by using the results of the two experimental techniques.

2.0 LITERATURE REVIEW

2.1 Thickness and Reinforcing Effects of Photoelastic Plastic

The use of a photoelastic coating is one method for determining the strains on a metal or other opaque body. The accuracy of this method is affected by the thickness of the coating used. Factors that influence the thickness effect are the strain gradients, the difference in Poisson's ratios between the coating and the base, and the geometry of the structure. A theoretical study of the thickness effect for an arbitrary one-dimensional variation of the displacement at the metal surface has been presented in [1] *. The solution is extended to a two-dimensional deformation with radial symmetry in [2]. Experimental investigation on various geometrical discontinuities has been presented in [3].

Duffy [1] has shown that strain gradients or curvature of the surface have a pronounced effect on the observed photoelastic fringes, and must be taken into consideration. This can be corrected by means of two correction factors derived in his paper which takes into account the elastic properties of the coating and its thickness.

The reference frame is set as shown in Figure 1. Let u_o, w_o be the displacements of the interface in the x and z direction; respectively, and t be the thickness of the coating. In a reflection polariscope, the fringe order "n" is obtained from

---

*Numbers in square brackets designate references at the end of paper.

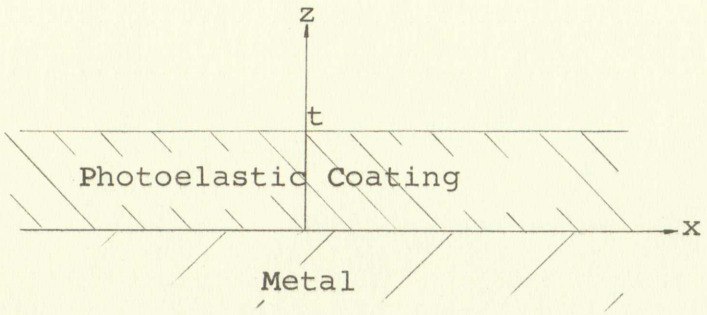

Figure 1. Section through coating and metal

the equation:

$$n = (\varepsilon_1 - \varepsilon_2)\frac{2t}{Q} \quad ;$$

where Q is the strain optical coefficient for the coating material and $(\varepsilon_1 - \varepsilon_2)$ is the principal strain difference; which in the present instance is in the plane of the interface between coating and metal. Duffy states that strain components can be obtained from the displacement by a summation of strain across the thickness, i.e.,

$$\varepsilon_1 = \frac{1}{t}\int_o^t \frac{\partial u}{\partial x}\, dz \ .$$

$\varepsilon_2 = 0$ is assumed a one-dimensional variation of the displacement and hence $v = 0$. Therefore, the expected fringe order is given by:

$$n = \frac{2}{Q}\int_o^t \frac{\partial u}{\partial x}\, dz \ .$$

It is convenient to express "n" in terms of the extensional strain at the interface, $\partial u_o/\partial x$, and the displacement of the interface normal to its plane, w_o. If the correction factor F and G are defined by:

$$F = \frac{1}{t}\int_o^t \left(\frac{\partial u}{\partial x}\right)_1 , \ dz \Big/ \frac{\partial u_o}{\partial x} \ .$$

$$G = \int_0^t \left(\frac{\partial u}{\partial x} \right)_2 \frac{dz}{w_o} ;$$

where $\left(\partial u / \partial x \right)_1$ is the strain at any point of the coating due to the longitudinal strain at the interface, and $\left(\partial u / \partial x \right)_2$ is the strain due to the curvature of the interface, then

$$n = \frac{2}{Q} \left[F t \frac{\partial u_o}{\partial x} + G w_o \right]$$

gives the fringe order at any point.

Lee, Mylonas, and Duffy [2] have extended Duffy's one-dimensional variation of strain to a two-dimensional deformation problem with radial symmetry.

Consider an infinite coating of thickness, t, and suppose that the interface between metal and coating is the r - θ plane of a cylindrical coordinate system and the z denotes the normal to this plane. (See Figure 2). Let u and w define the radial and normal displacements at any point of the coating; and u_o and w_o the corresponding displacements at the interface. It is clear that:

$$\left.\begin{aligned} u &= u(r,z) \\ w &= w(r,z) \end{aligned}\right\},$$

represent the displacement components at any point of the coating subject to the boundary conditions:

$$\left.\begin{aligned} u &= u_o \\ w &= w_o \end{aligned}\right\} \text{ at } z = 0,$$

$$\sigma_{zz} = \sigma_{zr} = 0 \text{ at } z = t;$$

where σ_{zz} and σ_{zr} are the stress components in the cylindrical coordinates and where the displacement components u_o and w_o are arbitrary functions of r.

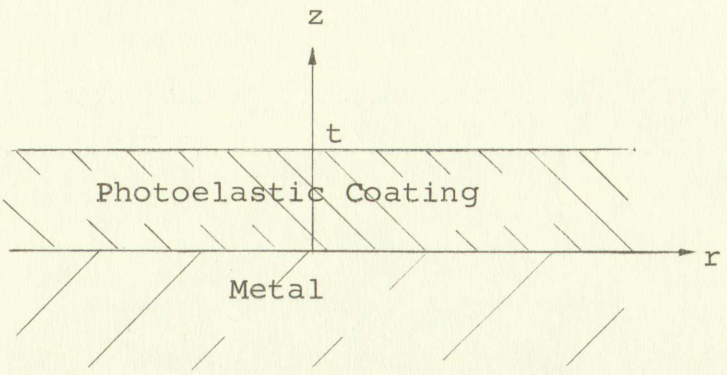

Figure 2, Section through coating and metal

The boundary conditions with no radial strain at the interface are:

$$\left.\begin{aligned} u_o &= 0 \\ w_o &= WJ_o(pr) \end{aligned}\right\} \text{ at } z = 0,$$

$$\sigma_{zz} = \sigma_{zr} = 0 \text{ at } z = t;$$

where W is an arbitrary constant representing the maximum normal displacement of the interface in the direction of z, $J_o(pr)$ is the Bessel function of the first kind of order zero, and p is an arbitrary constant.

The boundary conditions with no curvature at the interface are:

$$\left.\begin{aligned} u_o &= U\,J_1(pr) \\ w_o &= 0 \end{aligned}\right\} \text{ at } z = 0,$$

$$\sigma_{zz} = \sigma_{zr} = 0 \text{ at } z = t;$$

where the magnitude of U determines the amplitude of u_o, and $J_1(pr)$ is the Bessel function of the first kind of order one.

The relative retardation in wave length, dn, over a light path of length, ds, is given by:

$$dn = (\epsilon_1 - \epsilon_2)\ ds/Q;$$

where ϵ_1 and ϵ_2 are the secondary principal strains in the plane of the wavefront and Q is the strain optical coefficient

of the photoelastic medium. In the present problem the light is incident normally to the plane of interface, so that the wavefront is always parallel to the interface and the principal strains, ε_1 and ε_2 are the radial and circumferential strains, ε_{rr} and $\varepsilon_{\theta\theta}$. At any position (r, θ) the strains ε_{rr} and $\varepsilon_{\theta\theta}$ have a constant direction across the thickness "t" of the coating although they vary in magnitude. Since the light crosses the coating twice:

$$n = \frac{2}{Q}\int_0^t \left| \varepsilon_{rr} - \varepsilon_{\theta\theta} \right| dz$$

or, in terms of the displacement:

$$n = \frac{2}{Q}\int_0^t \left| \frac{\partial u}{\partial r} - \frac{u}{r} \right| dz .$$

For practical purposes, it is convenient to express "n" in terms of the strain and curvature of the interface, i. e., in terms of

$$\frac{du_o}{dr} - \frac{u_o}{r} ,$$

and

$$\frac{d^2 w_o}{dr^2} - \frac{1}{r}\frac{dw_o}{dr} .$$

This may be done by splitting "n" in two parts, so that:

$$n = n_1 + n_2$$

$$= \frac{2}{Q}\left[\int_0^t \left| \frac{\partial u}{\partial r} - \frac{u}{r} \right|_1 dz + \int_0^t \left| \frac{\partial u}{\partial r} - \frac{u}{r} \right|_2 dz \right];$$

where the subscript "1" denotes the part due to radial strain at the interface, and the subscript "2" denotes the part due to curvature of the interface. The actual birefringence can be

expressed in terms of the one for constant strains across the thickness of the coating by the correction factors:

$$F = \frac{\frac{1}{t}\int_0^t \left(\frac{\partial u}{\partial r} - \frac{u}{r}\right)_1 dz}{\frac{du_o}{dr} - \frac{u_o}{r}},$$

and

$$G = \frac{\int_0^t \left(\frac{\partial u}{\partial r} - \frac{u}{r}\right)_2 dz}{\frac{1}{P_2}\left(\frac{d^2 w_o}{dr^2} - \frac{1}{r}\frac{dw_o}{dr}\right)}.$$

Then one obtains for the actual relative retardation:

$$n = \frac{2}{Q}\left[F t\left(\frac{du_o}{dr} - \frac{u_o}{r}\right) + \frac{G}{P_2}\left(\frac{d^2 w_o}{dr^2} - \frac{1}{r}\frac{dw_o}{dr}\right)\right].$$

These papers [1, 2] have derived the two correction factors theoretically. Because of the way these two correction factors have been derived, their values are easy to obtain when the surface displacements of the metal are known. Since the object of the photoelastic method is to measure the unknown surface strains of a structure, using one of these two correction factors is not too practical. Although the authors of these papers have shown how to measure the unknown surface strains, the method involves much complicated work. This method will not be presented in this investigation.

Post and Zandman [3] have investigated the effect of coating thickness experimentally on four geometrical discontininties with coating thicknesses up to 0.9 inch and materials of unequal Poisson's ratios. The procedure is referred to in the original paper. Their conclusions on the effect of

coating thickness are as follows:

1. For the case of plane-stress problems and equal Poisson's ratio of structure and coating, the influence of coating thickness on birefringence developed along free boundaries is almost identically zero.

2. For unequal Poisson's ratios and singly connected structures in plane stress, birefringence developed along free bounderies is almost exactly independent of coating thickness. However, situations might arise in cases of complex geometry in which the shear tractions developed as a result of unequal Poisson contractions affect the state of stress and strain in the structure.

3. For singly connected structures in plane stress, very thick coatings behave essentially as independent bodies subjected to prescribed end displacements, i. e., as photoelastic models. In this case, birefringence is independent of Poisson's ratio.

4. In a three-dimensional problem in which coating deformation was controlled by shear traction developed at the coating interface, strains predicted by a thin coating were five percent greater than strains predicted by a thick coating. The difference is attributed to local reinforcement of the structure by the coating.

5. In the case of extremely high shear strains and strain gradients in plastically deformed mild steel, departures from linearity between birefringence and coating thickness qualitatively confirm the effects studied by Duffy. Extremely thin coating can be used for such studies.

6. In order to minimize the effect of dissimilar Poisson's ratios and local reinforcement, thin coatings are preferable. For most engineering problems, 1/8-inch coatings should be adequately thin. Plane-stress distributions for singly and multiply connected bodies and general surface-strain problems can be analyzed effectively by the method of birefringent-coating measurement.

There were two ambiguous points in the authors' statement. In statement (4) the authors do not state the criterion concerning the kind of coating thickness in relation to the thickness of the structure that attributed to the five percent of reinforcement. The second ambiguous point is in statement (6). Again the authors state that 1/8-inch coatings should be adequately thin, but have neglected to mention the thickness of the structure. Should the 1/8-inch coating be thin enough for any thickness or for a particular thickness of the structure they have in mind?

When a structure is coated with a photoelastic plastic, the coating carries a portion of the load that would otherwise be carried by the structure. Thus, strains at the interface of a coated structure are somewhat less than those in an uncoated structure for the same load. This reinforcing effect should be investigated when using the photoelastic coating method to find out whether it can be neglected or not. Correction factor for plane stress, flexure of plates, torsion of shafts, cylindrical pressure vessels, and the case of combined plane and flexural loads have been derived in [4].

Zandman, Redner, and Riegner [4] have a detailed discussion on the reinforcing effects under several loading conditions. Only the correction factor under plane stress conditions will be presented in this investigation.

The actual strains in the x and y directions of a structure can be obtained from the strains of the coated part by the equation:

$$\left|\varepsilon_{xx} - \varepsilon_{yy}\right|_s = \frac{1}{C}\left|\varepsilon_{xx} - \varepsilon_{yy}\right|_c$$

where the subscript"s" is the strain difference for an uncoated structure, and subscript "c" is for the coated structure, C is the correction factor which will be different under different loading conditions.

In the case of plane stress, an element (see Figure 3), is chosen such that x and y are the principal axes, hence, $\sigma_{xx}, \sigma_{yy}, \varepsilon_{xx}, \varepsilon_{yy}$ are principal stresses and strains.

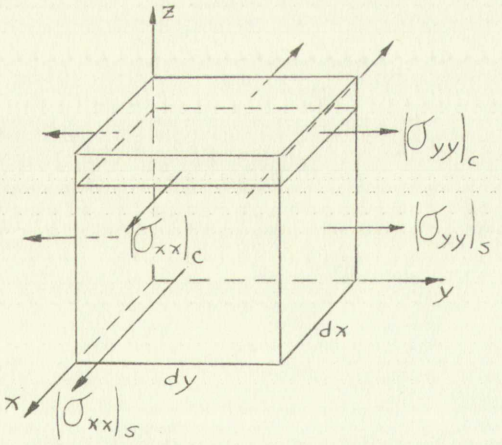

Figure 3, Coated Element From Plane Stress Structure

The influence of the load carried by the coating can be determined by equating the forces acting on the composite element to the forces acting on the uncoated element of the

structure. Hence,

$$t_s\, dy \left(\sigma_{xx}\right)_s = t_s\, dy \left(\sigma_{xx}\right)_s + t_c\, dy \left(\sigma_{xx}\right)_c ,$$

$$t_s\, dx \left(\sigma_{yy}\right)_s = t_s\, dx \left(\sigma_{yy}\right)_s + t_c\, dx \left(\sigma_{yy}\right)_c .$$

If strains are assumed to be constant across the thickness in the plane-stress problem, then:

$$\left(\varepsilon_{xx}\right)_s = \left(\varepsilon_{xx}\right)_c \quad , \quad \left(\varepsilon_{yy}\right)_s = \left(\varepsilon_{yy}\right)_c$$

at the interface. Hooke's law of elasticity for plane stress requires:

$$\sigma_{xx} = \frac{E}{1-\nu^2}\left(\varepsilon_{xx} + \nu\,\varepsilon_{yy}\right) ,$$

$$\sigma_{yy} = \frac{E}{1-\nu^2}\left(\varepsilon_{yy} + \nu\,\varepsilon_{xx}\right) ,$$

$$\sigma_{zz} = 0 .$$

Thus,

$$\left(\varepsilon_{xx} - \varepsilon_{yy}\right)_s = \left(\varepsilon_{xx} - \varepsilon_{yy}\right)_c \left[\, 1 + \frac{t_c E_c}{t_s E_s}\,\frac{1+\nu_s}{1+\nu_c} \,\right]$$

where ν_s and ν_c are Poisson's ratios of the structure and coating respectively. Comparing this with

$$\left(\varepsilon_{xx} - \varepsilon_{yy}\right)_s = \frac{1}{C}\left(\varepsilon_{xx} - \varepsilon_{yy}\right)_c$$

gives the correction factor for plane stress problems:

$$\frac{1}{C} = \left[\, 1 + \frac{t_c E_c}{t_s E_s}\,\frac{1+\nu_s}{1+\nu_c} \,\right] .$$

Since the factor $\left[(1+\nu_s) / (1+\nu_c)\right]$ is very close to unity and represents a second order effect in the correction term, the correction factor can be simplified to:

$$\frac{1}{C} = 1 + \frac{t_c E_c}{t_s E_s} .$$

The foregoing analyzis is restricted by the following assumptions,

and applies to any situation in which these conditions prevail:

1. Structure and coating are isotropic elastic materials.

2. Identical deformation of structure and coating exists at the interface.

3. Plane stress prevails in structure and coating.

It is clear from these restrictive conditions that this correction factor can only be applied within the elastic range of the material. If the structure is in the post-elastic range, the coating has a very significant reinforcing effect on the structure. This reinforcing effect on a post-elastic structure will be discussed later in this investigation.

2.2 Papers on Related Topics

The following is a review of the papers published by other authors on topics similar to the problem studied in this investigation. These papers are either on using the same experimental methods or on the same problem.

Gerberich [5] used the birefringent coating method for determining the stress distribution about a slowly growing crack. The test specimen was a ASTM recommended center notched flat plate. Using the electrical discharge process, crack tips were obtained which had root radii less than or equal to 0.001 inch. The material tested was 0.130 inch thick SAE 4340 steel, heat treated from 210 Ksi to 250 Ksi yield strength. The specimens were pulled in a 3,000,000 lb. hydraulic testing machine at a loading rate of approximately 13,000 lb./min. Load-versus-time was recorded so that the applied stress for a particular movie frame could be calculated later. An epoxy-polysulfide copolymer with a formulation of 15 parts epoxy to 12 parts polysulfide by weight was chosen by Gerberich as the

birefringent coating material. The properties of this plastic were as follows: elastic modulus, 220,000 psi; elongation, 15 percent; K factor, 0.056.

To check the thickness effect on accuracy of the birefringent coating in a high strain gradient region, a specimen of 0.10-inch thick 2024-0 aluminum with a yield strength of 15.4 ksi and an ultimate strength of 34.6 ksi was utilized by Gerberich. The specimen was loaded to an applied stress of about 90 percent of the yield strength and then relaxed. Two sets of pictures were taken of full-order and half-order fringes with the original thickness of the bonded plastic of 0.1096 inch. This procedure was repeated with the plastic milled down to 0.0551 inch and finally to 0.0279 inch. The strains obtained from these various thicknesses of plastic were compared. The author has claimed, even for 0.05 inch, the error is less than 10 percent.

Since the test was on slow growing cracks, the specimen would surely have reached the post-elastic range. At least the region surrounding the growing cracks would be in the post-elastic range of the specimen. However, Gerberich has neglected to mention the reinforcing effect of the plastic on the specimen in the post-elastic range.

Durelli and Sciammarella [6] have used the moiré method to analyze the distribution of stresses and strains on the transverse axis of a finite plate with a circular hole. The plate is subjected to unidimensional load as the plastic deformation increases and, for one of the loading stages, to study the strain distribution in a region surrounding the

hole. To improve the accuracy of the method an initial fringe pattern was introduced by grid "mismatching" the master and model screens. The advantages of "grid mismatch" discussed by the authors are as follows:

Calling "ε_m" the initial fictitious strain corresponding to the pitch mismatch and "p" the master grid pitch, the fringe spacing is:

$$\delta_m = \frac{p}{|\varepsilon_m|} .$$

If ε_d is the strain produced by the applied deformation, the corresponding fringe spacing is:

$$\delta_d = \frac{p}{|\varepsilon_d|} ,$$

The fringe spacing resulting from the superposition of ε_m and ε_d is:

$$\delta_f = \frac{p}{|\varepsilon_m| \pm |\varepsilon_d|} ;$$

where the plus sign applies to the case $\varepsilon_m \varepsilon_d > 0$ and the minus sign to the case $\varepsilon_m \varepsilon_d < 0$.

To increase the precision it is desired that :

$$\delta_f < \delta_d .$$

This is achieved by any:

$$|\varepsilon_m| > 0 \quad \text{if} \quad \varepsilon_m \varepsilon_d > 0 .$$

When $\varepsilon_m \varepsilon_d < 0$, the condition $\delta_f < \delta_d$ is fulfilled if

$$|\varepsilon_m| > 2 |\varepsilon_d| .$$

It is clear that a mismatch of the same sign will always produce more fringes and so always be advantageous, and that to be advantageous a mismatch of opposite sign must be of at least twice the magnitude of the strain to be analyzed.

An aluminum model, 24 inches long, 8 inches wide, and 1/8 inch thick was used by the authors. A circular hole, 1.25 inch in diameter, was drilled at the center. A grid of 300 lines per inch with lines parallel and perpendicular to the axial load was lithographically printed on one face of the model. The study of the deformations was carried out up to $\lambda = 0.82$, where $\lambda = \frac{\sigma}{\sigma^*}$. The stress "$\sigma$" is the applied stress to the specimen, and "σ^*" corresponds to the flat portion of the stress-strain curve, called "yield stress" by the authors. The elastic modulus of the specimen was 10,000,000 psi with $\lambda = 0.82$ the strain in the dimensionless form "$\frac{\epsilon E}{\sigma^*}$" is about 1.0, which is around the yield strength of the aluminum specimen. The authors did not investigate the strains in the fully plastic range of the specimen. The authors also did not investigate the possibility of using the moiré method to investigate strain distribution around a crack.

The study of plastic-strain pattern in a flat sheet with a hole has also been done by Merrill [7] using the photodot method. The photodot method is considerably more difficult to analyze than the moiré method or the photoelastic coating method. This method has not been considered in this investigation.

3.0 THE EXPERIMENTAL MODEL

The experimental model used for this investigation was a large tension plate with a centered circular hole as a stress raiser. The plate was subjected to a uniform, uniaxial loading by controlled rate of deformation. The nature of testing was to subject the plate to a continuous loading from the undeformed state to the fractured state. The loading rate employed in the testing was sufficiently low to consider the plate at the quasi-static state at all times.

The sample was made from 0.032 inch sheet stock of 6061-T6 aluminum alloy. The width of the plate was five inches with a one-inch diameter hole at the center. The mechanical properties of the 6061-T6 aluminum alloy by the manufacturer's specification are as follows:

Modulus of elasticity : 10.0×10^6 psi,

Ultimate strenght: 45,000 psi,

Yield strenght: 40,000 psi,

Elongation in two inches (1/16" thick specimen) : 12 percent

Due to the extremely slow loading rate of the specimen, the stress-strain relation is somewhat different from that given in the ASM handbook. Figure 4 shows the stress-strain relation of this aluminum alloy subjected to the same loading rate used in the tests. Since the rolled aluminum sheet stock is not an isotropic material, all the testing samples were with the roll-grain direction parallel to the loading direction to insure reproducibility of results of each model.

A whiffletree loading device was used to obtain the uniform, simple tensile load. The whiffletree and tension

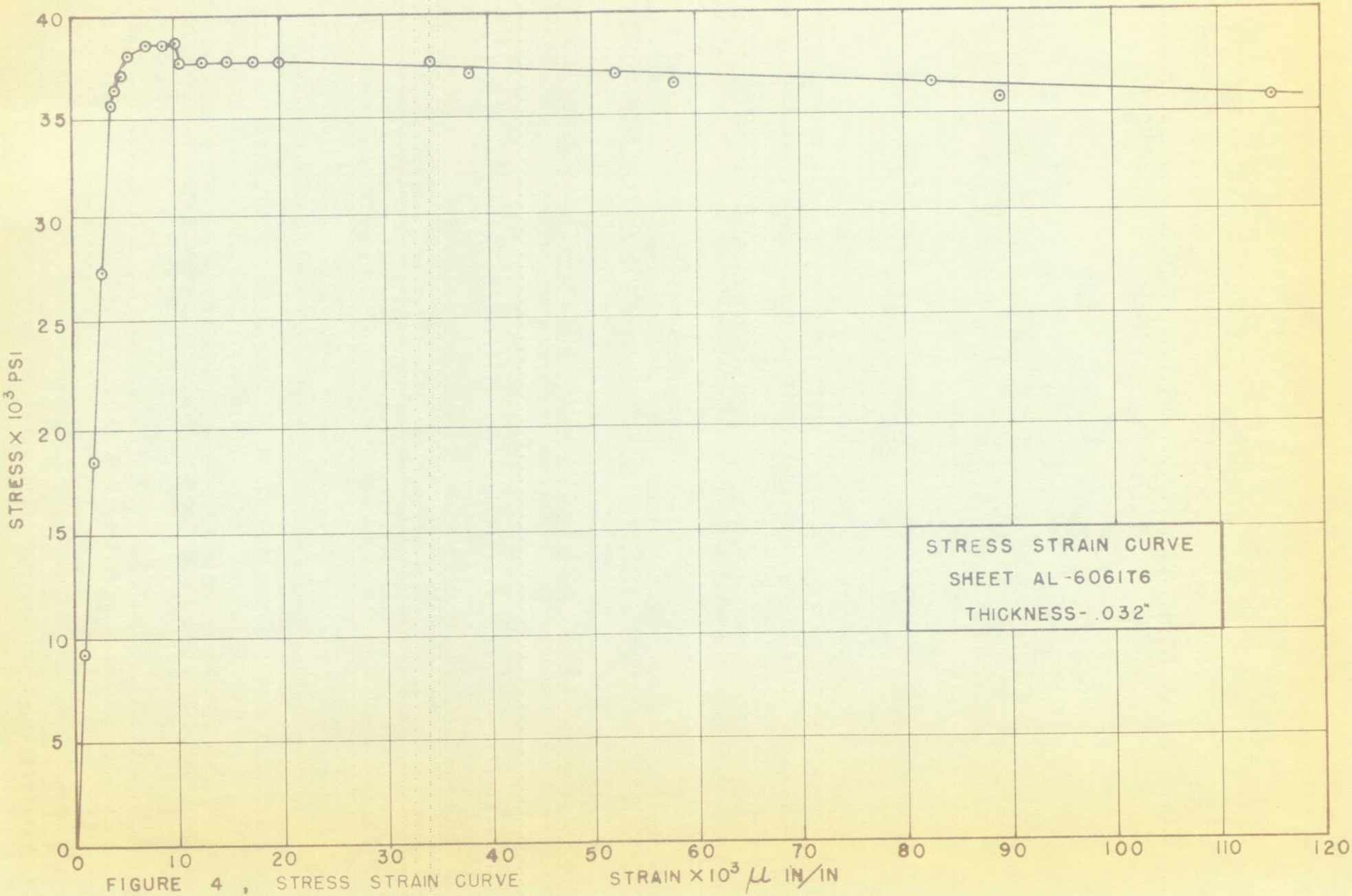

FIGURE 4 , STRESS STRAIN CURVE

plate assembly is shown in Figure 5. The square pull bar is doubled as a force link. Two SR-4 type A-14 gages were mounted on the square pull bar, item 2 in Figure 5. These gages were used as load transducers so that a record of the applied load would be obtained. The gages were mounted on opposite sides of the bar to eliminate signal produced by bending of the bar.

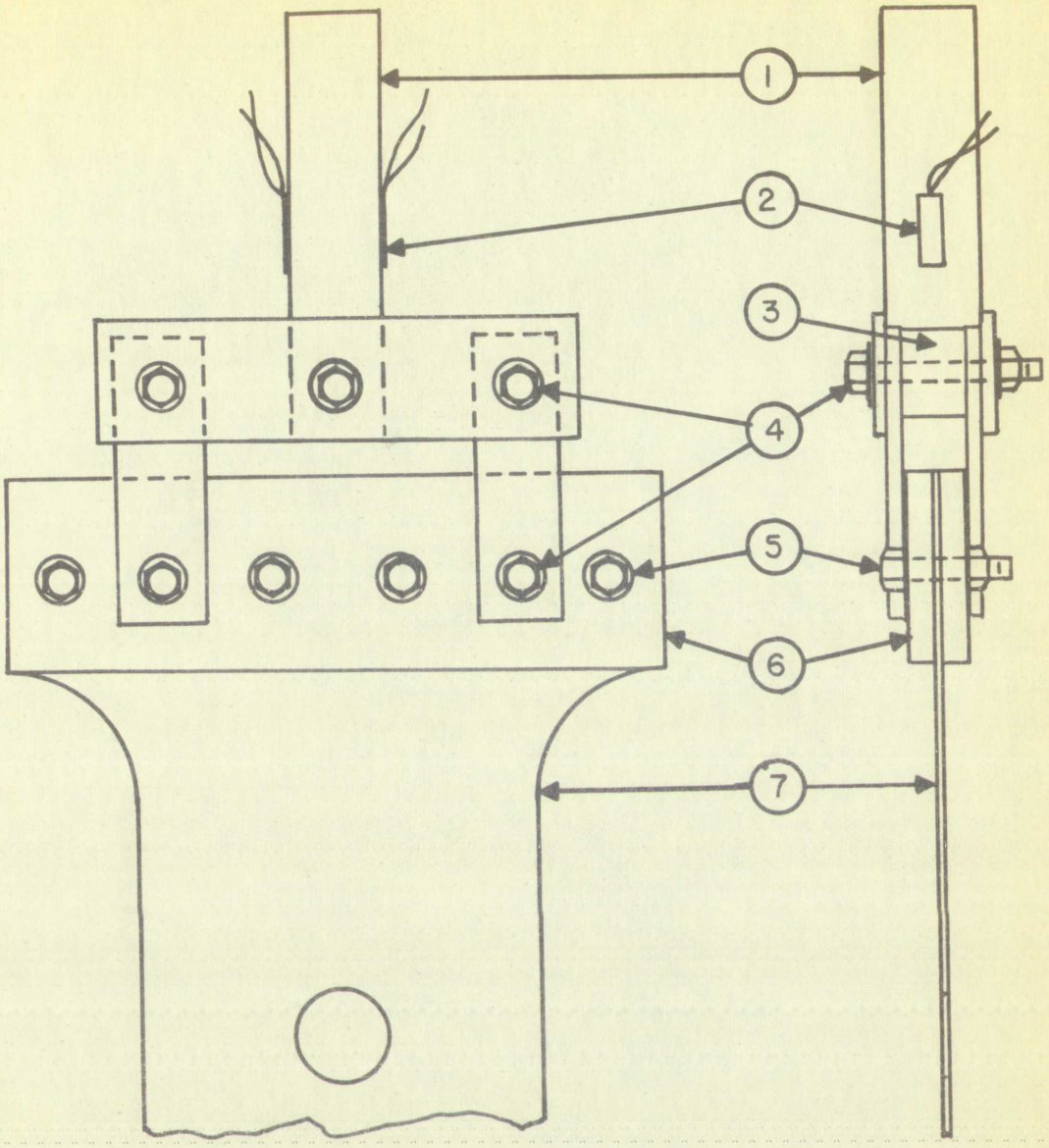

LEGEND

1. PULL BAR (1" SQUARE STEEL)
2. STRAIN GAGES (LOAD MEASUREMENTS)
3. SPACER
4. 3/8" PINS
5. 3/8" CLAMPING BOLTS
6. STEEL CLAMPING PLATE
7. ALUMINUM PLATE

WHIFFLETREE IS MADE OF STEEL

FIGURE 5, WHIFFLETREE & TENSION PLATE ASSEMBLY.

4.0 Moiré Method

The moiré method is a relatively new technique being used in the field of experimental stress analysis. Weller and Shepard [8] are believed to be the first to propose the use of moiré effect to measure displacement and deformation. The moiré effect is an optical phenomenon produced by mechanical interference of two screens with similar arrays of dots or lines superimposed on each other, resulting in the formation of alternating light and dark fringes. Since the fringes are the result of relative displacements of the two arrays, the moiré effect can be used as a tool to measure surface strain.

4.1 Theory

The moiré method for measuring surface strain consists of two identical screens of straight, parallel lines (see Figure 6a). A fixed screen is used as a reference both for analyzing the properties of the moiré effect and for the coordinate of direction. This screen is called the master screen. The other screen, printed on the surface of the test specimen to be strained, is called the model screen. Fringes are produced by either pure deformation, rigid body rotation, or a combination of pure deformation and rotation. In order to analyze a plane stress problem completely, two sets of screens are required. They are arranged so that the arrays of lines of the two screens are mutually perpendicular to each other (See Figure 7).

4.1.1 Pure deformation -- When a specimen is subjected to uniform tension in a direction perpendicular to its model screen lines, with the master screen superimposed onto it

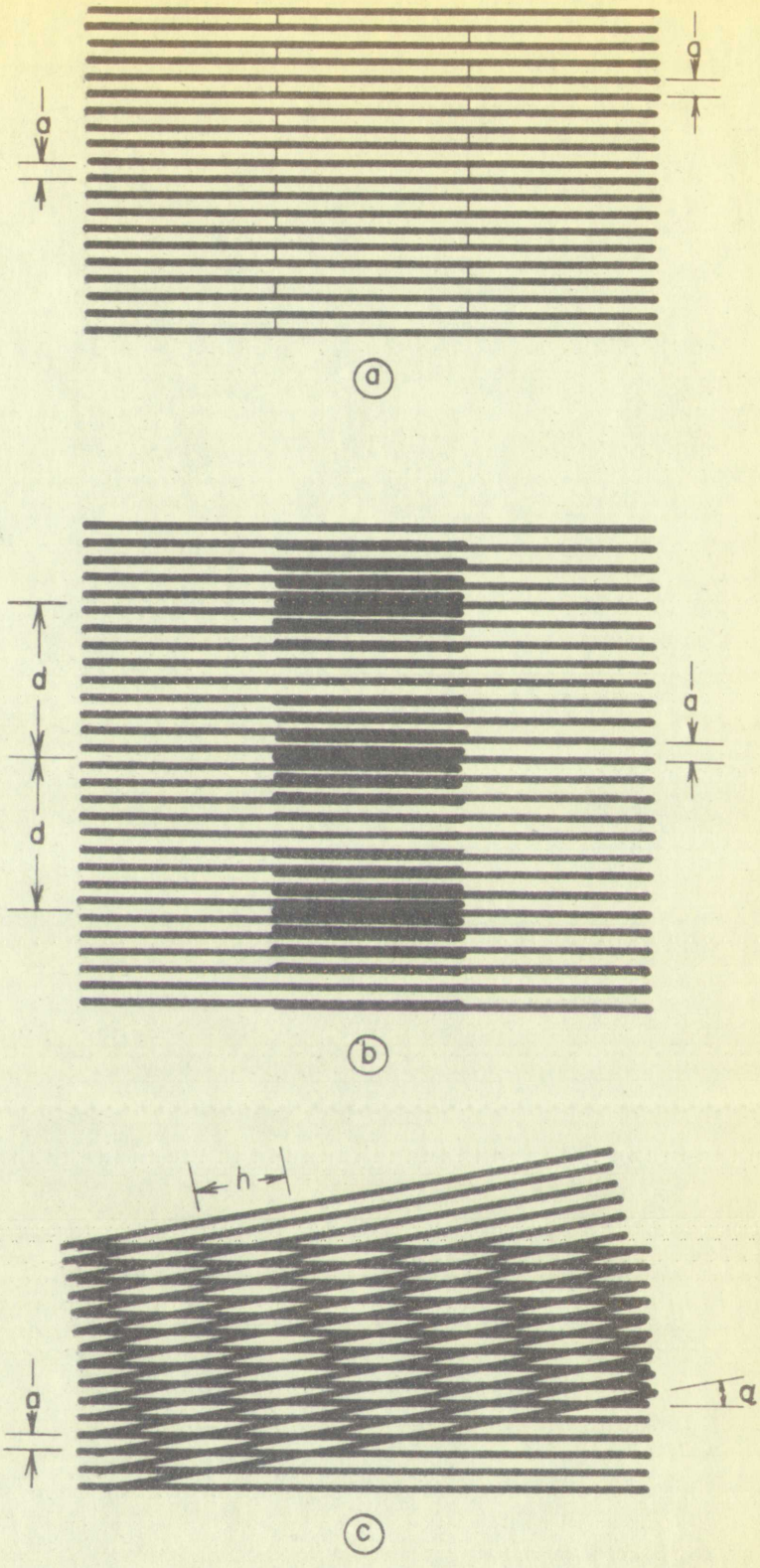

FIGURE 6 , THE MOIRÉ EFFECT

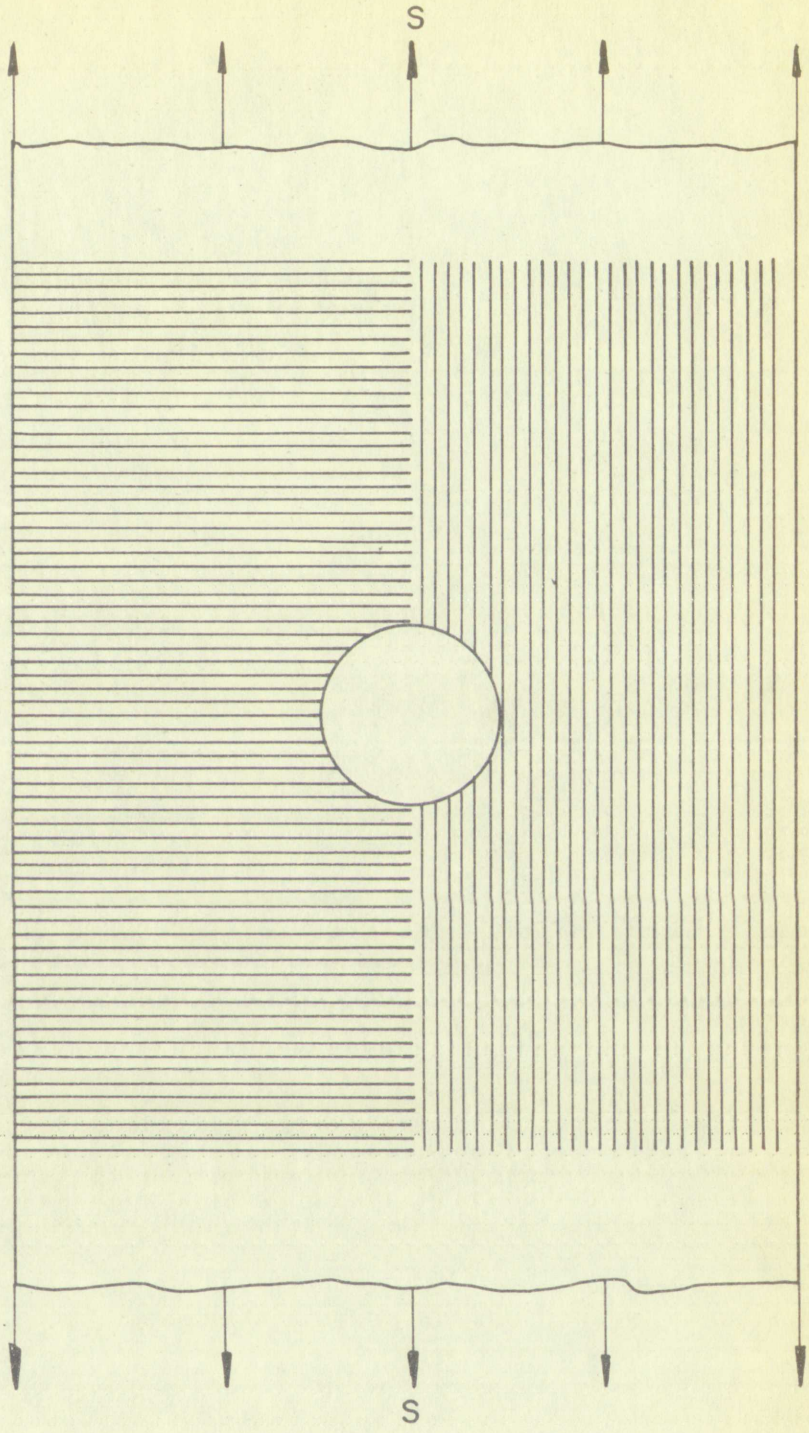

FIGURE 7 , MODEL SCREENS ARRANGEMENT ON TEST SPECIMEN

without rotation, moiré fringes are formed as those shown in Figure 6b.

In order to form the necessary fringes, the model screen must be strained so that its (n-1)-th line would interfere with the n-th line of the master screen. If it is in compression, it would be the (n-1)-th line of the model screen interfering with the n-th line of the master screen. If pitch of the screen lines is "a" and "d" is the distance between two neighboring fringes, see Figure 6b, the elongation "e" would be related to "a" and "d" by the equation:

$$n a = d = (n - 1)(1 + e),$$

or

$$e = \frac{a}{d - a} .$$

In the case of compression, the elongation "e" is in the form:

$$e = - \frac{a}{d + a} .$$

It is clear from the Figure 6b that the fringes formed are parallel to the screen lines, and the fringe spacing "d" must be measured perpendicular to the screen lines.

4.1.2 Rigid body rotation -- When the master screen is rotated slightly with respect to the undeformed model screen, interference fringes are formed as shown in Figure 6c.

If "h" is the distance between two fringes "h" is related to the pitch "a" of the screen and the angle of rotation "α" geometrically by the equation:

$$h = \frac{a}{\tan \alpha} + a \tan \frac{\alpha}{2} ,$$

or in simplified form

$$\sin \alpha = \frac{a}{h} .$$

For small rotation, where sin α is approximately equal to α, this equation can be written as:

$$\alpha = \frac{a}{h} .$$

As can be seen from the Figure 6c, the fringes are almost perpendicular to the lines of the model screen. So the fringe spacing "h" is measured parallel to the model screen lines.

The theory relating the moiré effect to the homogeneous deformation, plane stress, or plane strain problem, required more elaborate mathematical manipulation.

This theory can be found in references [9, 10, 11, 12]. In references [11 and 12] the authors used the geometrical approach to develop the matematical relation between the moiré effect and plane strain. In reference [10] the authors related the plane strain components to the moiré effect by means of linear transformation. Bromley, [9] using tensor calculus has analytically formulated the relationship between the moiré effect and strain components. Since the purpose of this investigation was to evaluate experimental techniques only, detailed mathematical theory concerning the moiré method will not be presented. References are listed at the end of this paper for the complete mathematical theory of the moiré effect.

4.2 Experimental Apparatus

4.2.1 Engraver's lithographic printing equipment --

The printing equipment consisted of a whirler and a vacuum arc printing machine. These were used to print model screens on the test specimen. The whirler had a 24-inch platform, which was capable of handling a plate up to 24" x 24". It was driven

by a motor at 60 cycles per minute. The purpose of the rotating platform was to spread the photo-sensitive solution evenly across the surface of the specimen. There was an electric heater in the whirler to dry the photo-sensitive solution.

The vacuum arc printing machine was a NuArc model RP-21A Rapid Printer. The printer had a single carbon arc light source. The arc could be controlled automatically or manually. It was capable of printing plates up to 21" x 24". There was a vacuum frame on top of the arc to hold the specimen tightly against the master negative to be printed on the specimen.

4.2.2 Tensile testing machine -- Two universal tensile testing machine were used at different times. The two machines were the Dillon Model "L" Universal Testing Machine and the Tinius Olsen Hydraulic "L" Type Universal Testing Machine courtesy of the Civil Engineering Department, U.N.M.

The Tinius Olsen machine is a controlled loading rate hydraulic machine of a capacity of 120,000 lb. The Dillon machine is a controlled deformation rate machine of a capacity of only 10,000 lbs. However, the Dillon machine was quite adequate for the purpose of this investigation because the tensile load at fracture for the test specimen was from 6,000 to 7,000 lbs. Loading mechanism was of the screw type, either motor driven or manually powered.

4.2.3 Photographic equipment -- Cameras were used to record the moiré fringe patterns. A Wollensak Fastax High-Speed Motion Picture Camera Model WF-4 ST and a Polaroid Land Camera Model 150 were used for this purpose at different times.

The Fastax camera used employs a rotating prism optical compensating device to obtain picture synchronization on the continuously moving film. It is a 400 foot capacity high-speed camera utilizing standard 16 mm Motion picture film, either black-and-white or color. The picture format is recorded on a 16 mm full frame. The camera is capable of taking pictures from approximately 150 to 12,000 frames per second. Two flood-lights were used for lighting.

The picture format recorded with the Polaroid camera model 150 is a 3" x 4" full frame. The camera has variable aperture openings with speed of the shutter limited to instant opening and shutting and the time exposure. The camera is capable of handling any standard Polaroid film.

4.3 Selection of Moiré Screens

With the moiré method, it is not possible to measure strain throughout a very wide range with a single specific set of screen lines. Therefore, care must be taken in selecting the screen lines to give the best resolution in the range of strain to be measured. For the case of a 200-line per inch screen, the pitch distance between two neighboring lines is 0.005 inch. To produce a fringe spacing of one inch, the model screen must be strained 5,000 μ in/in. Since the moiré effect measures the average strain within the fringe spacing, the usefulness of the average strain measured by this method depends upon the fringe spacing. The closer the fringes, the more nearly the average strain approximates the strain at a point

which is especially important when a strain gradient exists in the specimen. This is the criterion governing the lower limit of the strain to be measured by a specific screen. The higher limit of the strain to be measured is governed by the resolution of the fringe pattern shown on the picture taken by a camera. With the lens of the Polaroid camera placed eight inches away form the model screen, the picture could pick up fringes 0.025 inches apart with good resolution. Using the 200-lines per inch screen, fringe spacing of 0.025 inch represents a strain of 0.20 in/in. Closer fringe spacing could also be obtained by moving the camera closer to the specimen. When the fringes are closer together, the sharpness of the printed model screen on the specimen is an important factor in the resolution of the fringes. The sharper the model screen the better the resolution. This is especially true if the specimen is opaque, since in this case a reflection type of moiré method must be used. In general, the 200-lines per inch screen is capable of measuring strains ranging from approximately 3 to 30 percent with good accuracy.

Two types of screens, 200 and 1,000 lines per inch were available. The specimen used was made of 6061-T6 aluminum sheet, which had a manufacturer's given yield strain of 4,000 μ in/in and ultimate strain of 12 percent elongation. However, under the plane stress condition the ultimate elongation was recorded as over 30 percent. Since the post-elastic range was

of interest, the 200-lines per inch screen was used. A detailed account on the method of printing the model screen can be found in Appendix A.

4.4 Arrangement of Apparatus

The test specimen was mounted in the tensile machine, either the Tinius Olsen machine or the Dillon machine, by means of a set of whiffletrees. The master screen was glued on a sheet of 1/16-inch plexiglass plastic which then was clamped flat against the model screen on the specimen. Figure 7 shows the arrangement of the model screen on specimen. The Fastax camera was placed about 30 inches from the specimen and directly in front of it. The two flood-lights were placed by the sides and slightly behind the camera (See Figure 8). They were used to illuminate the specimen. On later tests the Fastex camera was replaced by a Polaroid Land camera, and the flood-lights were replaced by a circular fluorescent lamp. The Poloroid camera was placed about 8 inches from the specimen through the center of the circular fluorescent lamp (See Figure 9). Closeup lenses were needed for the Polaroid camera for close range picture taking.

4.5 Preliminary Investigations

The testing method was to subject the test piece to continuous loading from its unstrained state through final rupture. Following is an evaluation of the techniques and equipment used to determine the best approach to the problem using the moiré method.

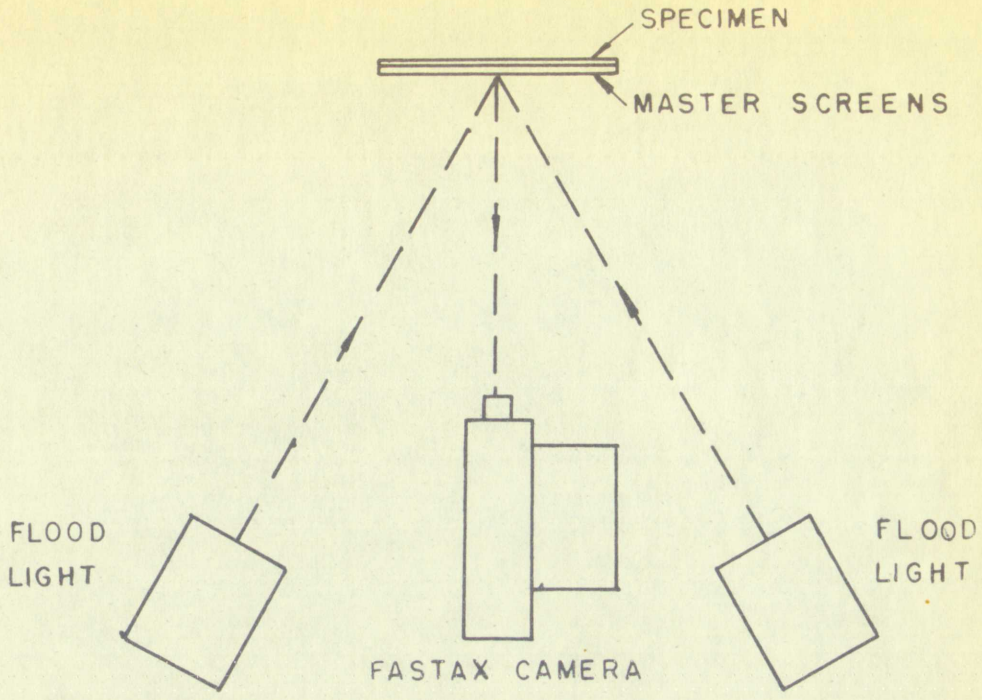

FIGURE 8 , FASTAX CAMERA AND LIGHT SOURCE SETUP FOR MOIRÉ METHOD

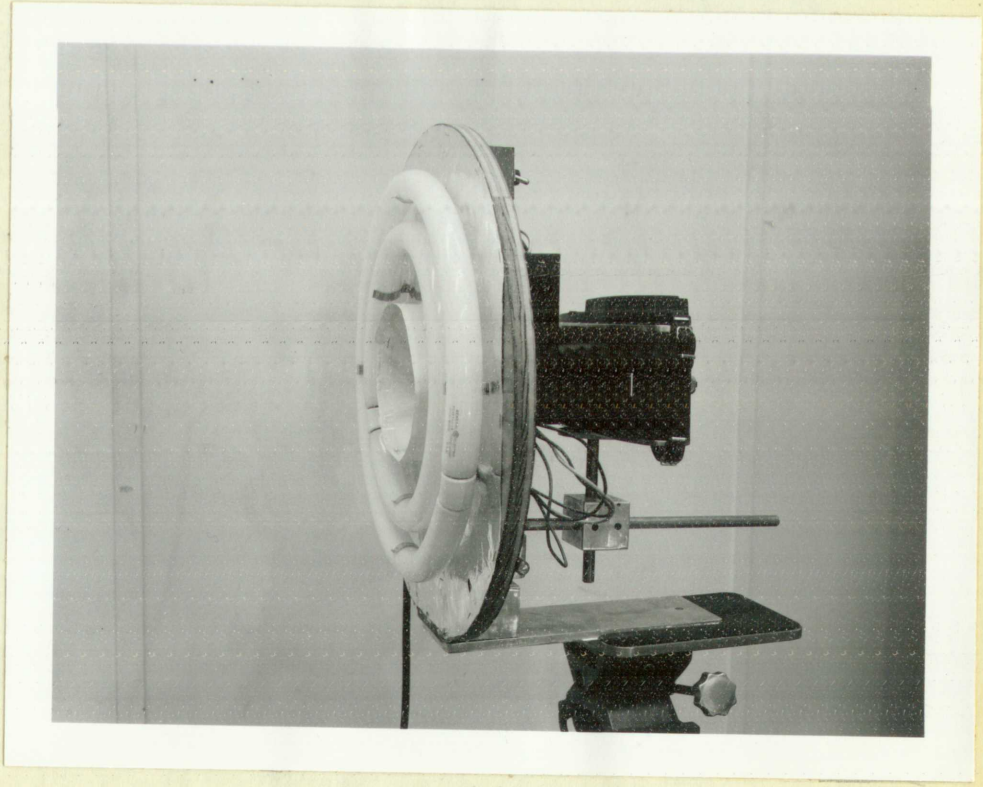

FIGURE 9 , CIRCULAR FLUORESCENT LIGHT SOURCE WITH CAMERA FOR MOIRÉ METHOD

4.5.1 Lithography as a means for printing model screens-- Several tests were run to check the merit of the lithographic method as a means for printing model screen on the metal specimen.

First, to find out the workability of the printed metal specimen, holes had been drilled in the plate. Then it was observed under a 30-power microscope. It was found that the printed grid lines ran right up to the edge of the drilled hole. The adhesiveness of the printed grid lines was also found to be excellent. They were not affected in any way by the drilling process. Before this method had been tried, model screen were printed on the metal specimen with a hole already in it. When this printed specimen was observed under a microscope, the printed grid lines had faded away at the region within 1/16 to 1/8 inch of the edge of the hole. Since the region at the immediate neighborhood of the hole was of utmost importance in this investigation, this defect rendered the specimen useless. Therefore, in all subsequent work the method of printing before drilling was employed to prepare the test specimens.

Other tests were conducted to investigate the adhesiveness of the model screen under actual test conditions. Screen lines were printed on tensile specimen strips of 1.5" x 8". The specimens were subjected to tensile loading until rupture. Then, the ruptured edges were observed under the microscope. Again it was found that the printed grid lines adhered to the surface extremely well right up to the very edge of rupture.

Great care was taken to keep the lithographically printed model screen dry at all times. If it is dry, the model screen can stand very rough abrasive handling. If it comes in contact with any liquid, either oil or water, the printed screen will easily wipe off.

4.5.2 Tinius Olsen Testing Machine as a loading device-- The first several tests using the moiré method were conducted using the Tinius Olsen Testing machine. This machine was chosen because of its ease of operation. Furthermore, different loading rates could be obtained in stepless intervals. However, its loadwas transmitted to the specimen by means of hydraulic pressure on the loading piston. This method of pressure loading did not suit the purpose of this project since the main interest here was in the relative displacement of the specimen. Therefore, it was abondoned for further use. The positive displacement Dillon testing machine was then used exclusively for the remaining tests.

4.5.3 Fastax camera as a recording device-- The Fastax camera was used along with the Tinius Olsen testing machine. The purpose of using this camera was to provide a continuous record of the formation of moiré fringes as the specimen was be being strained to rupture. It was also desired to record the moiré fringe pattern as cracks propagated through the specimen. In the first test, the Fastax camera was run at about 300 frames per second. In later tests, the camera was run at a speed of approximately 1,200 frames per second. It was found that the

Fastax camera was not satisfactory as a recording device. Due to the high propagation rate of cracks through the aluminum specimen only a few frames of the picture recorded the cracks propagating through the specimen even with the camera running at 1,200 frames per second. Since the Fastax camera is a high-speed camera, it required high-speed film.Unfortunately, coarse grains are generally associated with the high speed film. This coarse-grain structure in the film impairs the resolution of the picture. Also the picture format was only 16mm full frame. A great amount of detail essential in the analysis of the moiré fringes was lost due to the smallness of the film size. For example, in the largest strain region, where the moiré fringes would be closest together, the fringes were no longer visable in the 16 mm film. Furthermore, the cracks were so fine, that they too were not very distinctly shown in the film. Due to poor resolution of the Fastax camera picture, this camera was abandoned in favor of the Polaroid still camera.

4.5.4 Flood-light as a source of illumination -- Two 1,000 watt flood-lights were used to illuminate the specimen. They worked well as an illuminating source for the Fastax camera. However, they were not satisfactory as a light source for the Polaroid camera because uniformly reflected light from the specimen was not possible. In some areas the reflected light was too bright, and in other areas it was too dim. In either case, the resolution of the picture was impaired. Therefore, in later tests the flood-lights were replaced by a circular fluorescent lamp. The resolution of the pictures was improved

considerably with this new light source.

4.5.5 Final assembly -- The final assembly for tests using moiré method consisted of the Dillon testing machine, Polaroid camera, and the circular fluoresent light source. The load record of each test was also recorded by means of the force link in the whiffletree (See Figure 5).

Since the Polaroid camera was taking still pictures, there was a time lapse between pictures. With this positive displacement machine, the intention was to stop the loading while every picture was taken. Then the loading was started again whenever the camera was ready to take the next picture. It was hoped that the positive displacement loading nature of the machine would hold the strain pattern constant. However, it was found that when the specimen was in the post-elastic range, the strain would not remain constant. The reason for this was that although the total displacement was held constant it did not prevent the plastic strain in region of high stress concentration from flowing which, in turn, relaxed the strain in the lower stress region. Therefore, to prevent the plastic flow, the specimen had to be loaded continuously throughout the entire test. In order to obtain enough time between exposures , the machine had to be loaded as slowly as possible. The loading rate obtained by motor drive was found to be too fast. The slow loading rate had to be accomplished by hand loading the machine.

The final procedure used for these tests was to load the specimen at the slowest possible rate by hand until it ruptured. A sequence of pictures of the moiré fringe pattern was taken with the Polaroid camera. A complete record of the

load was also recorded on the CEC recording oscillograph. Markings were placed across the load record to correspond to each fringe pattern photographed. These data obtained from the test were then analyzed. However, once the cracks had started in final rupture of the specimen, they were propagating at such a high speed, they could not be photographed by the Polaroid camera.

4.6 Data Reduction

Since the average strain reduced by the moiré method depends on the fringe spacings, an accurate record of the fringe pattern is necessary. In order to relate the fringes in a picture to its actual size, a reference is needed. The reference used in the tests is a circular coin of exactly one inch in diameter, and the thickness is about 1/32 inch. It was taped to the specimen, where it would not interfere with the region of interest. When the fringe pattern was photographed, the coin would appear in the picture as a reference. A correction factor was then calculated from this reference to convert the measurement back to its actual dimensions.

The screen lines are arranged perpendicular to direction of the strain to be measured. In the case of the specimen under uniform uni-axial loading the screen is arranged with the lines perpendicular to the load. The moiré fringes will appear perpendicular to the direction of loading, parallel to each other, and evenly spaced. If the transverse strain due to Poisson's effect is to be measured, the screen lines should be

arranged parallel to the direction of loading. The fringes will appear parallel to the direction of loading. To obtain the strain will simply involve measuring the fringe spacings and knowing the pitch of the screen used. For the longitudinal direction, the average strain will be computed by the equation:

$$\varepsilon = \frac{a}{d-a} ,$$

and the average transverse strain will be:

$$\varepsilon = -\frac{a}{d+a} ;$$

because it is in compression produced by the Poisson's effect. In an uniform strain field the fringe spacing can further be checked by comparing the average fringe spacing of several fringes to the spacing of two neighboring fringes.

In a plane stress or strain field, where there is a gradient existed in the specimen, the average strain at a point would no longer be accurately approximated by the fringe spacing at that point. A more accurate method for approximating strain of this nature was illustrated in the following paragraph.

Taking a hypothetical case as shown in Figure 10. When strain at point A is to be measured. We will arbitrarily assign the fringe at which point A is situated as the zero fringe order. The next full fringe would be the first order fringe and so on, as shown in Figure A. On the opposite side, the fringe orders would be designated as the negative fringe orders as shown in the Figure (10a).

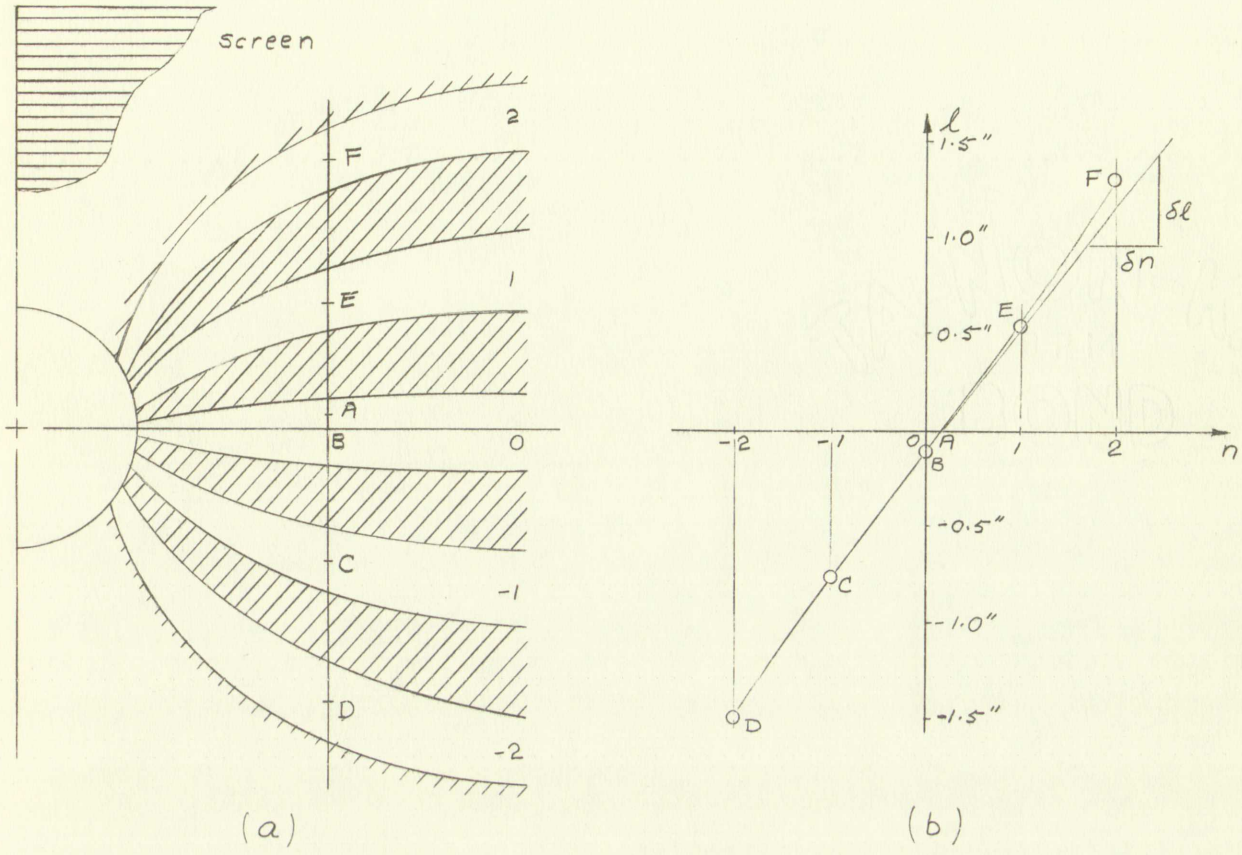

Figure 10, Moiré Fringe Pattern and Interpolation Curve

The centers of the full light fringes were designated by the letters B, C, D, E, and F. Note the full fringe order can be that from the center of a dark fringe to the center of its neighboring dark fringe. If the strain of the point to be measured is located inside a dark fringe, they will be designated the same way as that for the light fringes shown in Figure (10a) except that the zero and the full fringe orders would be the dark fringes.

To measure the strain at the point A the fringe orders were first plotted against the distances from A to the centers of the fringes as shown in Figure (10b). Then a smooth curve was constructed throught the points. The intersection of the curve

and the line where "1" is equal to zero will be the location of the point A. A tangent to the curve through A is constructed. The slope of the tangent line will be the fringe spacing at the point A:

$$d' = \frac{\delta \ell}{\delta n} ,$$

and the average strain at A will be:

$$\varepsilon = \frac{a}{d'-a}$$

in tension, or:

$$\varepsilon = - \frac{a}{d'+a}$$

in compression.

Under the plane stress or strain condition the fringes will no longer be parallel, but the fringe spacing will still be measured perpendicular to the master screen lines in the direction of the strain to be measured. Slopes of the fringes can be used to find other strain components. However, we were not interested in other strain components. They will not be considered here. A detailed discussion concerning other strain components can be found in reference [9].

4.7 Estimate of Error

An estimate of error for each method of determining the surface strain measurement was made to gain knowledge of the accuracy of the experimental work and to compare the two methods.

The estimate of error for the moiré method depends on the accuracy of the grid lines, the location of the center of the fringes, and construction of the line tangent to a point in the

fringe spacing versus fringe order curve, (See Figure 10b). The 200 lines per inch master grid negative was reproduced from a glass plate rulings. The glass plate ruling was done by Max Levy and Company, Philadelphia, and the rulings were a 50:50 dark and light lines and extremely accurate. However, the reproduced master negatives and model screens in the specimen lost some of its accuracy. The accuracy of the glass plate screen was reduced about $\pm$ 1 percent on the master negative when reproduced from the glass plate. The fringe spacing was then measured by a Bansch and Lomb's 7-power measuring magnifier. The linear measuring scale has a range of 0.75 inch and with each small division equal to 0.005 inch. The greatest error in locating the centers of fringe lines occurred when the fringes were closest together. The error was estimated to be $\pm$ 8 percent. The error could be reduced by enlarging the fringe pattern pictures. When the picture was enlarged to twice the normal size of the specimen the error was reduced considerably. It was estimated to be about $\pm$ 3 percent. However, the greatest error was introduced when constructing the tangent line to the fringe spacing versus fringe order curve. The error was sometimes as high as $\pm$ 10 percent. Hence, the total additive error introduced from this strain reduction process could be as high as $\pm$ 13 to $\pm$ 15 percent.

5.0 BIREFRINGENT COATING METHOD

The birefringent coating method is commercially called the Photostress method. The principle of Photostress is exactly the same as the principle of photoelasticity, except that a reflection polariscope is used and a birefringent plastic is bonded on the test specimen.

In recent years, the manufacturers have made available high elongation birefringent plastics. These high elongation birefringent plastics have made analysis of strain in the post elastic range of metals possible. Two companies are manufacturing these plastics commercially. The Budd Company is offering the high elongation type M Photostress plastic. It has a maximum elongation of 30 to 50 percent, according to the manufacturer. The modulus of this plastic is approximately 25,000 to 30,000 psi, while the strain senstivity for the plastic of 0.12 inch thickness is approximately 0.02. Two other high elongation plastics are available from Photoelastic Incorporated. They are called Photolastic PS-2 and PS-3. The maximum elongation for the PS-2 is 30 percent and for the PS-3 50 percent. The modulus of the PS-2 and PS-3 are 450,000 psi and 30,000 psi respectively. The manufacturers claim that the plastics have a constant strain optical coefficient over the stated usable range of elongation.

The Budd Company's type M Photostress plastic was used in the tests discussed here. Since the test specimen was made of 6061-T6 aluminum sheet, which has an ultimate elongation of

slightly higher than 30 percent under plane stress condition, the type M Photostress plastic should be capable of measuring strain up to the rupture point of the specimen.

5.1 Theory

The following theory developed by Zandman [13] is primarily for use with the Budd Company's Photostress plastics. However, the theory can be applied to other birefringent plastics manufactured by other companies as well.

The principal stress difference of any birefringent material is related to the fringes developed in the birefringent material when stressed by Newman's equation;

$$\delta_n = (n_1 - n_2)\,2t = C\,(\sigma_1 - \sigma_2)_p\,2t$$

or

$$\sigma_1 - \sigma_2 = \frac{\delta_n}{2tC} \qquad (1)$$

where δ_n is the relative retardation measured when polarized light is traversing the plastic under normal incidence. σ_1 and σ_2 are the principal stresses, t the thickness of the plastic, and C the stress optical constant. The subscript "p" was used to designate stresses of the plastic, and s would be used for test specimen. Note that 2t is used in the equation because the polarized light is being reflected from the surface of the specimen, and is passing through the plastic twice.

Since the tension plate used in this investigation represents a plane stress problem, the strains will be related to the stresses by the following equations:

$$\varepsilon_1 = \frac{\sigma_1}{E} - \nu\frac{\sigma_2}{E}$$

$$\varepsilon_2 = \frac{\sigma_2}{E} - \nu\frac{\sigma_1}{E}$$

where E is the modulus and ν is Poisson's ratio for the material. Hence, the principal stresses are related to the principal strains by the equation:

$$\sigma_1 - \sigma_2 = (\varepsilon_1 - \varepsilon_2)\frac{E}{1+\nu} \qquad (2)$$

By combining equations (1) and (2) for the plastic, we obtain the relation:

$$\frac{\delta_n}{2tC} = (\varepsilon_1 - \varepsilon_2)_p \frac{E_p}{1+\nu_p}$$

or

$$(\varepsilon_1 - \varepsilon_2)_p = \frac{\delta_n}{2tC}\frac{1+\nu_p}{E_p}$$

The plastic coating has exactly the same deformation as the specimen, i.e.,

$$(\varepsilon_1 - \varepsilon_2)_p = (\varepsilon_1 - \varepsilon_2)_s ,$$

so that the principal strain difference of the specimen can be expressed as:

$$(\varepsilon_1 - \varepsilon_2)_s = (\varepsilon_1 - \varepsilon_2)_p = \frac{\delta_n}{2tC}\frac{1+\nu_p}{E_p}$$

or

$$(\varepsilon_1 - \varepsilon_2)_s = \frac{\delta_n}{2tK} \qquad (3)$$

where

$$K = \frac{1+\nu_p}{CE_p}$$

K is called the strain sensitivity constant, whose value is generally specified by the manufacturer along with the thickness of the plastic.

The relative retardation δ_n can be expressed as

$$\delta_n = \lambda n$$

where λ is the relative retardation per fringe order and n is the fringe order. λ is a constant which has a value of 2.27×10^{-5} inch per fringe order for type M Photostress plastic. Hence, equation (3) can be rewritten into the familiar photoelasticity

equation:

$$(\varepsilon_1 - \varepsilon_2)_s = \frac{\lambda n}{2tK}$$

or

$$(\varepsilon_1 - \varepsilon_2)_s = \frac{Qn}{2t} \qquad (4)$$

where

$$Q = \frac{\lambda}{K}$$

Q is called strain optical coefficient. Since the plastic is following the deformation of the specimen, equations (3) and (4) should still hold true although the specimen is well beyond its elastic range. The high elongation birefringent plastic is still within its constant strain optical coefficient range, and the stress-strain relation is applied to the plastic only.

5.2 Experimental Apparatus

The Polarizing Instrument Company's regular eight-inch-field polariscope was used for birefringent coating studies. This regular eight-inch-field polariscope is primarily intended to be used with ordinary transparent photoelastic models. There is a focus lens in front of the illuminator to converge light into a columnated light beam. The light bulb socket, which is primarily fitted for a mercury vapor light bulb, can be replaced to accommodate a white light bulb for color fringes. Beyond the analyzer is a projection system so that the fringe pattern image can be projected on a screen or into a camera to be photographed. The columnated light source, polarizer, analyzer, quarter-wave plates, and projection system are each mounted on an individual stand. These may then be arranged in any fashion desired, if necessary.

5.3 Arrangement of Apparatus

The test specimen was mounted in the Dillon machine in the same way as when moiré method tests were conducted.

Due to the bulkiness of the polariscope, it could not be arranged with the polarizer and analyzer place side by side and still be close enough to the specimen without inducing a large incident angle. The incident angle is an important factor because it is assumed so small that it can be neglected in the development of the birefringent coating theory. The analyzer should be placed as close to the specimen as possible so that the specimen will show up in the photographed picture as large as possible for better resolution of the fringes.

To accomplish these factors, first a half-mirror was used. Figure 11 shows the arrangement of the reflection polariscope using a half-mirror. The columnated light source, polarizer, and quarter-wave plate were offset to one side making a 90-degree angle with the specimen. The polarized light was reflected 90-degrees by the mirror to shine on the specimen. Then it was reflected directly back from the specimen passing through the half-mirror, quarter-wave plate, analyzer, and into the camera. Ideally, this setup is perfect for use in the birefringent coating method because it eliminates the incident angle completely. However, the intensity of the light was cut down considerably by the half-mirror. When the polarized light was first reflected by the half-mirror, only half the light intensity was reflected

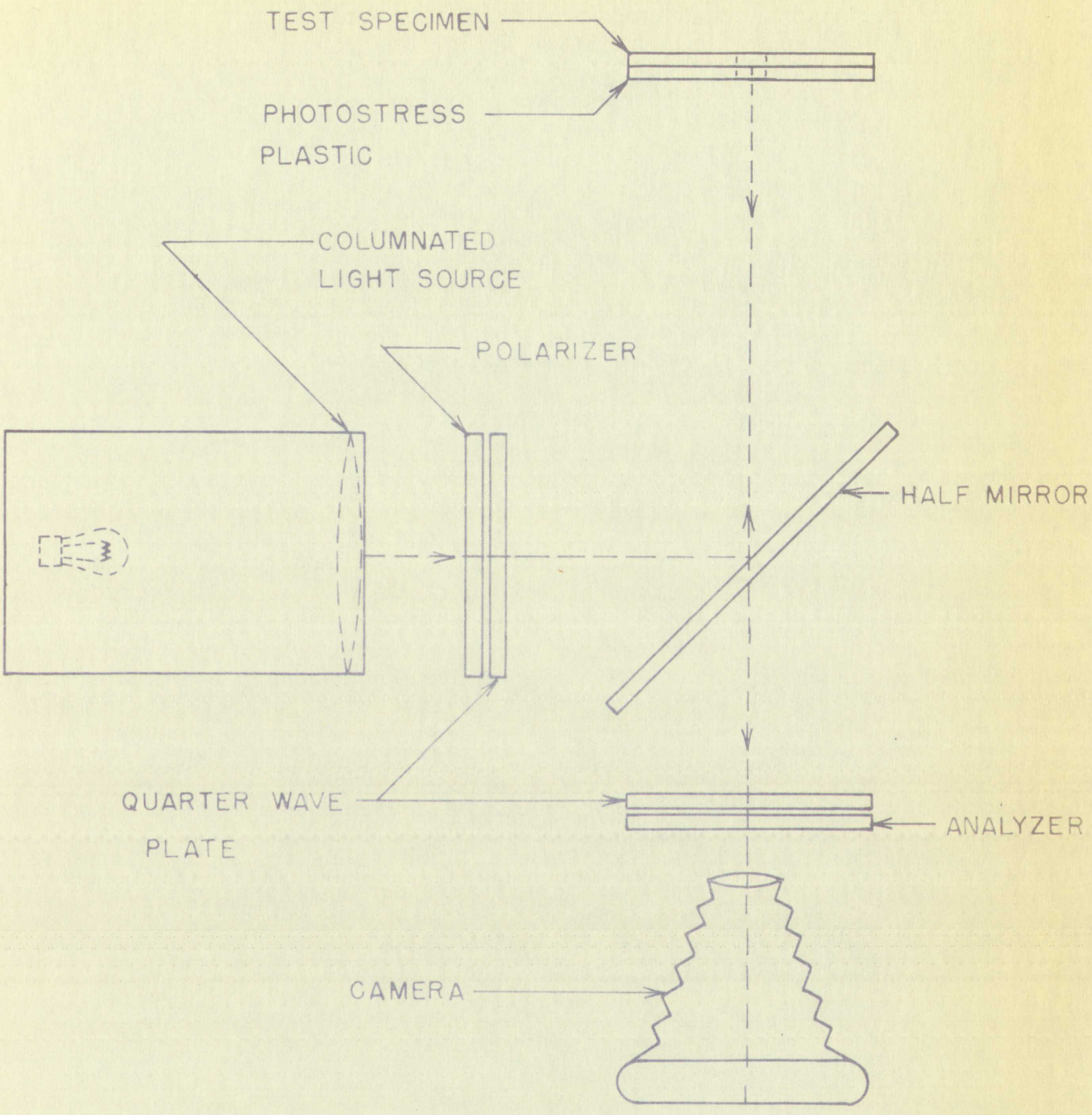

FIGURE II , PHOTOELASTIC EXPERIMENT WITH HALF MIRROR

to shine on the specimen. The other half of the light intensity was allowed to pass through the half mirror. Again, only half of the light intensity reflected back from the specimen passed through the half-mirror and into the camera, while the other half was reflected away. Therefore when the polarized light had reached the camera its intensity was almost reduced to a quarter of the original light intensity from the illuminator. Due to this reduction in light intensity, time exposure was needed to photograph the fringe pattern. For the type 47 Polaroid film, with an ASA speed rating of 3,000, ten to fifteen seconds were needed in order to get enough exposure for the picture. Since the specimen must be loaded continuously, (See previous section), the fringe pattern could very well have changed during this duration of time.

In order to get more light intensity, a full mirror was substituted for the half-mirror, and the polariscope was rearranged as shown in Figure 12. The polarized light was reflected by the full mirror to shine on the specimen at an angle. Then the light reflected from the specimen bypassed the mirror and went through the quarter-wave plate and analyzer into the camera. Although the light intensity had increased considerably, it still required five seconds for the film to be exposed. Finally, the blue filter had to be taken out of the light source in order to get enough light intensity for near instant exposure of the film.

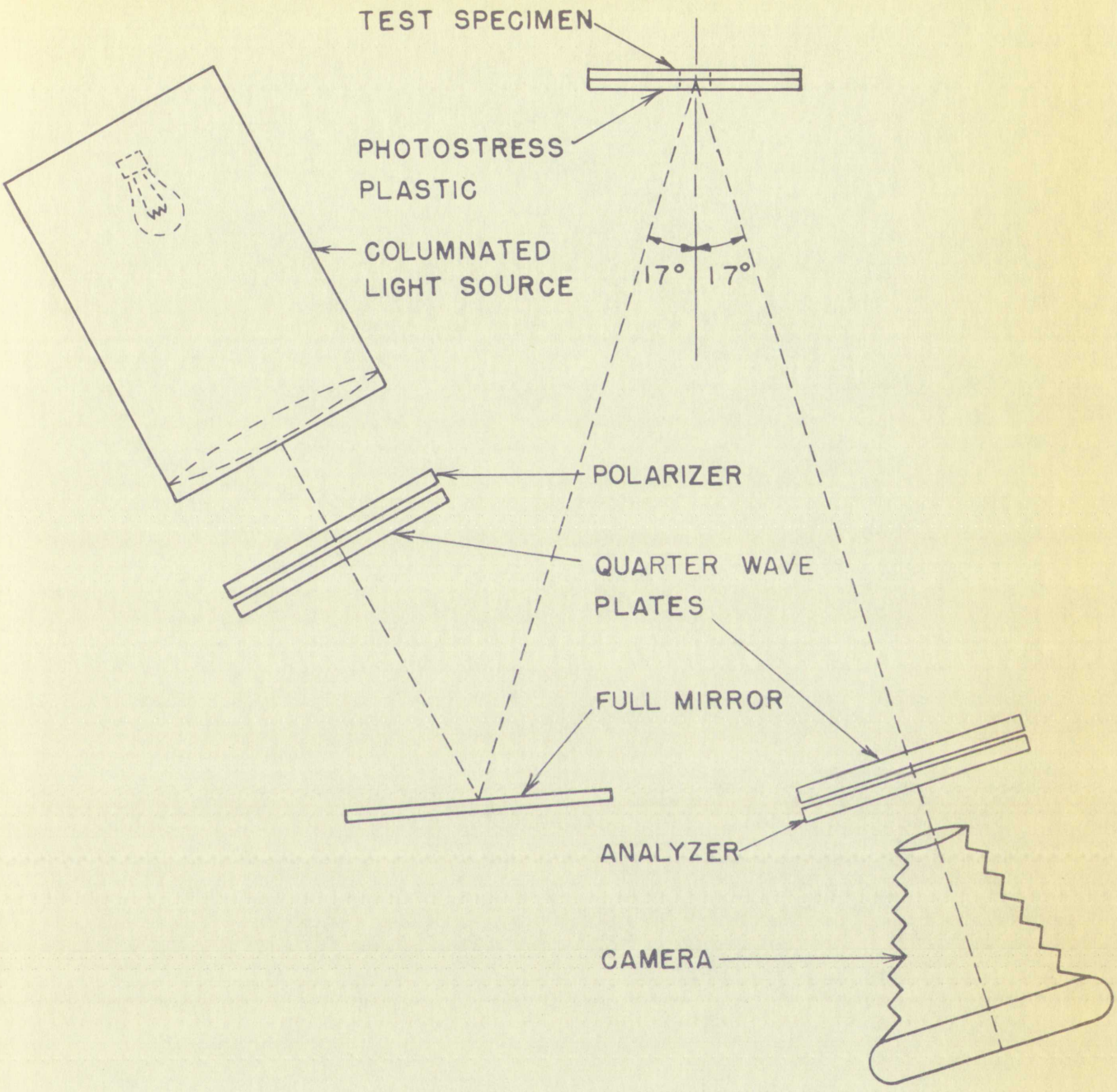

FIGURE 12 , PHOTELASTIC EXPERIMENT WITH FULL MIRROR

A test was conducted to check the effect on the fringes without the blue filter. It was found that there was no noticable distortion of the fringes without the flue filter. Hence, this final arrangement of the reflection polariscope was used for the tests.

5.4 Calibration of the Type M Photostress Plastic

The strain optical coefficient of the type M Photostress plastic was claimed to be constant up to from 30 to 50 percent elongation by the manufacturer. To check this, calibration tests were conducted on this plastic. It was found that the actual constant strain optical coefficient range of the plastic was only approximately 8 percent of elongation. Since this Photostress plastic was used on a tensile specimen, it was calibrated in tension.

The first calibration model designed was intended to be used with a white light source. The reason for using white light was so that better resolution might be obtained from the first three color fringes. The first model was a tapered specimen. It was coated with a sheet of type M plastic of 0.072 inch thickness. Three SR-4 type A-8 strain gages were mounted in the one-inch, two-inch, and three-inch sections of the model on the side opposite the plastic coating. (See sections A, C, and D of Figure 13b.) These gages were used to record strains at these three sections. It was hoped that the first three color fringes formed would be distributed across these sections.

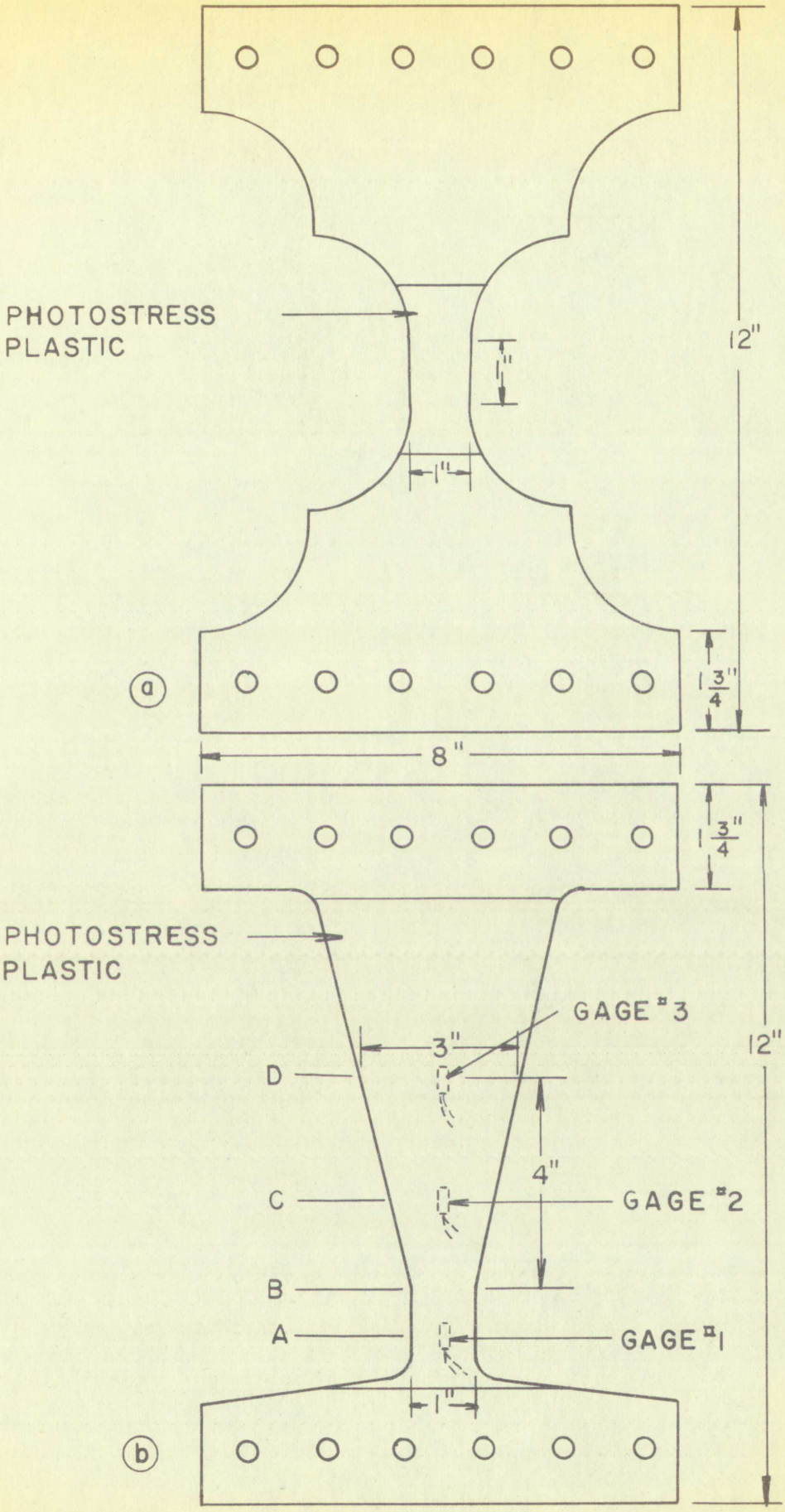

FIGURE 13 , PHOTOSTRESS PLASTIC CALIBRATION MODELS

However, due to the low sensitivity of this type M plastic, it would require a principal strain difference of approximately 10,400 μin/in, to produce the first fringe order. Since the yield strain of the aluminum model is only about 4,000 μin/in, it is well beyond its elastic region when the first full fringe develops. The one-inch section, having the smallest cross-section, reached its elastic limit first. Once the strain was in the post-elastic region it would keep increasing with only slight increase in load, while the tapered section of the model remained in the elastic range. As a result, a steep strain gradient existed in the section denoted "B", (See Figure 13b), and all of the photoelastic fringes accumulated there. Since these fringes were so close together, the resolution of the color fringes had no marked advantage over the monochromatic fringes. Besides, when color fringes were photographed with a color film, the resolution was further decreased, i.e., not all the hues of the color fringes showed up in the photograph. A 35 mm Nikon camera and Ektachrome color film were used.

The second calibration model was designed for monochromatic fringes only. (See Figure 13a). As before, it was coated with a piece of type M plastic. The moiré method was used to measure the strain corresponding to each fringe order of the plastic. A 200 lines per inch screen was printed on the surface of the model opposite the photoelastic coating. The model was mounted in the Dillon machine and subjected to tension.

A reflection polariscope equipped with a camera was placed in front of the plastic coating. On the opposite side a light source and camera were mounted to photograph the moiré fringe pattern. A picture was taken when each photoelastic fringe order had formed in the coating. The corresponding moiré fringe pattern was also photographed so that each photoelastic fringe order could be related to the strain required to produce it. Both cameras used were Polaroid Land type, and the film used was the type 47 Polaroid film with an ASA speed rating of 3,000. This calibration test was run until rupture of the aluminum model occurred.

A fringe order versus principal strain difference curve was plotted from the results of this test. This curve clearly shows that the constant strain optical coefficient range of the type M plastic is well below the 30 percent claimed by the manufacturer. The actual maximum value was about 8 percent of elongation; beyond that the strain sensitivity constant K drops sharply. The strain versus fringe order plot is shown in Figure 14. However, the K factor calculated from the straight portion of the curve checked with the value given by the manufacturer, 0.015 for the type M plastic with a thickness of 0.072 inch. Due to the fact that the K factor is not constant the calibration curve was used to convert fringe orders to strain readings instead of using a single K value.

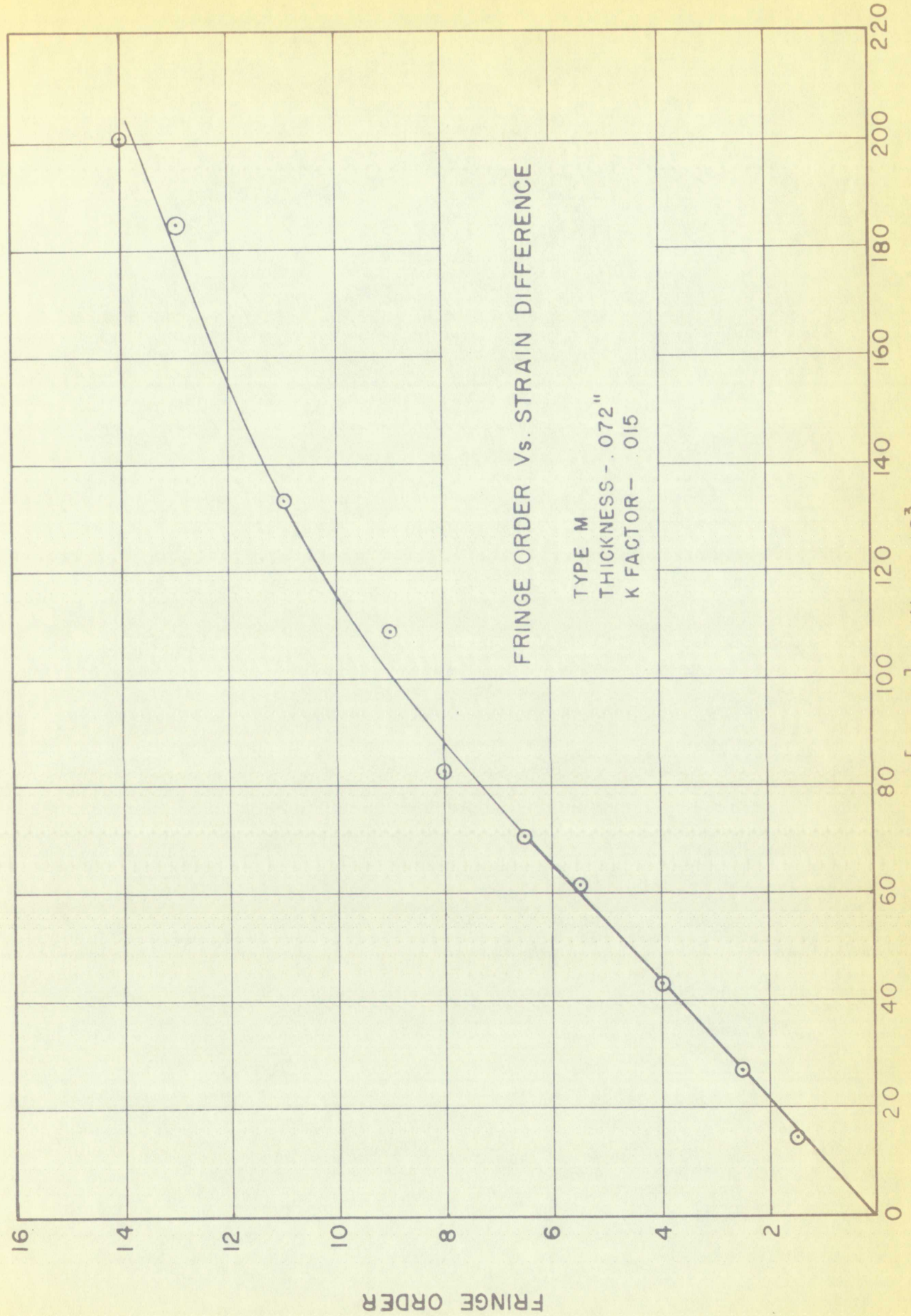

FIGURE 14 PHOTOSTRESS PLASTIC CALIBRATION CURVE

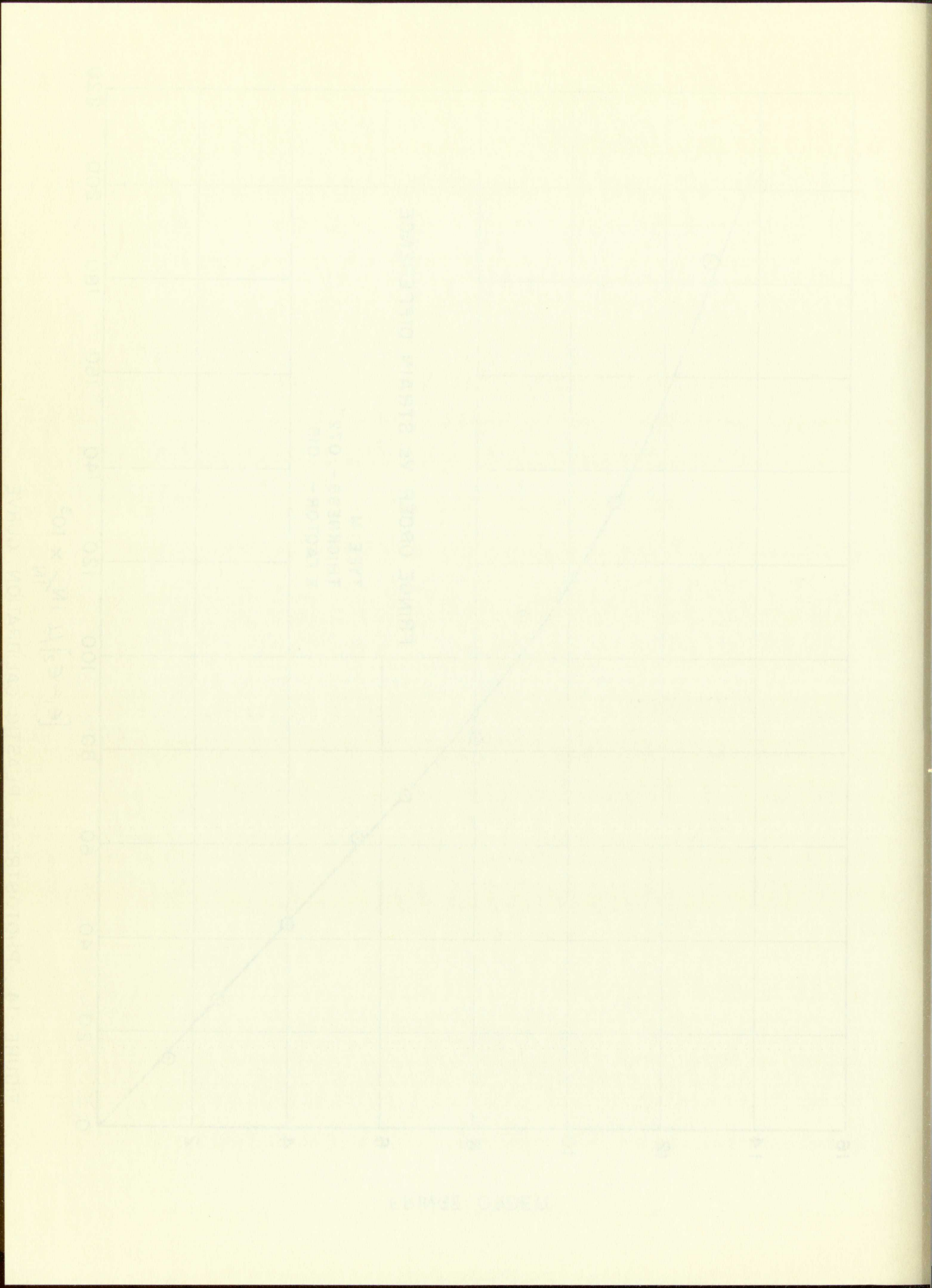

5.5 Preliminary Investigations

5.5.1 Strain distribution in the neighborhood of a crack-- Due to the difficulty of finding a birefringent plastic that would develop a crack following exactly the one developed in the metal, a test specimen was designed to check the effect on the strain distribution if the plastic does not develop a crack following that in the metal. The test piece consisted of a tension plate with a central hole which had two artificial cracks cut at each side to one radius length of the hole. The width of each crack was about 0.015 inch. After a birefringent coating was bonded to the specimen, an artificial crack was cut in the plastic directly over one of the cracks in the metal so that the crack in both plastic and metal had the same form. Over the other crack the plastic was left uncut, so that the discontinuity was in the metal only.

This test piece was loaded until three or four fringes had formed in the plastic. A picture of the fringe patterns developed around the cracks was taken for analysis. The picture of the fringe pattern is shown in Figure 15.

5.5.2 Accuracy check of coating by strain gages -- The purpose of using strain gages was to check the accuracy of the birefringent coating readings. Ten variable resistant strain gages were mounted on the surface of the specimen opposite the coated surface. The arrangement and locations of the gages are shown in Figure 16. These gages were the Budd Company Metalfilm C12-111 strain gages, which have a 1/16-inch gage length.

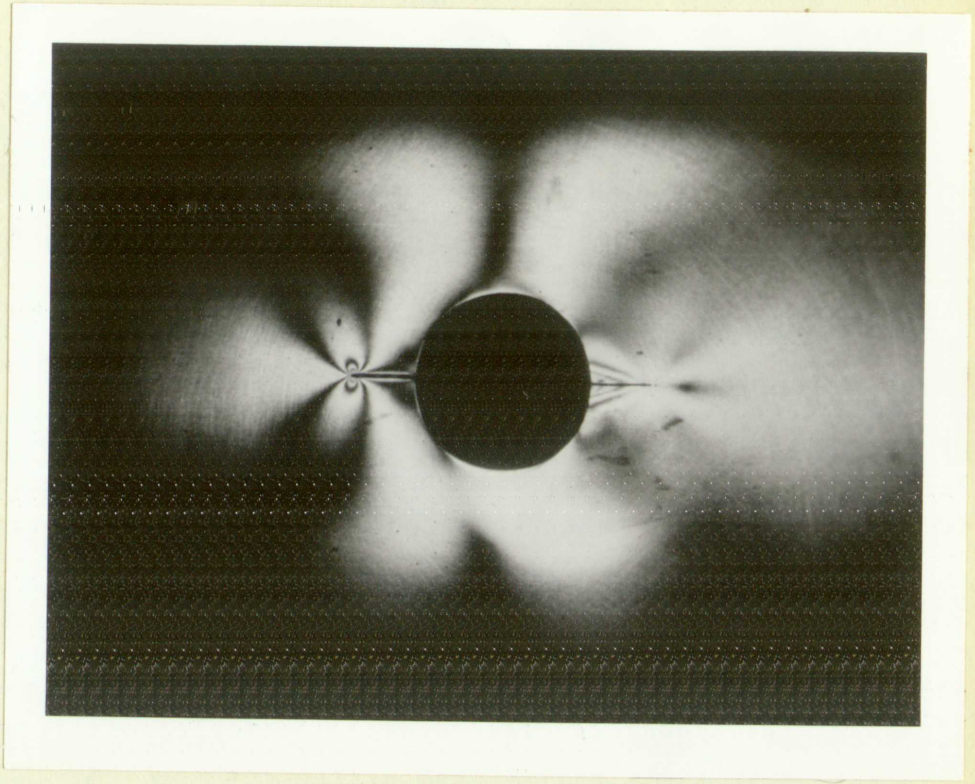

FIGURE 15, BIREFRINGENT PATTERN SHOWING EFFECT OF COATING ON CRACK IN METAL SPECIMEN

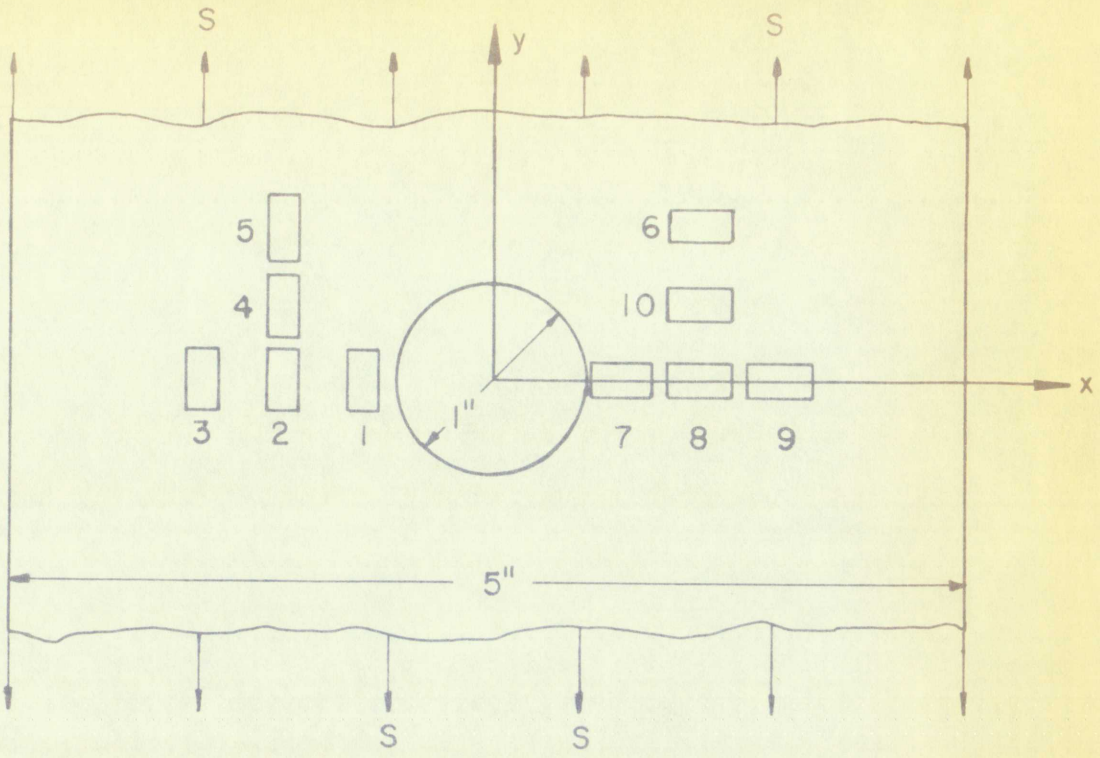

GAGE		POSITION	
LONGITUDINAL	TRANSVERSE	X	Y
1	7	0.5426"	0
2	8	0.7521"	0
3	9	1.0147"	0
4	10	0.7521"	0.2906"
5	6	0.7521"	0.5811"

GAGES ARE BUDD METALFILM - C12 - 111

GAGE RESISTANCE - 120 OHMS

GAGE FACTOR - 2.02

FIGURE 16 , GAGE POSITIONS IN PHOTOELASTIC EXPERIMENT

The gage resistance and gage factor are 120 ohms and 2.02 respectively. The gages along the x-axis in both transverse and longitudinal directions were used to check the accuracy of the plastic. The rest of the gages were used to check the strain distribution.

All ten of these gages were connected to the ten channel, individual bridge board with a common power supply, (See Figure 17). The outputs of these ten bridges were fed into the CEC recording oscillograph, so that a continuous record of the output could be obtained. The two gages mounted on the pull bar were connected to the two opposite arms of a bridge circuit, (See Figure 18), to serve as a load transducer. The load transducer output was also fed into the recording oscillograph. A marking trace was also devised for the oscillograph record so that the strain and load outputs could be synchronized with the photographed fringe pattern. The ten channel, individual bridge board was first powered by a Hewlett Packard Model 712B power supply. Since this is a high voltage, low current power supply, a stable constant current supply to the bridge board could not be obtained from this unit when used at low voltage. Therefore it was replaced by a six-volt wet cell battery.

A preliminary test was conducted. The specimen was loaded just below the elastic limit of the metal. The outputs of the gages were recorded so that they could be compared to theory to check the accuracy of the gages. After the accuracy of the gages had been checked, the specimen was loaded beyond its

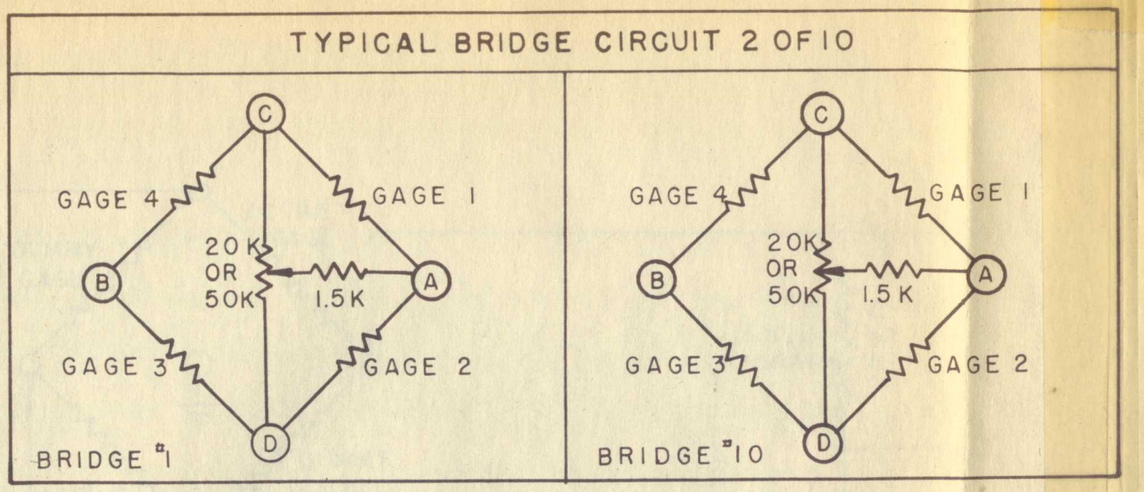

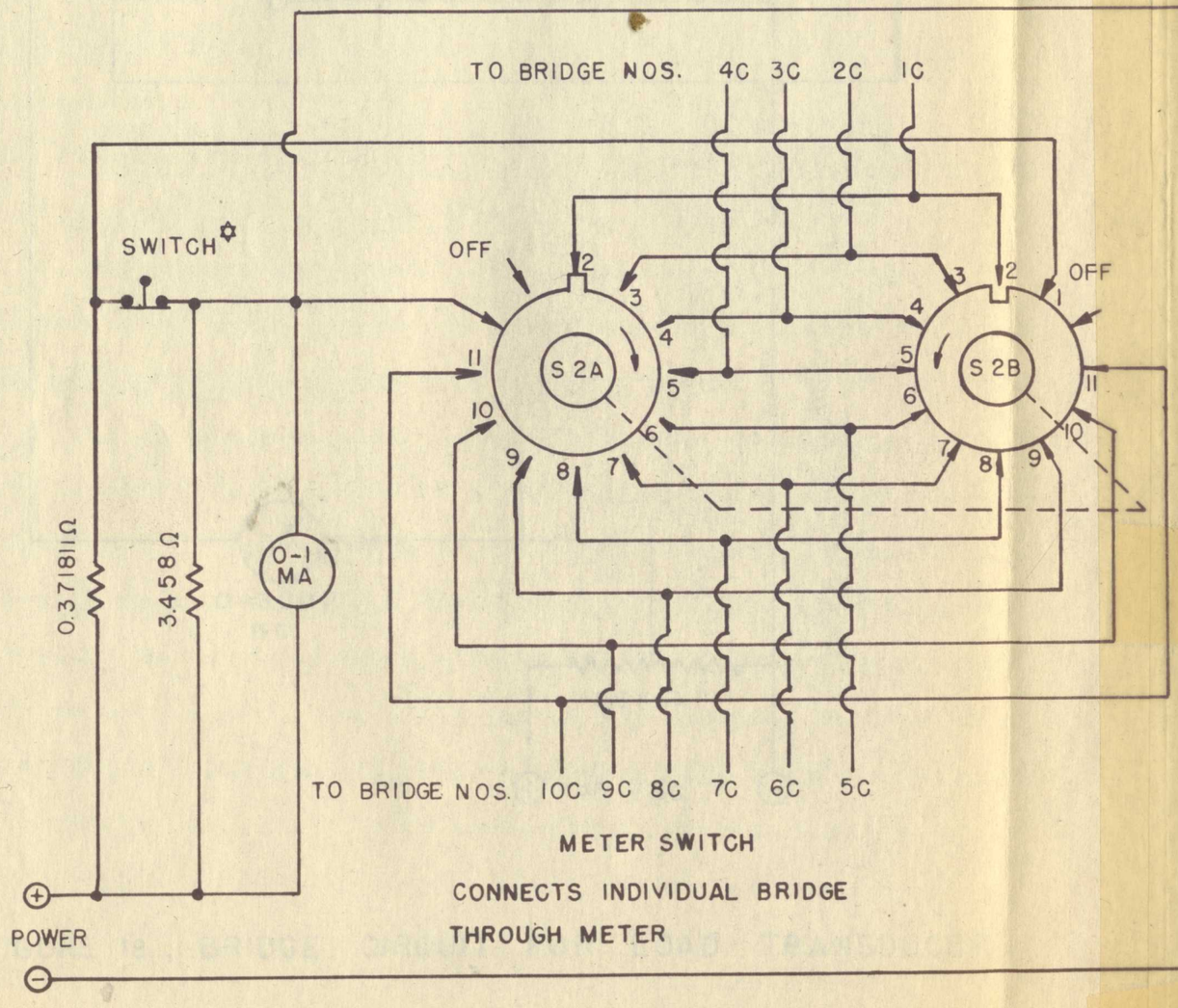

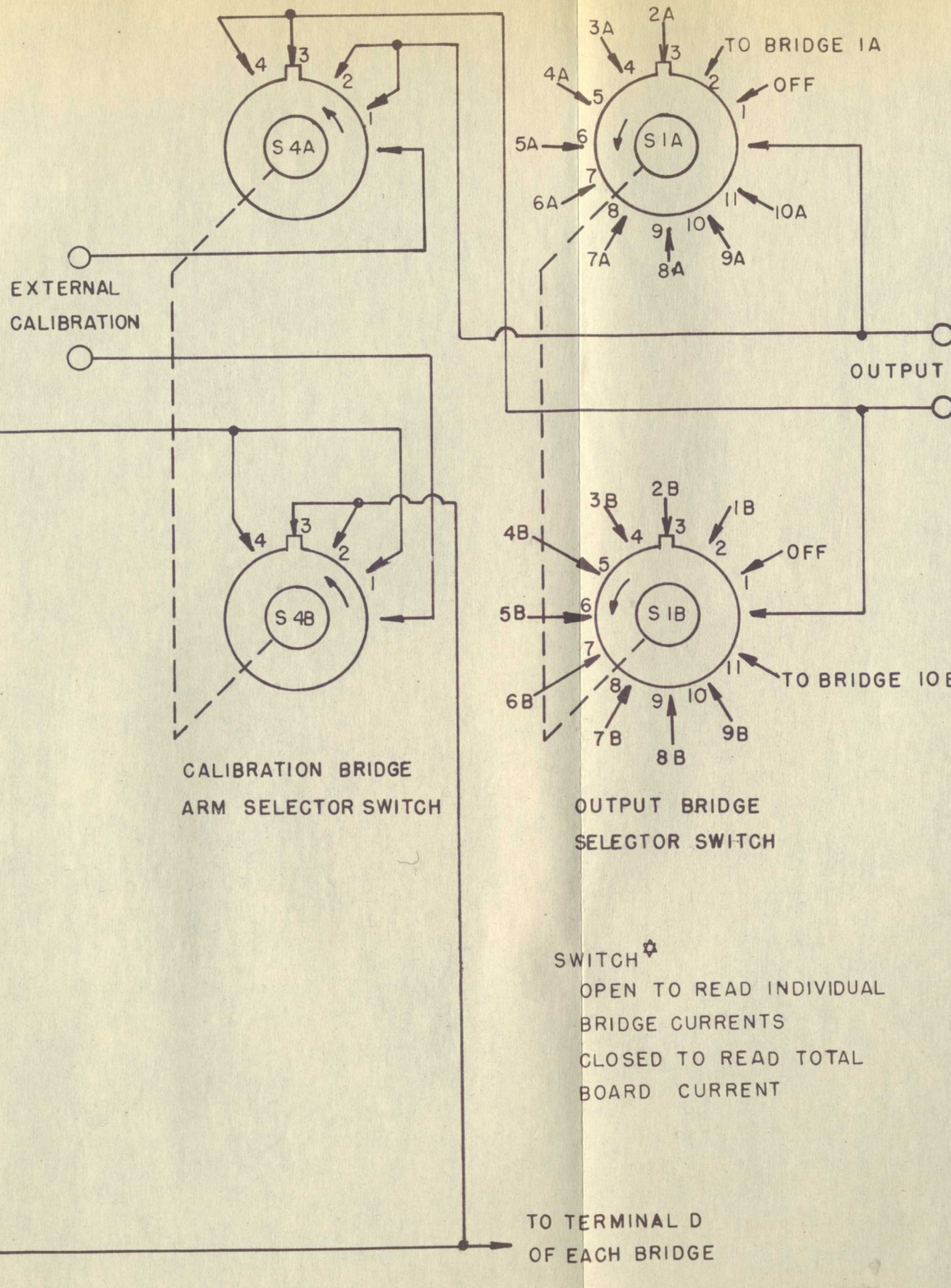

FIGURE 17 ,TEN CHANNEL, INDIVIDUAL BRIDGE BOARD WITH COMMON POWER SUPPLY

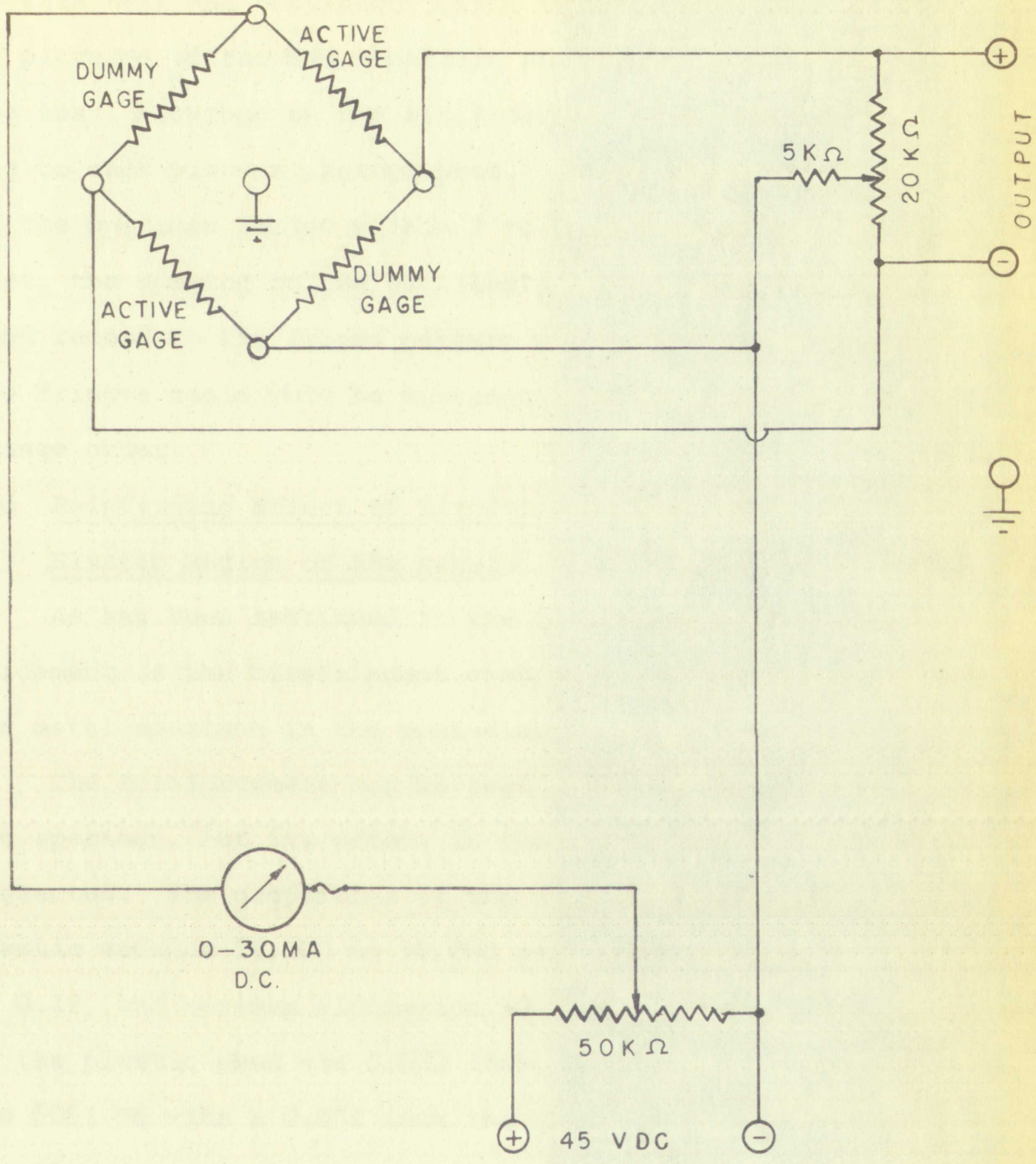

FIGURE 18, BRIDGE CIRCUIT FOR LOAD TRANSDUCER

elastic limit to check the accuracy of the coating. The loading in this test was continuous until rupture occurred. A sequence of pictures of the fringe pattern was photographed throughout the test. Markings on the oscillograph record were made corresponding to each picture photographed. It was found that all the gages on the specimen failed within 2 to 3 percent of strain. Beyond that, the marking on the oscillograph were used for relating load record to the fringe pattern photographed. It was found that the fringes could only be distinguished up to the sixteenth fringe order.

5.6 Reinforcing Effect of Birefringent Coating in the Post-Elastic Region of the Metal

As has been mentioned in the literature review, the reinforcement of the birefringent coating has a pronounced effect on the metal specimen in the post-elastic range.

The reinforcement may be negligible in the elastic range of the specimen, but its effect in the post-elastic range cannot be neglected. The properties of the type M Photostress plastic are: elastic modulus 25,000 to 30,000 psi, K factor 0.02 for thickness of 0.12, and maximum elongation 30 to 50 percent. The thickness of the plastic used was 0.072 inch. The aluminum specimen used was 6061-T6 with a 0.032 inch thickness. The reinforcement in the elastic range of the specimen was calculated using the correction factor equation for plane stress problem:

$$\frac{1}{C} = 1 + \frac{t_c E_c}{t_s E_s}$$

and

$$(\varepsilon_1 - \varepsilon_2)_s = \frac{1}{C}(\varepsilon_1 - \varepsilon_2)_c$$

It was found that C = 0.9933 with the elastic modulus of the plastic at 30,000 psi and 10,000,000 psi for the aluminum specimen. However, the reinforcement increases progressively with the post-elastic strain in the specimen. Figure 19 clearly shows the effect of the coating on the specimen in the post-elastic range. This picture was taken from a specimen 1.5 inch wide and 10 inches long with a 3-inch long strip of plastic bonded to the central portion of the specimen. The thicknesses of the plastic and specimen were mentioned above. A 200-line per inch model screen was lighographically printed on the opposite surface of the specimen. At the center of the picture the moiré fringes are farther apart. This is due to the reinforcing effect of the bonded coating on the opposite surface of the specimen. In the regions outside the bonded coating area, top and bottom of the picture, the moiré fringes are much closer together. The applied stress was about 38,000 psi. The measured longitudinal strain was 31, 460 μin/in for the uncoated part and 11,212 μin/in for the coated part of the specimen. It was found that C = 0.3564 or that the measured strain of the coated part was about 64.36 percent lower than the uncoated part. Since the thicknesses of the plastic and the aluminum specimen were kept constant in this test, it is the belief of this author that reinforcing effect is mainly dependent on the tangent modulus of the specimen in the post-elastic range.

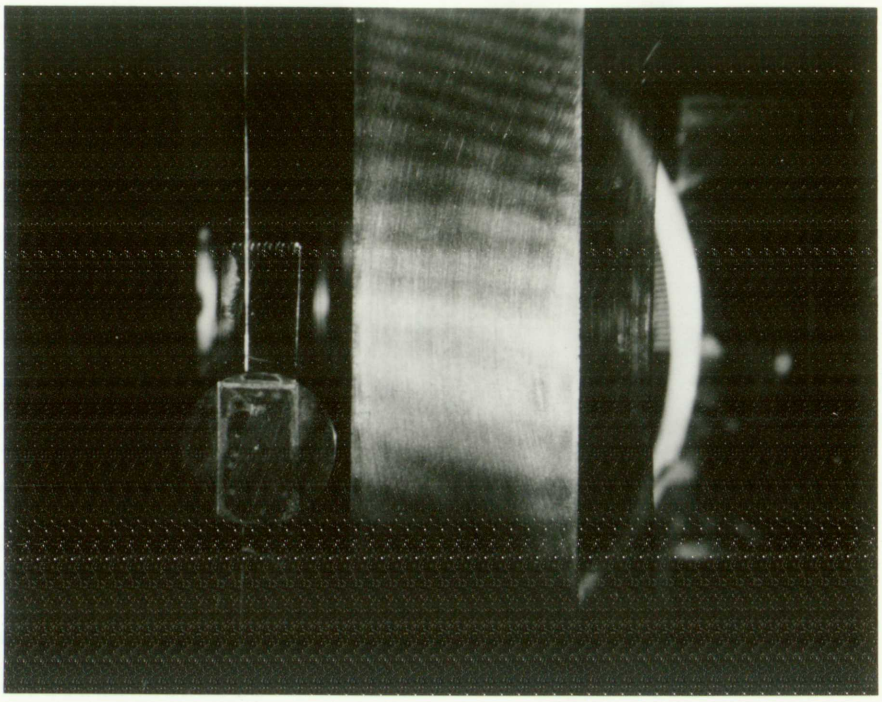

FIGURE 19, MORIÉ FRINGES SHOWING REINFORCING EFFECT OF TYPE M PLASTIC, t= 0.072", ON SPECIMEN

Another important factor is how this reinforcing effect of the plastic in the post-elastic range of the metal affects the strain distribution. The comparison was made on pictures of the moiré fringe patterns taken from specimens with and without a birefringent coating, (See Figure 20). The basis of comparison was to obtain the same longitudinal strain at a reference point on both the coated and uncoated specimens. The reference point was located at the edge of the hole where there was the highest strain concentration. A sequence of pictures of the fringe patterns in the coated specimen was first photographed. The fringe spacing at the reference point was measured for each picture of the fringe pattern. Then a divider was set at that fringe spacing. When the uncoated specimen was tested, the divider was placed against the reference point on the specimen. As soon as the fringe spacing at the reference point of the uncoated specimen had reached the spacing set in the divider, a picture of the fringe pattern was photographed. Due to the nature of testing, it was impossible to obtain pictures of the coated and uncoated specimens with exactly the same strain at the reference point. Therefore, a sequence of pictures was taken. Then the set of pictures of the coated and uncoated specimens with the fringe spacings at the reference closest together was chosen for comparison. A quick qualitative comparison can be made by observing the fringe patterns of the coated and the uncoated specimens. The greatest distinction is shown on the fringes produced by transverse strains, i.e.,

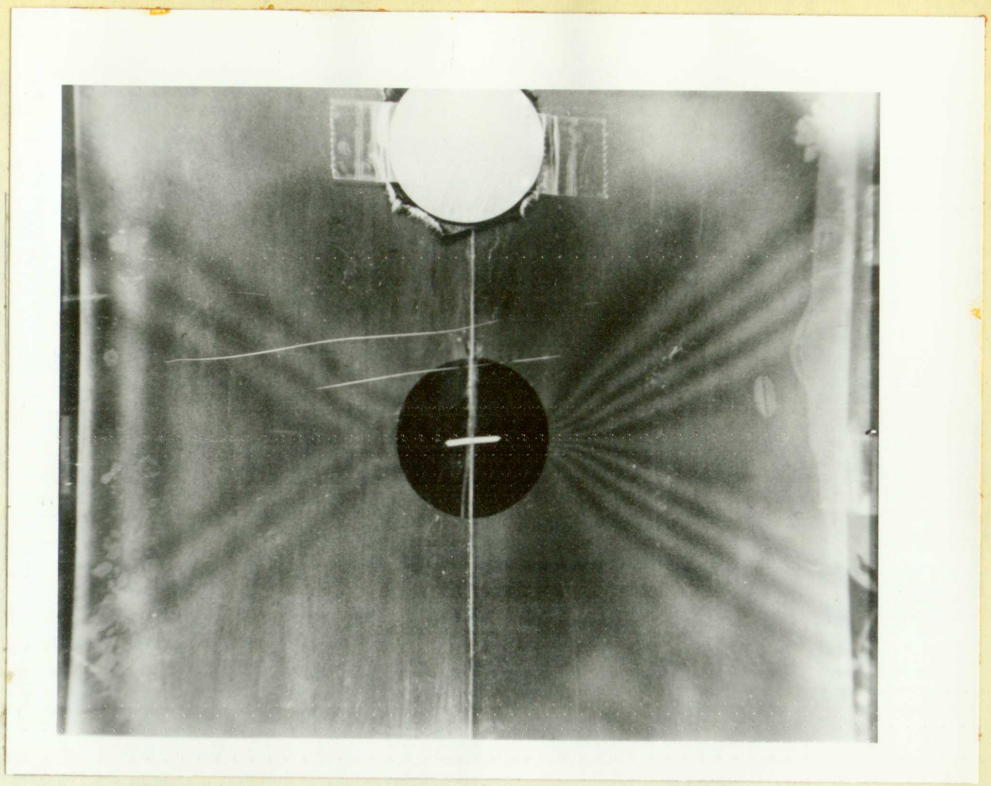

(a) UNCOATED SPECIMEN P = 5,676 Lb

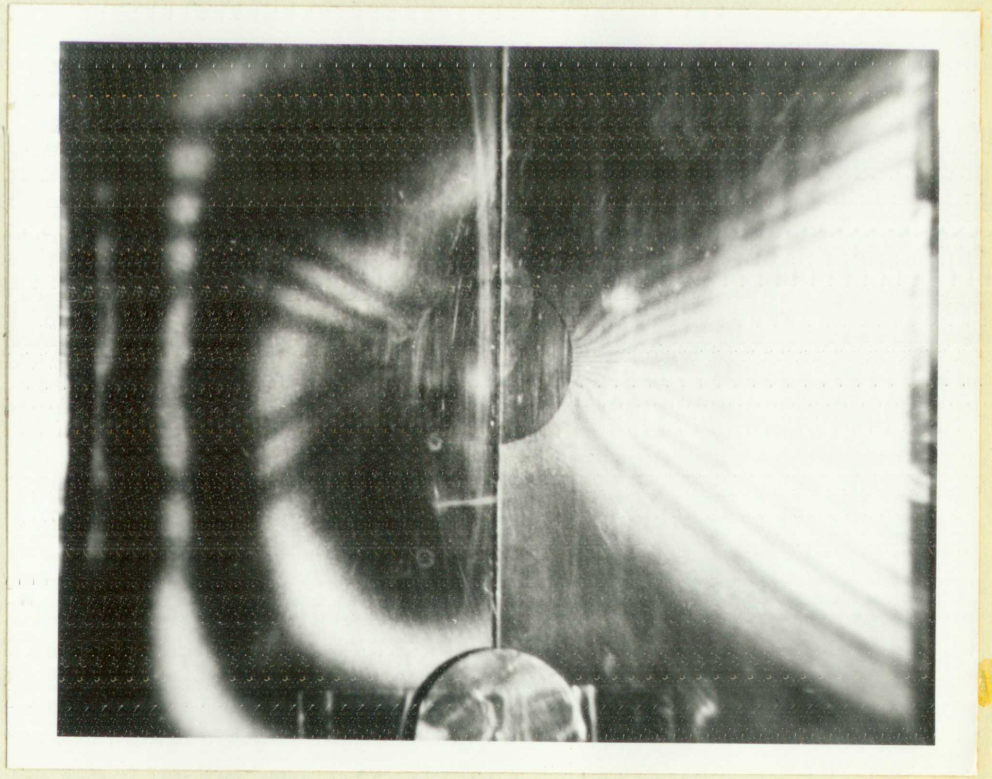

(b) COATED SPECIMEN P = 5,820 Lb

FIGURE 20, MORIÉ FRINGE PATTERNS OF THE COATED AND UNCOATED SPECIMENS

the left half of the pictures in Figure 20. The fringes of the coated specimen had rotated more than 90 degrees from the longitudinal direction near the outer edge of the plate. Evidently, this was due to rigid body rotation on the part of the specimen induced by the coating. This phenomenon did not occur in the uncoated specimen. The second noticable point from the pictures is that the strain gradient across the specimen is much higher on the uncoated specimen than on the coated specimen. This can be verified by the fact that the fringe spacings, produced by longitudinal strains, are farther apart near the outer edge of the uncoated specimen. Figures 21 and 22 show the comparison of longitudinal strain distributions along longitudinal lines located one inch and one-and-one-half inches from the edge of the hole. These curves show clearly that the coating does affect the strain distribution in this specimen.

The reinforcement of the plastic not only affects the strain distribution but, in addition, since the plastic carries a portion of the applied load, it also holds the specimen together and allows the plastic strains to flow to a much higher elongation before rupture. It was observed in these tests, that a crack formed in the plastic first. The crack in the specimen followed that in the plastic. The series of pictures, shown in Figure 23, show the crack propagation in coated specimen. Once the crack had started to propagate, the loading was stopped. It was observed that when the cracks in coated specimen had

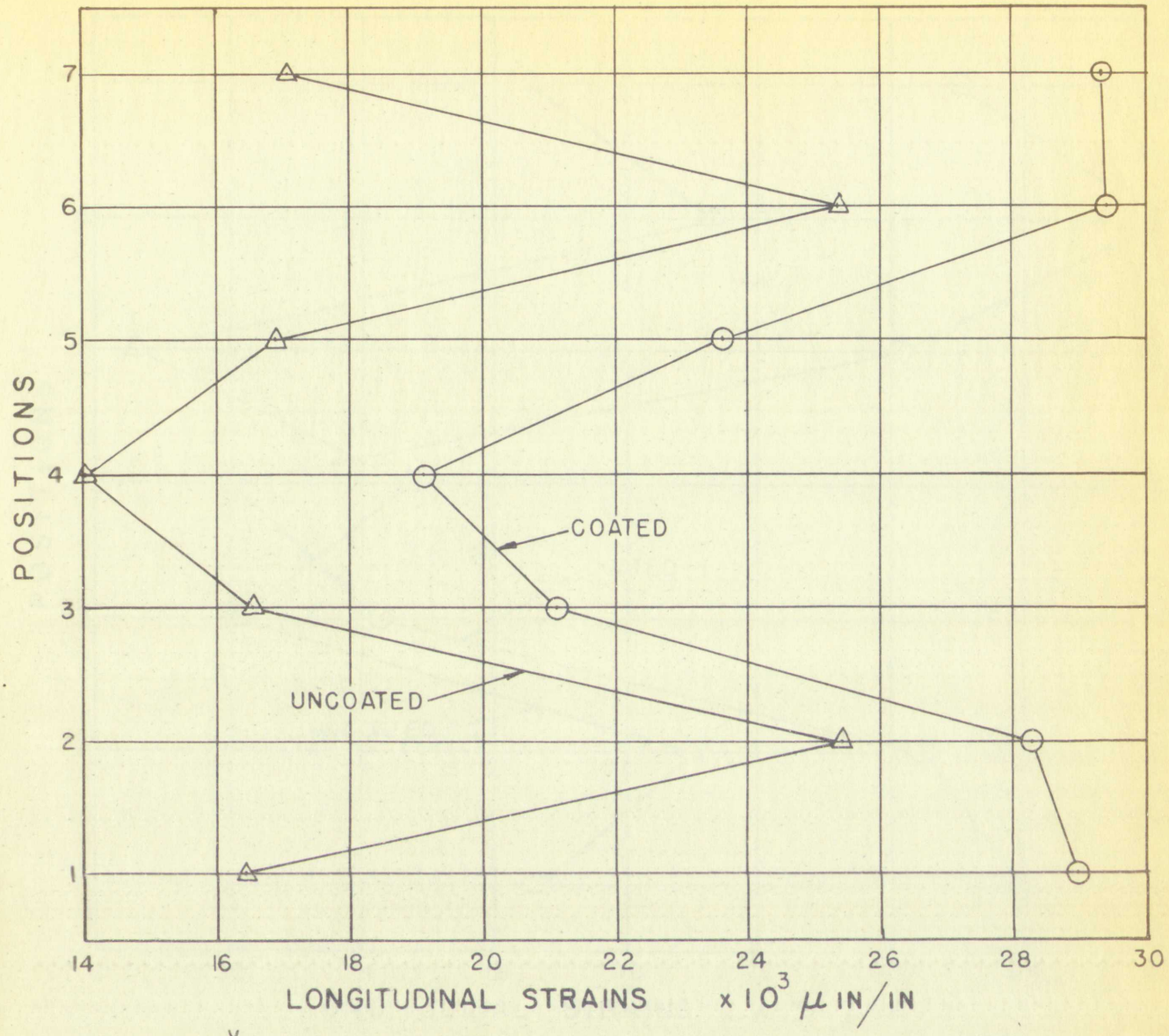

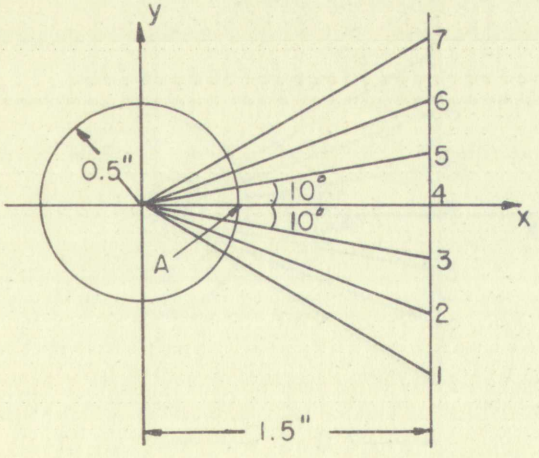

STRAINS AT REFERENCE POINT "A"

COATED = 177,630 μ IN/IN

UNCOATED = 164,375 μ IN/IN

APPLIED LOAD

COATED = 5,820 Lb

UNCOATED = 5,676 Lb

FIGURE 21 , STRAIN DISTRIBUTIONS OF COATED AND UNCOATED SPECIMENS

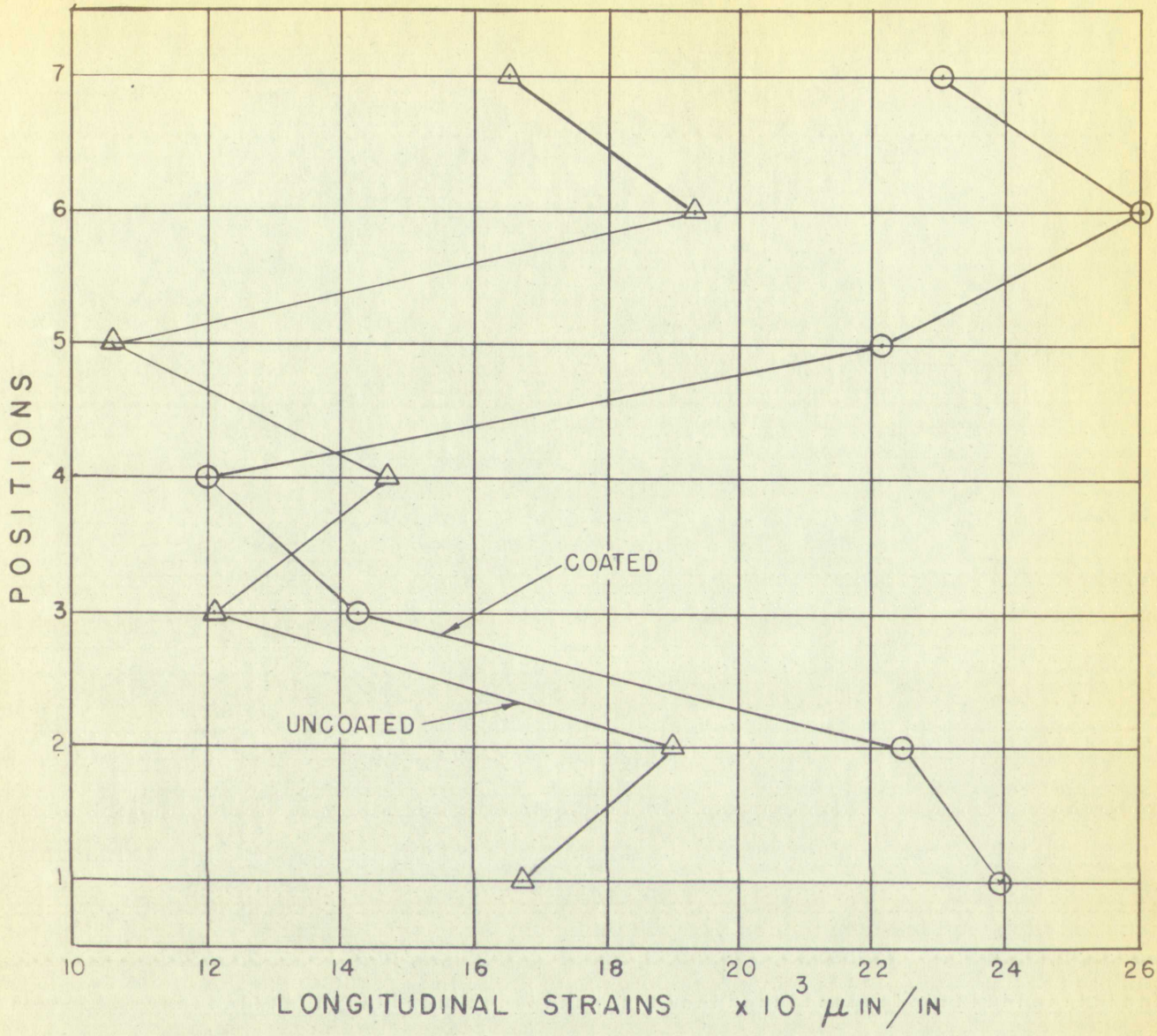

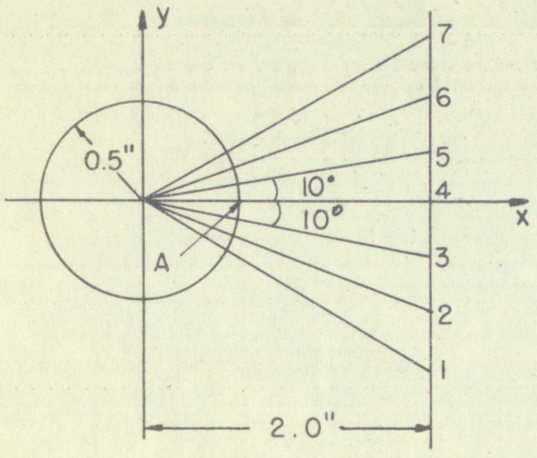

STRAINS AT REFERENCE POINT "A"

COATED = 177,630 μ IN/IN

UNCOATED = 164,375 μ IN/IN

APPLIED LOAD

COATED = 5,820 Lb

UNCOATED = 5,676 Lb

FIGURE 22, STRAIN DISTRIBUTIONS OF COATED AND UNCOATED SPECIMENS

(a) CRACK HAS FORM IN THE PLASTIC COATING AT P= 5,663 Lb

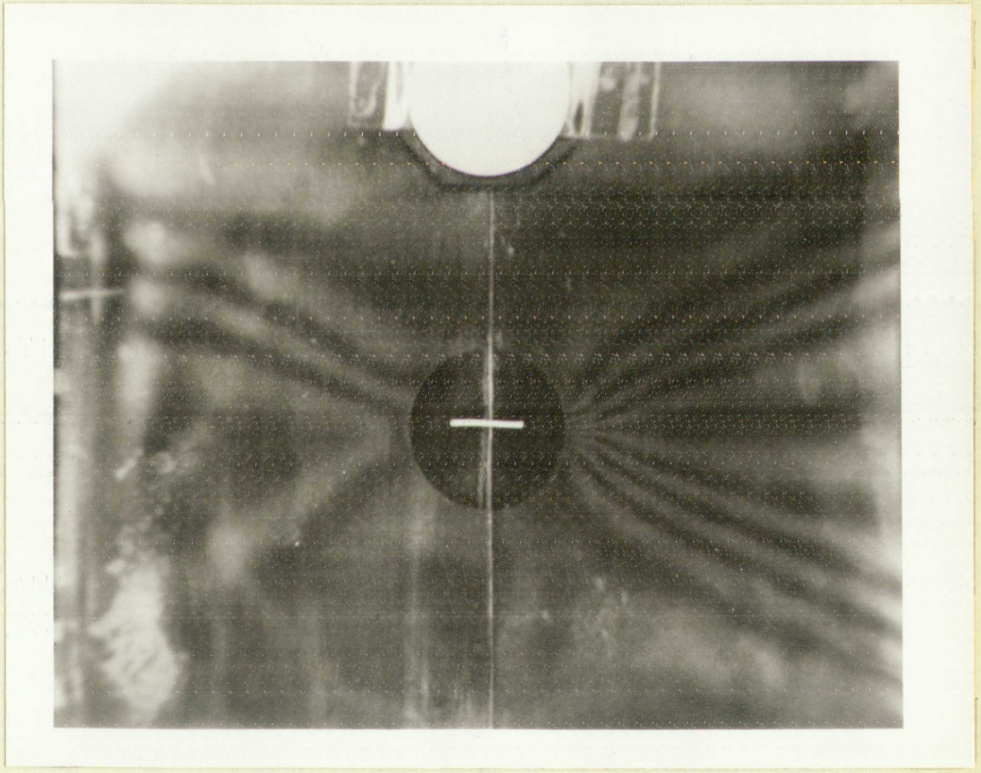

(b) TAKEN AT THE SAME INSTANT AS FIGURE (a) ABOVE, ON THE OPPOSITE SIDE OF SPECIMEN

FIGURE 23, SEQUENCE OF PICTURES SHOWING EFFECT OF COATING ON CRACK PROPAGATION IN SPECIMEN

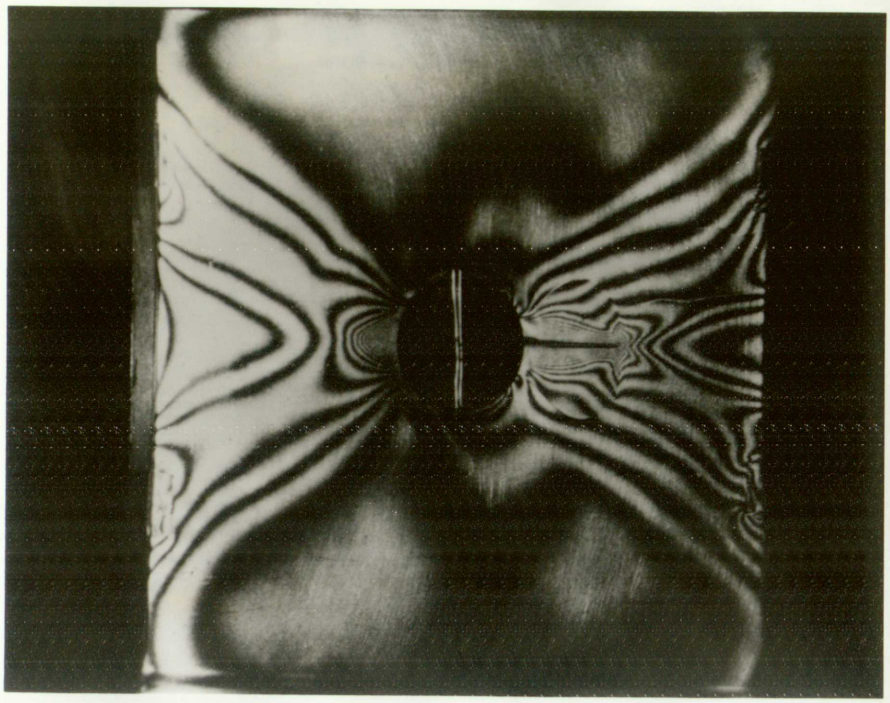

(c) CRACK HAS FURTHER PROPAGATED THROUGH THE BIREFRINGENT COATING P = 4,504 Lb

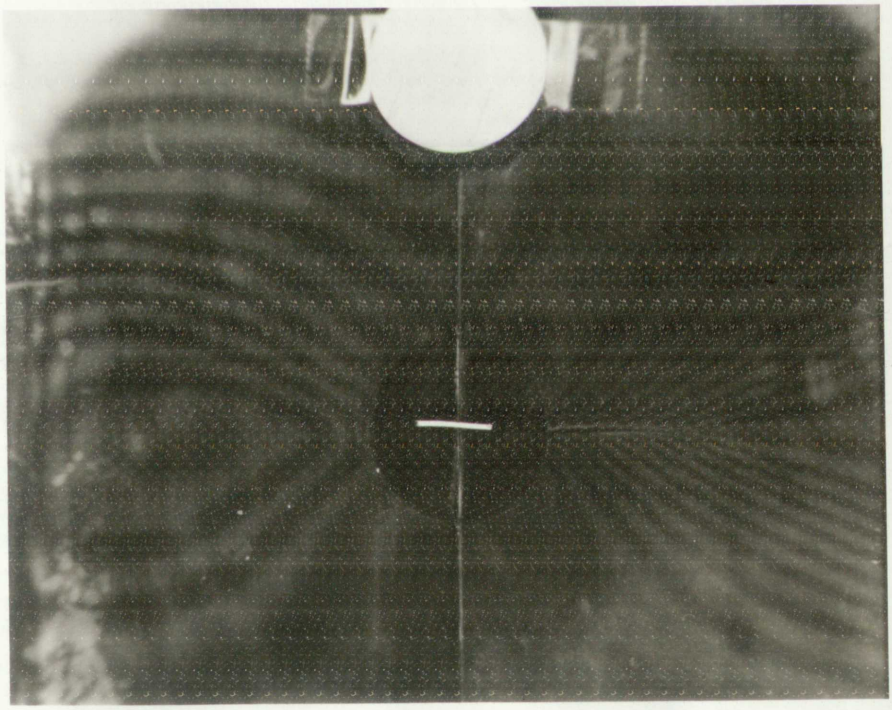

(d) CRACK IN SPECIMEN HAS FOLLOWED THAT OF THE COATING P = 4,504 Lb

FIGURE 23 , CONTINUED

propagated to about one diameter length of the hole, the cracks stopped for a few seconds. Then the crack continued to propagate through the whole width of the specimen. Therefore, it was possible to use the Polaroid camera to photograph the cracks. However, once the cracks had started in an uncoated specimen, the cracks would not stop until final rupture of the specimen. Also the crack propagation rate increased as the crack length increased. The cracks of the uncoated specimen were propagating at such a high speed that even with the Fastax camera running at about 1200 frames per second only a few frames recorded the crack growth. The crack propagating phenomenon of the coated and uncoated specimens can be explained by the strain energy principle. Evidently, when a crack has occurred in the coating, it has released enough strain energy in the specimen so that the crack would stop growing until the strain energy has built up to its maximum again. In the uncoated specimen the cracks in the metal do not release enough strain energy for the cracks to stop propagating.

5.7 Data Reduction

Reducing the photoelastic fringes into strains involves a very simple method. By knowing the fringe order, the principal strain difference can be calculated by the equation:

$$\varepsilon_1 - \varepsilon_2 = \frac{Q n}{2 t}$$

where "t" is the thickness of the photoelastic coating, "n" the fringe order, and "Q" the strain optical coefficient.

Q is computed from the equation

$$Q = \frac{\lambda}{K}$$

where λ is a constant and equal to 2.27×10^{-5} inch per fringe order, and K is the strain sensitivity constant which is generally given by the manufacturer accompanying the plastic.

Another method is to calibrate the photoelastic coating. The fringe orders are plotted against the measured principal strains difference; then this calibration curve will be used to relate fringe order into principal strains difference.

The latter method was used in this thesis for the following reason; it had been found out during the calibration that the strain optical coefficient 'Q' was not constant throughout the range claimed by the manufacturer. In this region where the strain optical coefficient "Q was not constant the above equation would no longer hold true. Instead the calibration curve was used for strain reduction.

The principal strain directions could be obtained from the isoclinic lines of the photoelastic method. However, this method could not be used for our problem. Since the specimen was loaded continually, it was impossible to obtain the isoclinic lines under such condition.

5.8 Estimate of Error

The greatest error of the birefringent coating method is introduced when interpolating the fractional fringe between two full-order fringes. The linear interpolation method was used

to determine the fractional fringes. Since the strain difference between two full fringe orders is 10,400 μin/in for the type M photostress plastic, the error can be quite large. The accuracy also depends on the linearity of the strain gradient in the specimen. The more the strain gradient approaches a straight line, the more accurate the linear interpolation method is. When the strain gradient deviates from linearity, the error introduced by the linear interpolation method can be very serious. The percentage of error at low-fringe order region would undoubtedly be much higher than that at region with higher fringe order. The maximum error introduced by this linear interpolation method was estimated to be approximately from 8 to 10 percent. Another error might be introduced when locating the center of the full fringe order. The percent of error is about the same as that of the moiré method. It is about $\pm$ 3 percent when the picture is enlarged to twice the normal size of the specimen. Thus, the total additive error introduced from the firefringent method in strain reduction could be as high as 10 to 12 percent.

6.0 THE COMBINATION WHOLE-FIELD METHOD

The separation of principal stresses or strains using one experimental method had always involved a very complicated, time consuming, if not difficult, procedure. For example, using the photoelastic method, it would require either the relaxation method or the equation of equilibrium method, to be combined with the isoclinic lines, or the oblique incidence method to determine the principal stresses or strains. Using the moiré method to determine the principal strains would require that the shearing strain must also be known. However, the shearing strain obtained from the moiré fringes have very poor resolution because it must be separated from the effect on the fringes due to rigid body rotation. The amount of rigid body rotation which is usually an unknown quantity in a specimen would render the shearing strain obtained from the moiré fringes useless. The combination whole-field method is therefore designed to combine the characteristic information from the moiré fringe and birefringent coating experiments to separate the principal strains. The birefringent method determines the magnitude of the difference between the principal strains; while the moiré fringe method will yield the value of the dilatation. Therefore, it is possible to devise an experiment which combines both methods to determine the principal strains. The measurement of dilatation or sum of normal strains in orthogonal directions of a plane stress problem is quite simple if the test specimen has an axis

of symmetry. Two moiré model screens can be arranged on both sides of the axis of symmetry to measure strains of two orthogonal directions. When symmetry is not present, two specimen under identical loading would be needed to measure strains in two directions.

Two types of test models were designed for this combination of whole-field method. One of the models was a transparent plastic model. The other model was made of aluminum plate. The design of models and test procedure are explained in the following subsections.

6.1 Adiprene Plastic Model

To investigate the possibility of applying the above mentioned method, an Adiprene plastic was used to model the tension plate. Properties of the Adiprene plastic can be found in Appendix C. The dimensions of the model were as shown in Figure 24. On each side of the center line two screens of 200-lines per inch were printed on the model by means of the lithographic printing method. The screens were arranged perpendicular to each other with one set of the model screen lines parallel to the direction of loading.

The specimen was mounted and loaded in a dead weight loading frame. Then the whole setup was placed in a polariscope, and the image of the fringe pattern (either moiré or photoelastic fringe pattern) was projected into a Polaroid camera. When the moiré fringe pattern was being photographed, only the master screen was mounted against the model screen on the specimen

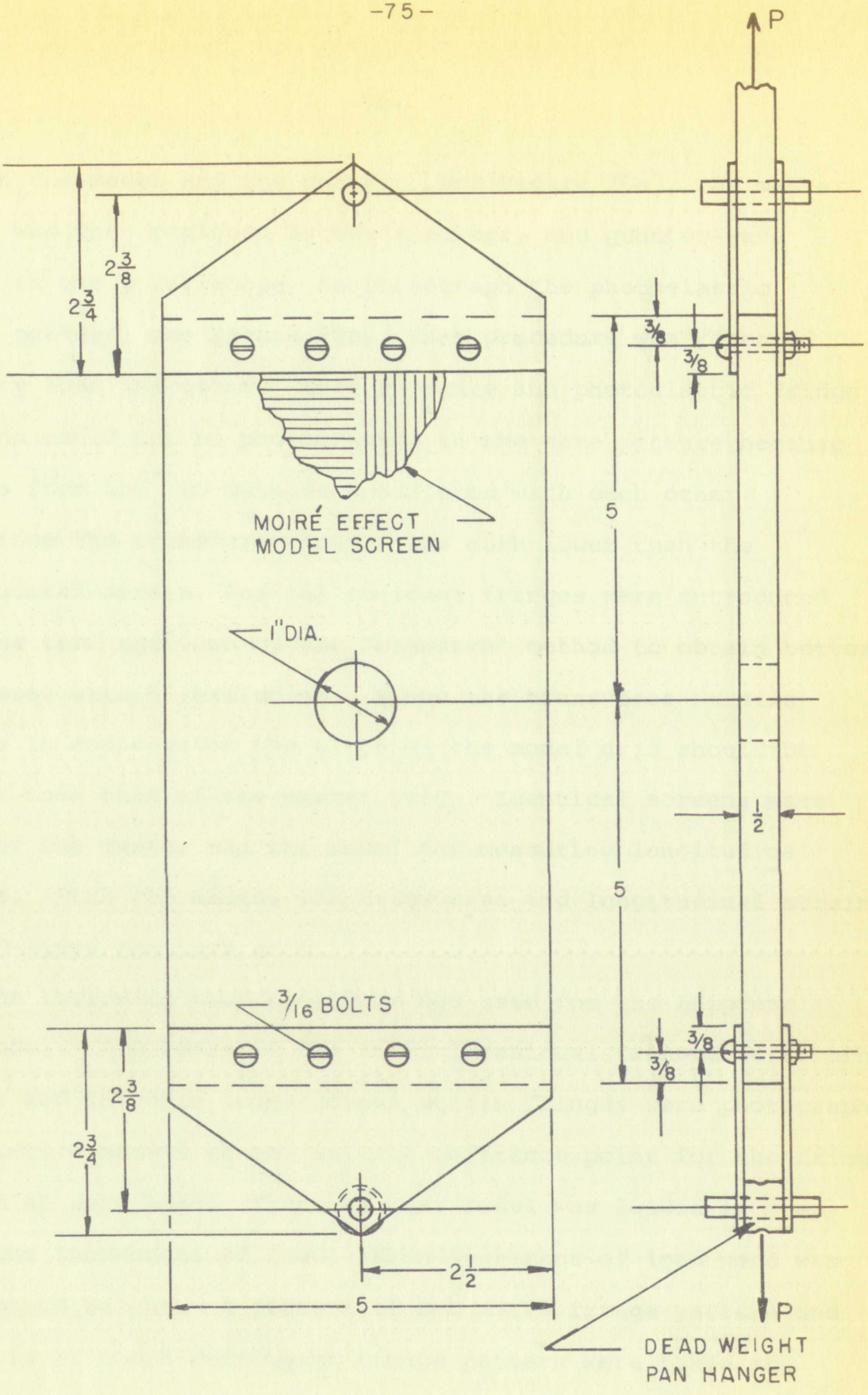

FIGURE 24, ADIPRENE PLASTIC TEST MODEL

between the model and the camera, (See Figure 25a). The master screen was then replaced by the analyzer, and quarter-wave plates in the polariscope, to photograph the photoelastic fringe pattern, see Figure 25b. This procedure was repeated at every load increment. Both the moiré and photoelastic fringe patterns could not be photographed in the same picture because fringes from the two methods interfered with each other.

Since the transverse strain was much lower than the longitudinal strain, initial residual fringes were introduced into the test specimen by the "mismatch" method to obtain better transverse strain resolution. Since the transverse strains will be in compression the pitch of the model grid should be smaller than that of the master grid. Identical screens were used for the master and the model for measuring longitudinal strains. Both the master for transverse and longitudinal strains had 200-lines per inch grid.

The following test procedure was used for the Adiprene test model. A picture of the initial residual transverse strain fringes and the zero longitudinal strain fringes were photographed. This picture served as the initial reference point for the fringe pattern at zero load. Then the test model was loaded in steps by adding increments of load. Each increment of load used was a ten-pound weight. A picture of the moiré fringe pattern and a picture of the birefringent fringe pattern were taken at each increment of load. Pictures of the fringe patterns

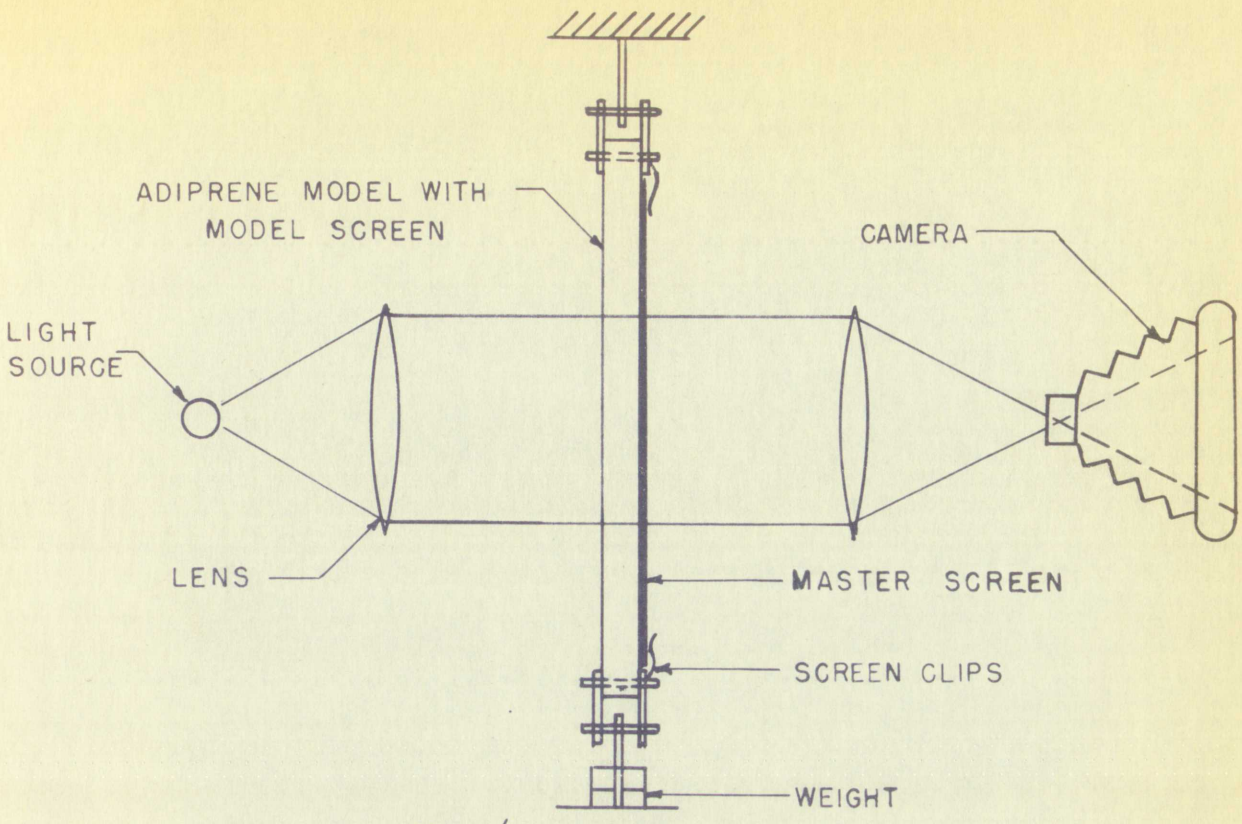

MOIRÉ METHOD SETUP

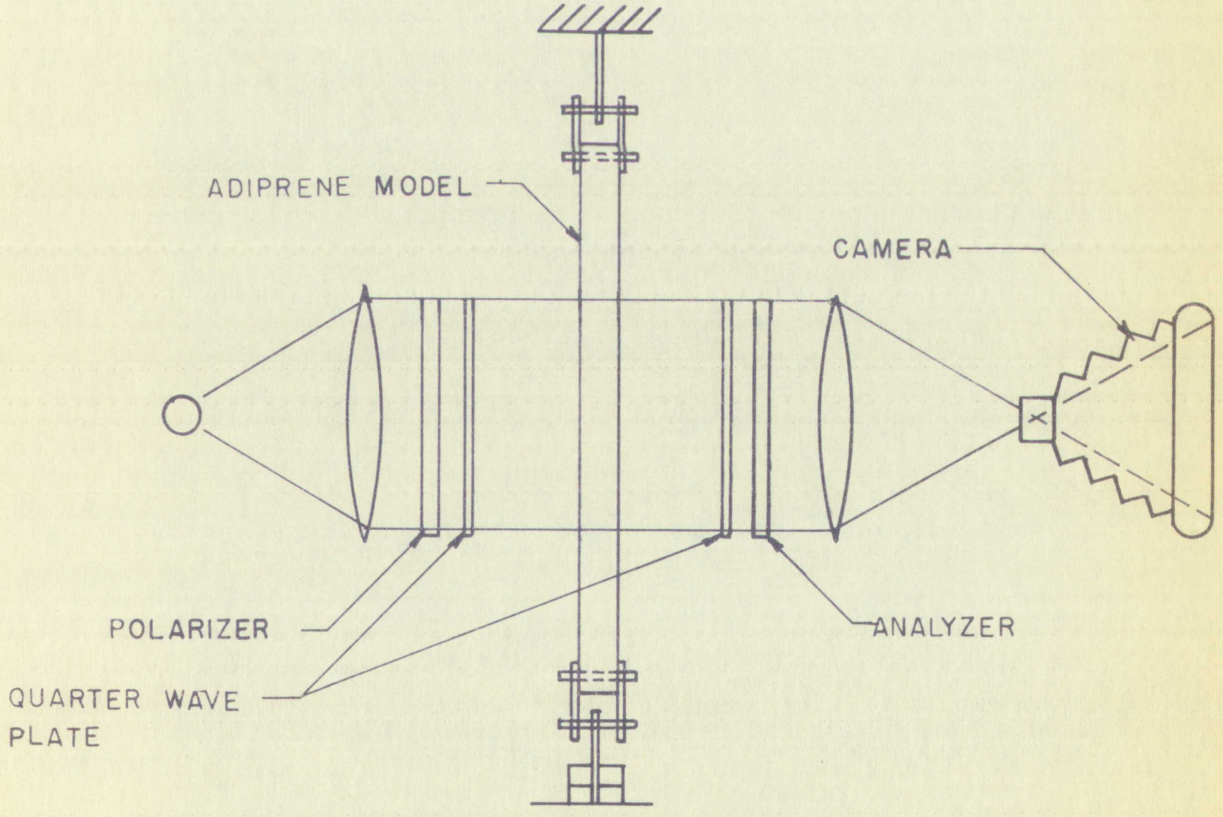

PHOTOELASTIC METHOD SETUP

FIGURE 25 , APPARATUS SETUPS FOR BOTH METHODS

(both moiré and birefringent coating) were taken at 10 and 20 pounds of applied loads.

6.2 Metal Model

Since metal is an opaque material, birefringent coating and reflection moiré effect methods must be used. The metal test model was exactly the same as the one described in Chapter 3. The arrangement of the model screens were as shown in Figure 7. Both the master and model screen grid was 200-lines per inch. Instead of using separate but identical test models for each method, the birefringent coating was bonded on the surface of the specimen opposite to the surface printed with the grid. The photoelastic coating material used was the type M Photostress plastic, and clear bonding cement was used. The model screens were printed on the specimen before the bonding of the birefringent coating. This procedure was important because during the printing process the specimen was submerged in the developing solution and water, and was also subjected to high temperature for prolonged period of time. Either the submergence in liquid or the exposure to high temperature for a long period of time could have weakened the bonding of the plastic to the specimen. Furthermore, the developing solution could impair the transparency of the plastic.

The specimen was mounted in the Dillon tensile machine by means of the whiffletree. The reflection polariscope and the light source for the moiré method used were the same as mentioned

in previous sections. The reflection polariscope was placed in front of the coating; while the fluorescent light source was placed in front of the moiré screens. Since post-elastic strains in the aluminum specimen were to be measured, the specimen had to be loaded continuously for the reasons mentioned in Chapter 4. The machine was loaded by hand at the slowest speed possible. Due to the light interference of the two sources, the moiré fringes and the birefringent fringes could not be photographed at the same time. Hence, the birefringent fringes were photographed first with the moiré light source turned off. Following this, the moiré light source was turned on immediately, then with the polariscope light source blocked off, the moiré fringes were photographed. The polariscope light source could not be turned off and on because when it is turned off, it requires more than twenty minutes for the mercury light bulb to cool and be ready to turn on again. The pair of pictures, moiré fringe pattern and the birefringent fringe pattern, should be taken with the shortest time lapse between them to insure the state of strain of the two pictures is nearly the same. A sequence of pairs of pictures was photographed until the plate ruptured.

6.3 Data Reduction

The strains in x and y directions can be obtained using the moiré method by placing the screens in the y and x directions of the specimen. By definition, the sum of normal strains is invariant therefore the sum of the principal strains will be

$$\varepsilon_1 + \varepsilon_2 = \varepsilon_{xx} + \varepsilon_{yy}$$

where $\varepsilon_{xx} + \varepsilon_{yy}$ is a known quantity obtained by the moiré method. The principal strain difference can be obtained from the isochromatic fringes of the birefringent coating method, where:

$$\varepsilon_1 - \varepsilon_2 = \frac{Q n}{2 t}$$

or that the value $(\varepsilon_1 - \varepsilon_2)$ can be obtained from the calibration curve of the plastic. Hence, by solving the above two equations simultaneously the individual values of ε_1, ε_2 can be obtained.

7.0 DATA AND RESULTS

7.1 Moiré Method Applied to the Study of Strain in the Neighborhood of a Crack

The possibility of using moiré method as a means to measure strains in the neighborhood of a crack was the primary concern of the investigation. Figure 26 shows pictures of the moiré fringe patterns just before the crack developed and when cracks propagated to approximately one diameter length from the hole. Figure 27 shows a comparison of the longitudinal strain distribution curves across the specimen reduced from the two pictures. The strains were measured along the line 1/16 inch from the crack. It can be seen from the curves that, after the cracks had formed, the strains near the edges of the crack relaxed considerably. Hence, part of the strain energy in the specimen was released due to the relaxation of strains near the edges of the cracks. Due to the limitation of the camera resolution, the fringe lines at the tip of the crack could not be recorded in the picture. The fringes at the tip of the crack seems to converge together and become one fringe line. However, this appearance of forming one fringe line in the highest strain region cannot be true because of the fact that the higher the strain the more fringe lines there should be. It was mainly due to the poor resolution of the camera which had made the extremely fine fringe lines appear to be one thick fringe line. These fine fringe lines could probably be photographed using a special setup for the camera. If strain determination at the very edge of the crack is desired, an extrapolation method will be needed.

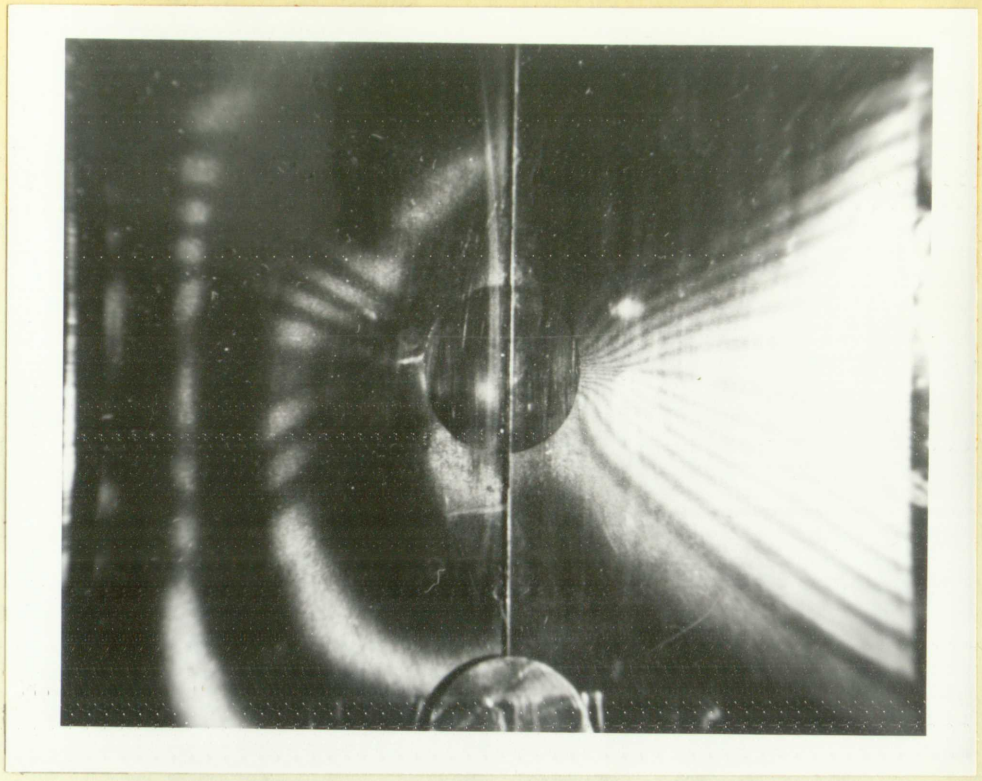

(a) MORIÉ FRINGE PATTERN JUST BEFORE CRACKS HAD FORMED P= 5,790 Lb

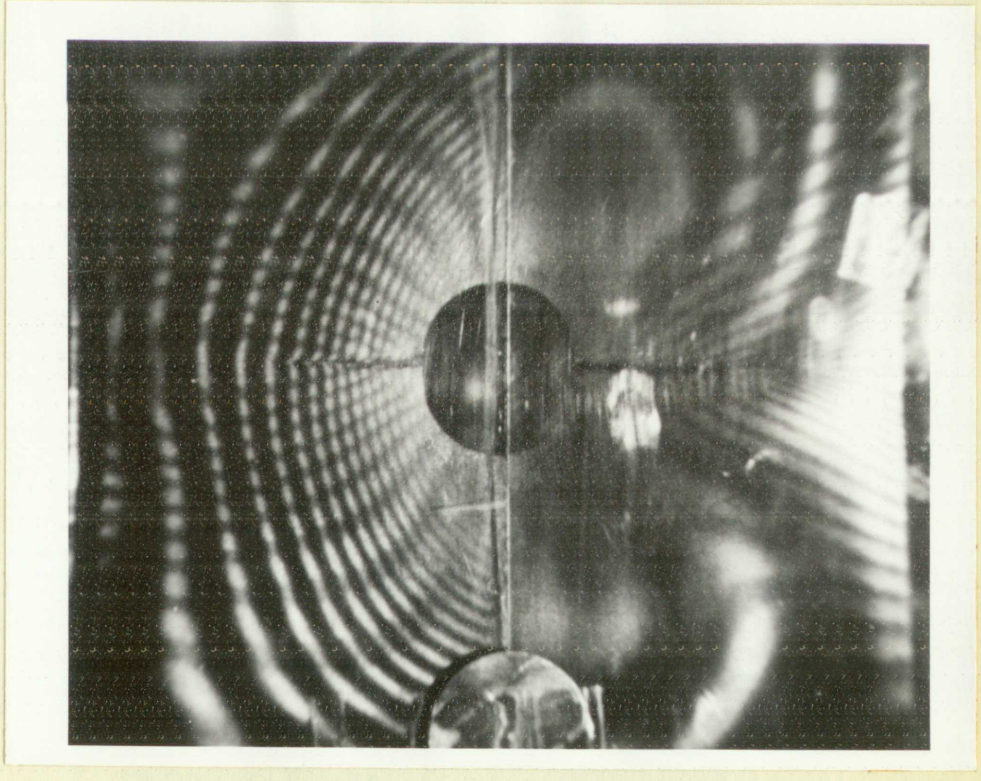

(b) MORIÉ FRINGE PATTERN AFTER CRACKS REACHED ONE DIAMETER LENGTH OF HOLE

FIGURE 26 , MORIÉ FRINGE PATTERNS BEFORE AND AFTER CRACKS DEVELOPED IN COATED SPECIMEN

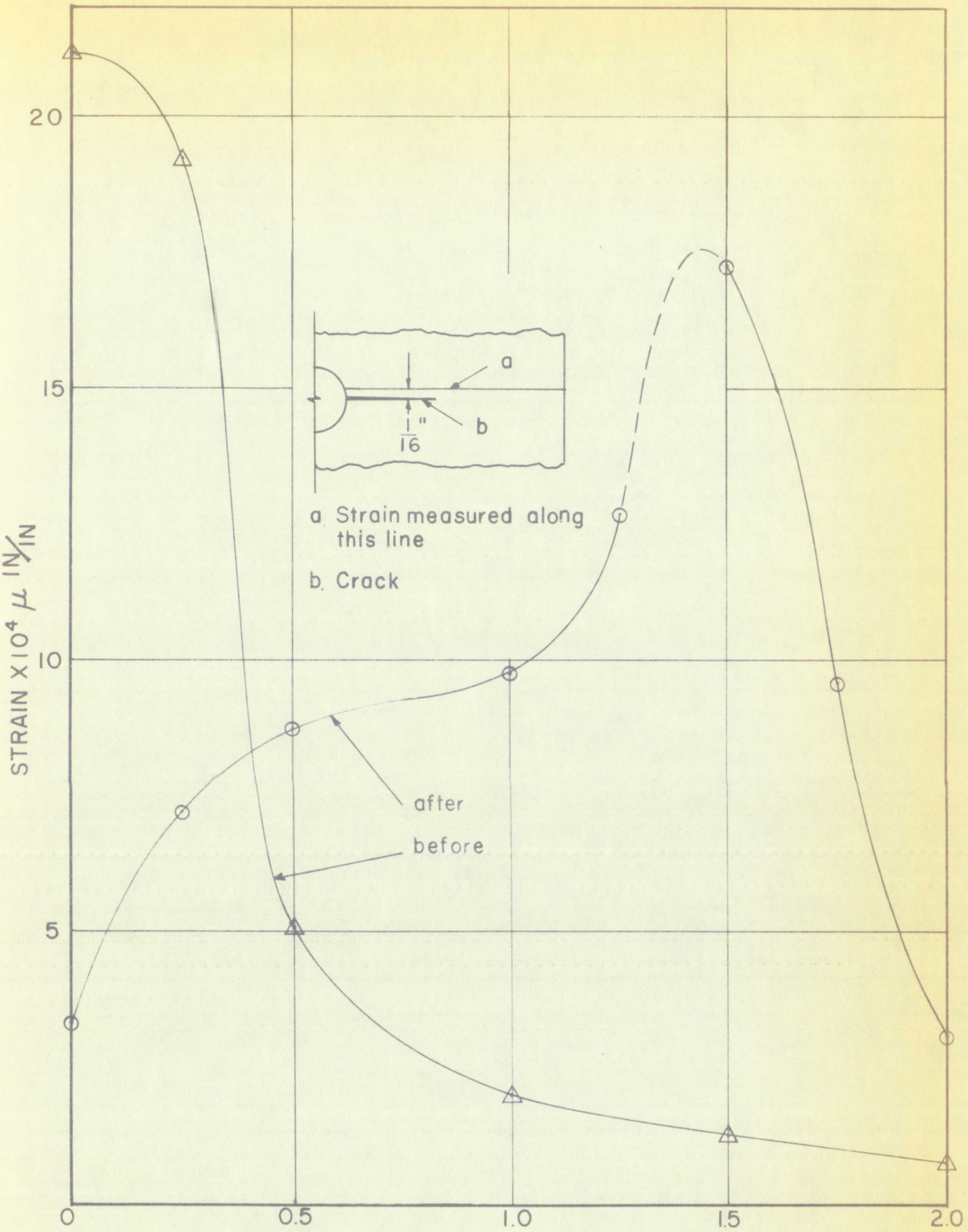

FIGURE 27, STRAIN DISTRIBUTION ACROSS SPECIMEN BEFORE & AFTER CRACKS HAD DEVELOPED

7.2 Birefringent Coating Method

7.2.1 Effects of coating on crack formation in metal--

Since it is very difficult to find a plastic that will follow a crack in the metal specimen, a test was designed to investigate the effect on the birefringent fringe pattern when a crack exists on the metal only. Figure 15 shows the fringe patterns when cracks formed in both plastic and metal (left hand side of the picture), and when the crack was formed in metal only (right hand side of the picture). It can be seen from the picture that the birefringent fringe patterns are greatly different from each other. A qualitative analysis has shown that the fringe order at the tip of the crack is 3.5 for the crack formed both in metal and plastic. Along the edges of crack there is only half a fringe order. But at the tip of crack formed in the metal only, the fringe order is shown to be 1.5. Along the crack formed in metal only the fringe order is higher nearer to the edge of the hole, and is 4.5 at the very edge of the hole. The load of the specimen, at which the picture was taken, was 1,960 pounds. Thus, when a crack does not form in both metal and coating at the same time, the birefringent pattern will be vastly different from what it should be.

The accuracy of the birefringent coating was checked when cracks in the plastic had followed those in the metal specimen under actual loading conditions. Results obtained by the moiré method and birefringent coating method are shown in Table I. The readings were taken at the evenly spaced points along the line from the tip of the crack to the outer edge of

the specimen. Figure 23 c and d show the crack developed in both metal and plastic due to an applied load. The load, at which the pictures were photographed, was 4,504 pounds.

TABLE I, Comparison of Strain Reading Reduced by Moiré and Birefringent Coating Methods

Strain Reading Positions	Longitudinal Strains ε_{yy} (μin/in)	
	Moiré	Birefringent
1	40,323	40,769
2	33,057	26,538
3	20,084	21,307
4	17,812	17,923

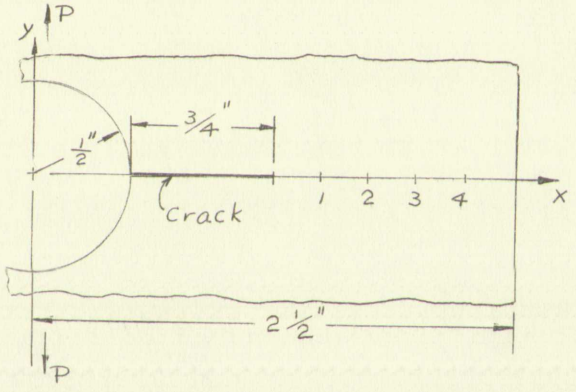

The birefringent readings were divided by the value $(1 + \nu)$ to obtain the longitudinal strains, which were the principal strains along the x-axis. The aluminum specimen was assumed to retain its Poisson's ratio "ν" in the post-elastic range. The longitudinal strains along the x-axis obtained by the above assumption checked extremely well with that obtained by the moiré method. However, the birefringent coating fringes did not show up near the edges and tip of the crack. Hence, the accuracy of the coating could not be checked very near the crack.

7.2.2 Accuracy check on birefringent coating by strain gages-- Before the strain gages were used to check the accuracy of the birefringent coating, the accuracy of the strain gages readings were checked using the strains calculated by the Kirsh theory for a tension plate. The calculated strains and measured strains from the gages are shown in Table II. The gage positions are shown in Figure 16. A typical curve of the theoretical and measured strain readings versus stress curve is shown in Figure 28.

After the gages had been checked out, the specimen was loaded until all the strain gages had failed. Figure 29 shows the strain readings obtained from the strain gages and the birefringent coating from the edge to about one radius length of the hole. The strains obtained from both methods check with each other extremely well except at the gage position closest to the edge of the hole. The strains obtained from the strain gages nearest the hole were much lower than that obtained from the birefringent reading. This may be due to lack of a good bonding at the edge of the hole. Also, as the strains become larger the gages might have slipped due to poor bonding.

7.2.3 Reinforcing effect of the birefringent coating-- The percentage of reinforcement of coating on aluminum specimen within its elastic range was calculated to be 0.67 percent. However, in the post-elastic range of the specimen the percent of reinforcement could be well over 50 percent. For example, the percent of reinforcement shown in Figure 19 was calculated

TABLE II

Calculated and Measured Strain Gage Readings

Gage Position	Loads (lb)	500	1,000	1,500	1,950
1	Calculated Strains (μ in/in)	765	1,530	2,293	2,995
	Measured Strains (μ in/in)	700	1,460	2,240	3,000
2	Calculated Strains (μ in/in)	437	874	1,301	1,704
	Measured Strains (μ in/in)	400	840	1,310	1,770
3	Calculated Strains (μ in/in)	354	706	1,060	1,378
	Measured Strains (μ in/in)	330	685	1,050	1,430
4	Calculated Strains (μ in/in)	426	853	1,279	1,662
	Measured Strains (μ in/in)	390	800	1,220	1,660
5	Calculated Strains (μ in/in)	383	709	1,157	1,365
	Measured Strains (μ in/in)	495	815	1,215	1,585
6	Calculated Strains (μ in/in)	-133	-255	-413	-398
	Measured Strains (μ in/in)	-140	-290	-450	-625
7	Calculated Strains (μ in/in)	-175	-350	-518	-720
	Measured Strains (μ in/in)	-170	-360	-540	-725
8	Calculated Strains (μ in/in)	- 26	- 52	- 78	-101
	Measured Strains (μ in/in)	- 20	- 40	- 70	-100
9	Calculated Strains (μ in/in)	- 27	- 54	- 81	-105
	Measured Strains (μ in/in)	- 20	- 50	- 90	-140
10	Calculated Strains (μ in/in)	- 82	-165	-247	-321
	Measured Strains (μ in/in)	- 80	-170	-270	-360

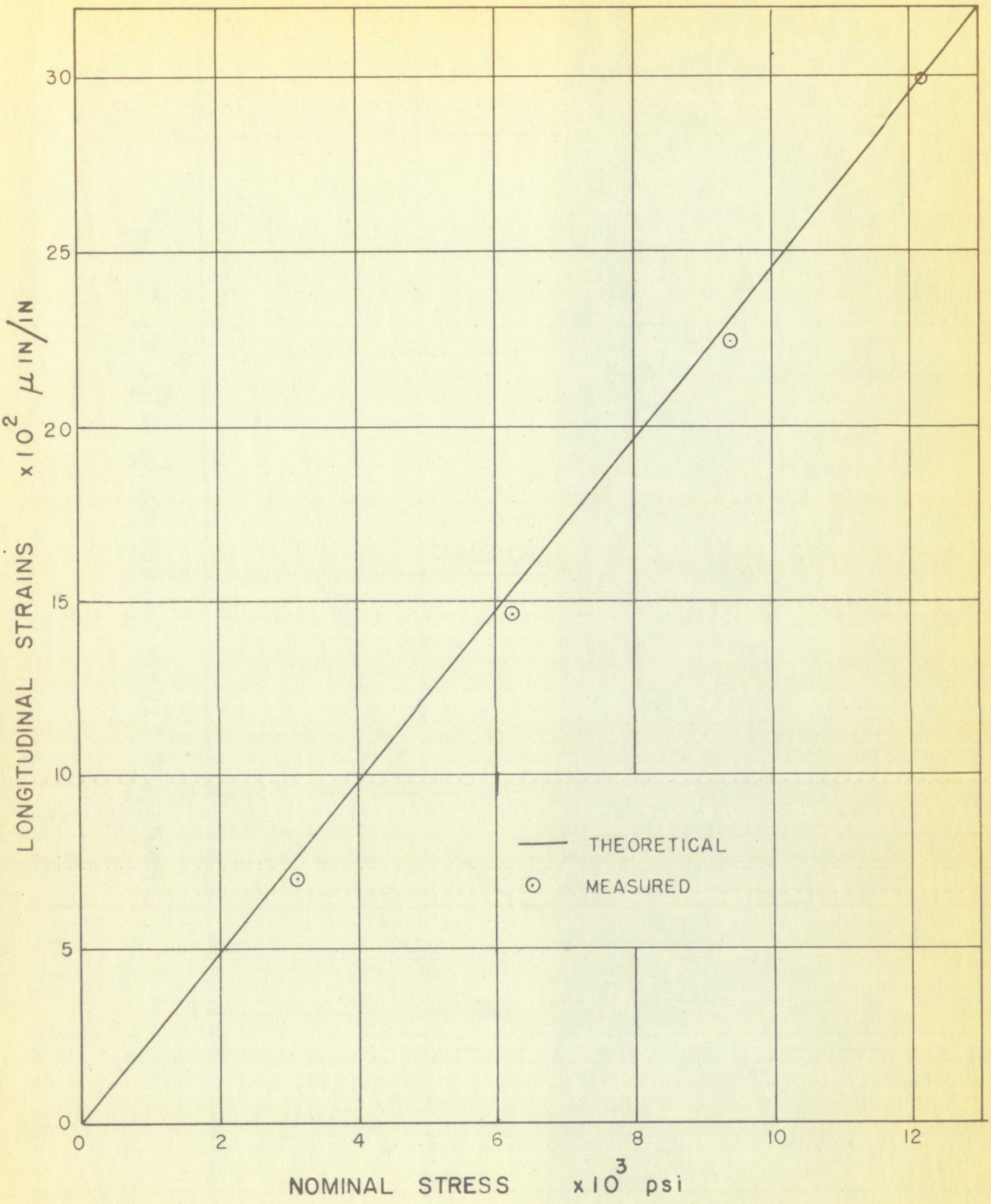

FIGURE 28 , THEORETICAL AND MEASURED STRAINS OF GAGE # 1

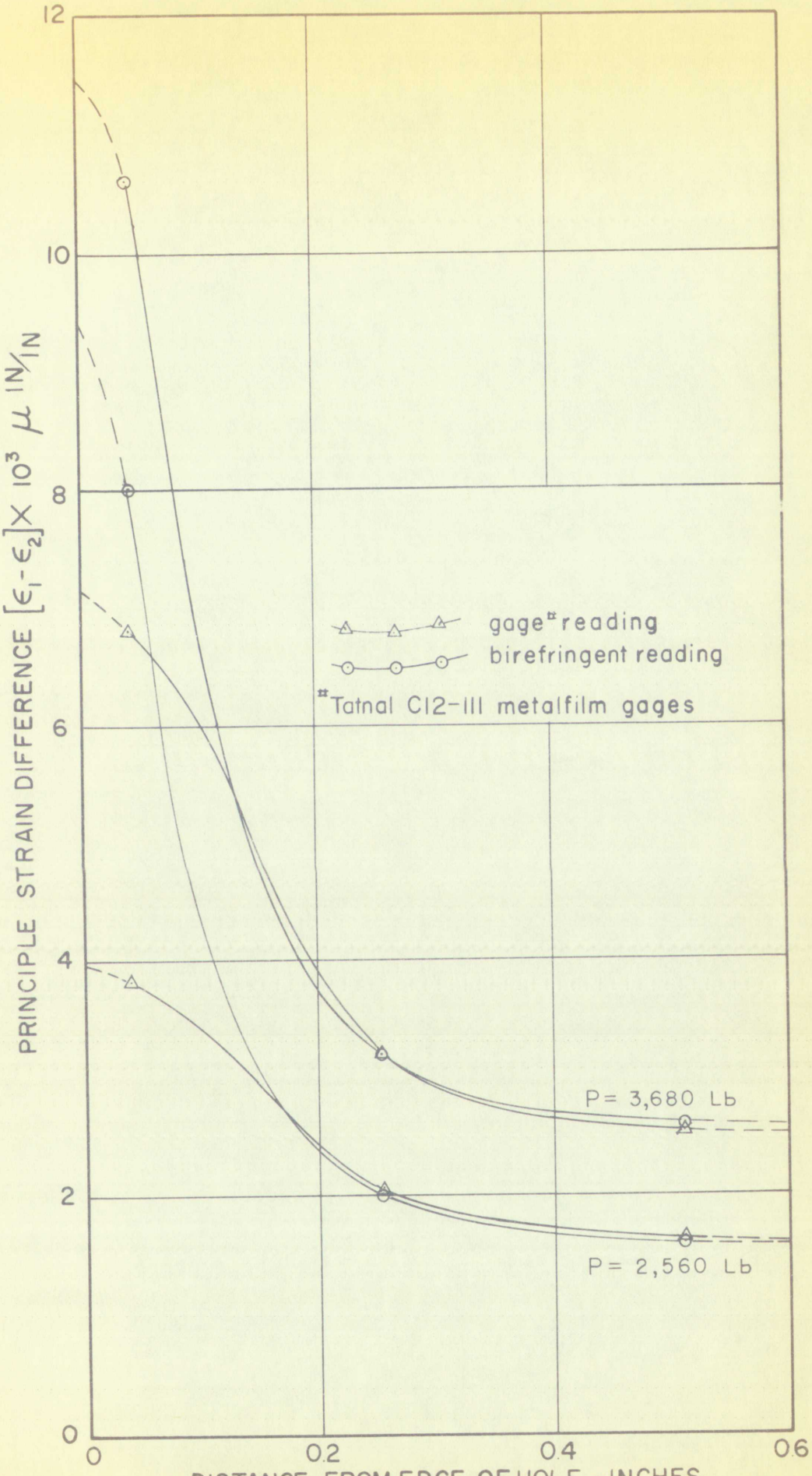

FIGURE 29, STRAIN DISTRIBUTION FROM EDGE OF HOLE TO ONE RADIUS LENGTH FROM THE HOLE

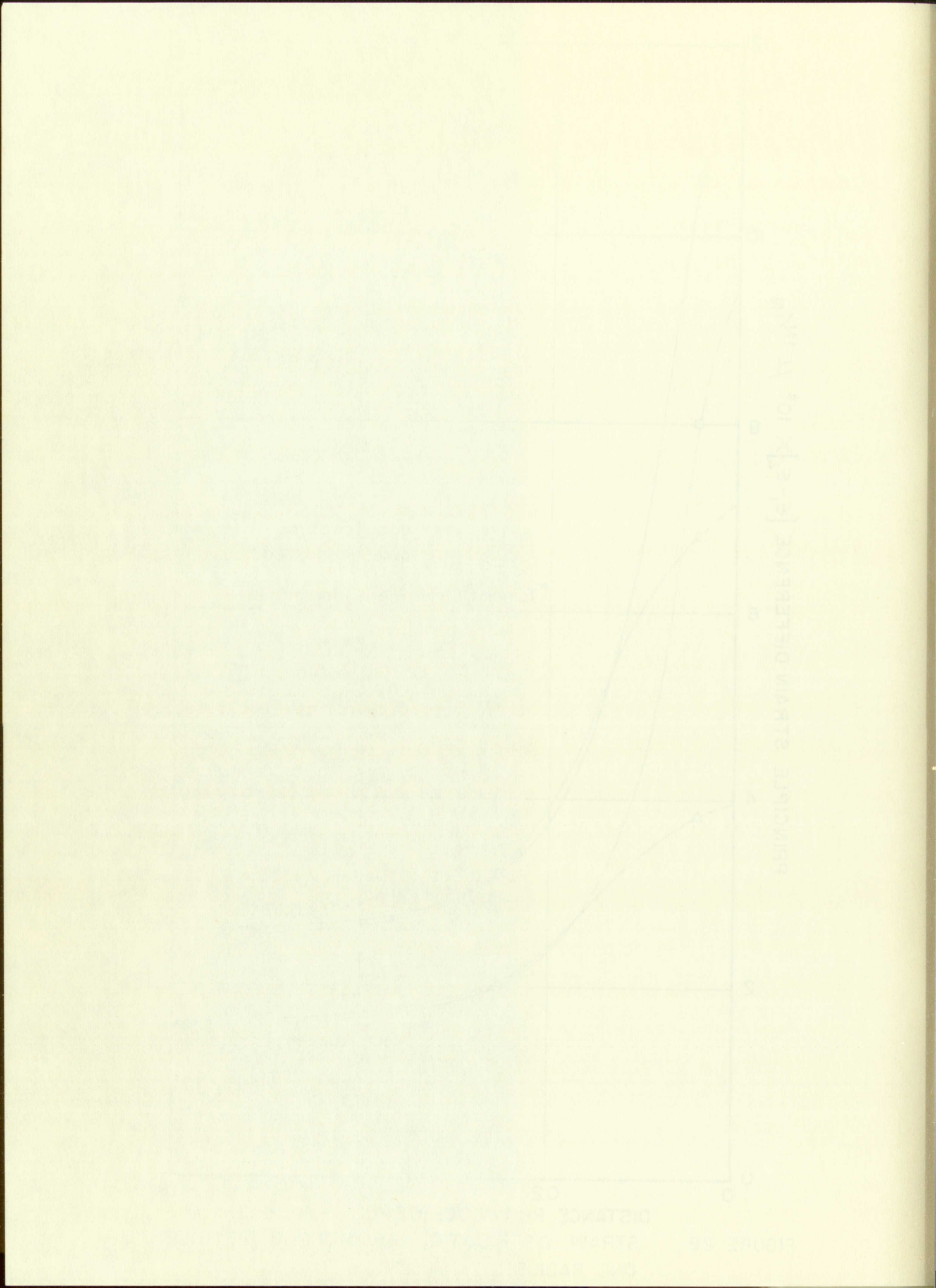

to be 64.36 percent for the coating and 14.44 percent for the strain gage.

The coating not only reinforces the specimen, but also affects the strain distribution in the specimen. Figures 21 and 22 show the longitudinal strain distributions in the coated and the uncoated specimens. The comparison was made with the same strain value at a reference point located at the edge of the hole.

7.3 Combination Whole-Field Method

Since strains in two orthogonal directions can be obtained by the moiré method and principal strains difference by the birefringent coating method, the combination of these two methods can be used to obtain individual principal strains. The combination whole-field method was first applied to an Adiprene plastic model and then to a metal specimen. The results obtained from the Adiprene plastic model are as shown in Table III; the measured principal strains were compared to the principal strains calculated using the Kirsch theory. No attempt was made to reduce the data from the metal specimen since, due to the small values of the transverse strains, the 200-line screen did not produce enough moiré fringe lines to give an accurate mapping of the transverse strains. Table IV shows the moiré and calculated normal strain readings obtained from the Adiprene plastic model.

TABLE III

Results of Principal Strains of Adiprene Model
by the Combined Method

Position	Strain	ε_1 (μ in/in)	Error of ε_1* (%)	ε_2 (μ in/in)	Error of ε_2* (%)
1	Calculated	38,800	+0.515	-18,400	-96
	Measured	39,000		- 800	
2	Calculated	17,380	-5.60	- 4,520	-22.6
	Measured	16,400		- 3,500	
3	Calculated	18,040	-6.9	- 8,200	-36.6
	Measured	16,800		- 5,200	

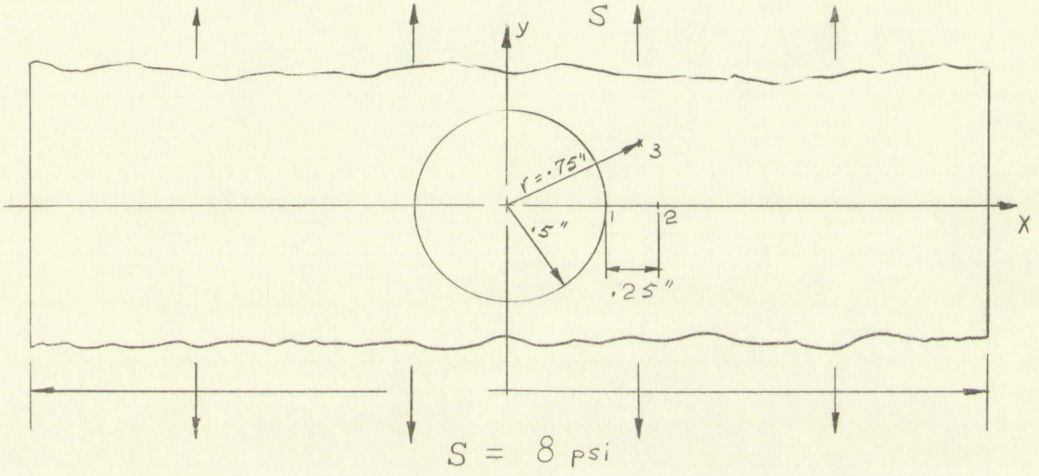

TABLE IV

Transverse and Longitudinal Strains Obtained
by the Moiré Method

Position	Strain	ε_{xx} (μ in/in)	Error of ε_{xx}* (%)	ε_{yy} (μ in/in)	Error of ε_{yy}* (%)
1	Calculated	-18,410	-61	38,800	17.3
	Measured	- 7,200		45,500	
2	Calculated	- 4,520	39.4	17,380	10.5
	Measured	- 6,300		19,200	
3	Calculated	- 8,160	29.9	17,990	23.4
	Measured	-10,600		22,200	

* The percentage of error in Table III and IV is computed using the calculated strains as references, and the negative sign denotes measured strain lower than the calculated strain.

8.0 DISCUSSIONS

8.1 Moiré Method

A study of the results obtained by the moiré method shows that the 200 lines per inch screen is not suitable for measuring strains lower than 3 percent. For small strain measurement either a finer line screen or the mismatch method suggested by Durelli and Sciammarella [6] can be used.

At a region of high strain concentration, as at the tip of the crack shown in Figures 23d and 26b, the fine fringe lines were so close together that they appeared as only one fringe line in the picture. If the whole specimen has reached a high strain level, a coarse line screen is desirable. However, when higher strain is concentrated at a small region of the specimen, where only a few coarse grid lines occupy the whole region, the coarser line screen is not desirable since the coarse screen lines will not produce a good mapping of strain distribution in that region. Therefore, a fine screen is desirable for measurement of high strain concentration in a small region. The way to photograph these fine fringe lines is to mount a low power microscope or a good quality magnifier in front of the camera.

Figure 27 shows that the moiré method is capable of measuring strain distribution in the neighborhood of a crack developed in a specimen. This leads to the possibility of using the moiré method in the measurement of surface strain distribution in the neighborhood of any type of dislocation in

a plate. The strain at the very edge of a crack can be obtained by extrapolating the moiré fringes. However, the extrapolation method could introduce an error as high as 20 to 25 percent. Another disadvantage of this method is that the displacement of of the crack may introduce rigid body rotation of the specimen, and as a result produces rotational fringes. If the exact shape of the crack is known, the amount of rotational effect can be determined from the theory of the moiré method.

8.2 The Birefringent Coating Method

Figure 29 shows that, once the birefrigent coating is calibrated, the birefringent coating method is a fairly accurate technique for the measurement of large strain. However, the profound effect of reinforcement on the specimen in the post-elastic range by the coating has made this method less desirable as a technique for measuring post-elastic strains. A detailed discussion on this reinforcing effect can be found in previous section.

8.3 Combination Whole-field Method

The combined methods of moiré effect and birefringent coating for separation of principal strains is much easier to use than that by a single method. However, the results shown in Table III shows that the measured strains deviate from those calculated by the Kirsch theory. Most of the error can be attributed to the results obtained by the moiré method; as is shown in Table IV. The large percentage error may be due to the following: Since the strains in the Adiprene plastic are rather low for the 200-lines per inch screen, the fringes are

too far apart to give a good approximation of strain at a point. This statement is justified by the results shown in Table IV. Since the strains in the transverse direction are lower than the strains in the longitudinal direction, the transverse moiré fringes are spaced farther apart. Hence, the percent of error is much larger for the transverse strain.

In addition some of the error can be attributed to the theoretical values. It is very likely that the theoretical results should not have been used as a reference. The Kirsch theory developed is based on two assumptions, namely that the specimen is an infinite plate with a finite hole, and it undergoes small deflection only. The Adiprene model does not fulfill these two assumptions. Due to the relatively low elastic modulus of the plastic, it undergoes large deformation. Under small deflection theory the hole should remain circular, but it can be seen that the hole is somewhat elliptical. Furthermore, the ratio of the hole to the width of the hole is only 1/5.

8.4 Conclusion and Recommendation

As a whole the moiré method is a much better technique than the birefringent coating method for the measurement of post-elastic surface strains in metals. The advantages of the moiré method as compared to the birefringent coating method are as follows:

1. The most important advantage is that the moiré method does not reinforce the specimen while the coating has a profound reinforcing effect on the post-elastic range of the metal. Furthermore, the thickness effect on the accuracy of the birefringent coating must also be taken into consideration.

2. The moiré method does not require any calibration procedure. While calibration is necessary for the coating to check the linearity of the plastic.

3. The apparatus used with the moiré method is much less than that for the birefringent coating method. Only a light sourse and a camera are needed for recording the moiré fringe pattern. The camera can be placed at any distance from the specimen. While with the birefringent coating method a light source, a camera, a polarizer, an analyzer, and two quarter-wave plates are required. Since the camera has to be placed behind the analyzer, the distance between the camera and specimen is more or less restricted by the arrangement of the polariscope.

Both of these methods are like any other strain measuring technique in that they can not use a single set of screen lines or a certain type and thickness of plastic to measure strain over a large range with good resolution throughout. The best way is to estimate the strain level to be measured, then select the screen lines or the type and thickness of plastic that will give the best resolution at that strain level.

A study of the results has suggested the moiré method is a very promising technique for the measurement of surface strains in a plane dislocation problem. A comprehensive investigation of the reinforcing effect of the birefringent coating on the post-elastic range of metals should merit consideration as an extension to this study. This profound reinforcing effect should be understood more fully.

REFERENCES

REFERENCES

1. Duffy, J., "Effects of the Thickness of Birefringent Coating", Experimental Mechanics, Vol. 1, No. 3, March 1961.

2. Lee, T. C., Mylonas, C., and Duffy, J., "Thickness Effects in Birefringent Coating with Radial Symmetry", Experimental Mechanics, Vol. 1, No. 10, Oct. 1961.

3. Post, D. and Zandman, F., "The Accuracy of the Birefringent Coating Method for Coating of Arbitrary Thickness", Experimental Mechanics, Vol. 1, No. 1, Jan. 1961.

4. Zandman, F., Redner, S. S., and Riegner, E. I., "Reinforcing Effect of Birefringent Coatings", Experimental Mechanics, Vol. 2, No. 2, Feb. 1962.

5. Berberich, W., "Stress Distribution About a Slowly Growing Crack Determined by the Photoelastic Coating Method", Jet Propulsion Laboratory, Technical Report No. 32-208, 1962.

6. Durelli, A. J., and Sciammarella, C. A., "Elastoplastic Stress and Strain Distribution in a Finite Plate with a Circular Hole Subjected to Unidimensional Load", ASME, Journal of Applied Mechanics, Paper No. 62-WA-152, May 1962.

7. Merrill, P. S., "Photodot Investigation of Plastic-strain Pattern in Flat Sheet with a Hole", Experimental Mechanics, Vol. 1, No. 8, Aug. 1961.

8. Weller, R. and Shepard, B. M., "Displacement Measurement by Mechanical Interferometry", SESA, Vol. VI, No. 1, 1948.

9. Bromley, "Two Dimensional Strain Measurement by Moiré", Proceeding Physical Society, London, Vol. 1, Part 1, 1956.

10. Vinckier, A. and Dechaene, R., "Use of the Moiré Effect to Measure Plastic Strains", Transactions of the ASME, Vol. 82, Series D, No. 2, June 1960.

11. Morse, S., Durelli, A. J., and Sciammarella, C. A., "Geometry of Moiré Fringes in Strain Analysis", ASCE, Engineering Mechanics Division, Vol. 86, E M 4, Aug. 1960.

12. Sciammarella, C. A. and Durelli, A. J., "Moiré Fringes as a Means of Analyzing Strains", ASCE, Engineering Mechanics Division, Vol. 87, E M 1, Feb. 1961.

13. Zandman, F., "Photostress-Principles and Application", Tatnall Measuring System, A Division of the Budd Company.

Other references of interest

14. Frocht, M. M., Photoelasticity, John Wiley & Sons, Inc., New York, 1941, Vol. 1 & 2.

15. D'Agostino, J., Drucker, D. C., Lin, C. K., and Mylonas, C., "An Analysis of Plastic Behavior of Metals with Bonded Birefringent Plastic", SESA, Vol. XII, No. 2, 1955.

16. Slot, T., "Reflection Polariscope for Photography of Photoelastic Coating", Experimental Mechanics, Vol. 2, No. 2, Feb. 1962.

17. Durelli, A. J. and Riley, W. F., "Development in the Grid Method of Experimental Stress Analysis", SESA, Vol. XIV, No. 2, 1957.

18. Ligtenberg, F. K., "The Moiré Method - A New Experimental Method for the Determination of Moments in Small Slab Models", SESA, Vol. XII, No. 2, 1955.

APPENDIX

APPENDIX A

Lithographic Printing Process

The following is a step-by-step procedure for printing 200-lines per inch screen on an aluminum specimen surface:

1. The surface of the metal is cleaned and polished with water and grade 600 water-proof sand paper to remove any grease or oxide coating. Circular motion is used in polishing until the surface is bright and shiny. Then the plate is rinsed thoroughly with tap water. When a thin coat of water is spread evenly throughout the plate, the surface is free of grease or other grey deposits.

2. Leaving water on the cleaned surface the plate is placed on the platform of the whirler. Drain or whirl excess water from the plate. Gaco Engrowers Sensitized Resist can then be poured on the surface of the plate. The Gaco Resist should be poured when the surface is still overflowing with water. The whirler, spinning at about 60 rpm will spread the Resist evenly across the surface. The lid of the whirler with the heater is closed. The heater switch is set at medium. The plate is left in the whirler from 25 to 30 minutes for the coating to dry thoroughly. The plate should be quite warm to touch when removed from the whirler.

Note: Plates can be coated several days in advance of the date of use. The pre-coated plates should be stored in dry, light-proof cabinets.

3. The master screen negative is aligned on the coated surface of the plate, and Scotch tape is used to hold the screen in place. The emotion side of the master negative should be right against the coated surface to prevent any distortion of the printed lines.

4. The plate with the master screen is placed in the vacuum frame of the electric arc printing machine for exposure. Length of exposures range from 10 to 12 minutes.

5. After exposure the plate is immersed in the developing solution for at least five minutes. It is then rinsed thoroughly by spraying lukewarm tap water over it. The spraying pressure should be low enough to prevent the printed grid from washing away. Drain excess water from plate and let it dry.

Note: Care must be taken to prevent any liquid, either oil or water, to come in contact with the printed grid. The printed grid can be rubbed off readily when wet. If it is completely dry, the printed grid can stand considerable abrasive handling without damage to the grid.

APPENDIX B

Instruction for applying Birefringent Sheet Plastic

I. Preparation of Reflective Metal Surface

a. The surface should be relatively smooth. It may be polished with grade 600 sand paper to give a bright shiny surface but still leaving the surface slightly scratched. A very high polish is prohibitive because it is detrimental to good bonding. The final step should be a circular motion.

b. Clean the surface with acetone to remove all traces of grease. After degreasing, use a dry cotton swab to remove all traces left on the surface by the solvent.

II. Preparation of the Plastic Sheet

a. Select a thickness of plastic suitable for the strain level expected on the test piece (in our case, Type M Photostress plastic with a thickness of 0.072 inch and 10,400 microinch per inch per fringe was used).

b. Saw, drill, file, or machine the sheet to the proper size, taking care not to generate excess heat during the machining.

Note: Due to the low modulus of the Type M plastic, it has a tendency to warp upward at the edges when excess cement starts flowing back into the interface between the plastic and base. The plastic should be cut at least 1/8 inch larger overhanging the edges of the base metal to avoid this warping. For a hole in the specimen, the hole in the plastic should be drilled undersize accordingly. Only after the bonding cement

is completely set should the plastic be cut down to the exact shape of the specimen.

c. File an approximate 45° level from top surface to bottom edge of the plastic at all locations where the base extends beyond the plastic (the bonding cement overflowing the top of bevel to prevent the edges from warping).

d. Clean the bonding surface of the plastic with acetone to remove any trace of grease or dirt. After degreasing, wipe plastic surface with dry clean cotton swab.

III. Preparation of the Bonding Cement

a. Pour desired amount of resin into a beaker or cup and weigh (no more than 100 grams of resin should be mixed at one time). For a 6" x 6" sheet plastic, fifteen grams of resin should be sufficient. Clear bonding cement is used for the reflective metal surface, as in our case. Heat resin to 140° - 220° F for about 20 to 25 minutes to remove air bubbles and any trace of moisture which might be present in the bonding cement. Then allow to air cool to room temperature.

b. Add hardener (12 percent by weight for clear bonding cement) to the cooled resin. Then mix thoroughly with glass stir-rod until a homogeneous liquid is obtained. The mixture should be mixed slowly to avoid introducing air bubbles. After thoroughly mixing, allow to stand for 8 to 10 minutes. The bonding is now ready to be used.

IV. Bonding Procedure

a. Brush or pour bonding cement on base surface about 1/16 inch thick. Carefully place plastic sheet on the prepared part.

b. To remove any air bubbles that may be entrapped under the plastic, press gently, starting at one edge and slowly press down toward the other edge. All air bubbles will flow out with the excess bonding cement. If some bubbles persist in returning, brush additional resin at the edge while releasing pressure, so that resin will flow back instead of air.

c. Let the bonded specimen stand for approximately 24 hours before using. To test hardness, press fingernail into plastic bonding, and if no indentation is made, it is ready to use. If indentation is made, wait one more day and test again.

Note: If the bonding interface between base and plastic appears foggy, it indicates that the hardener and resin were not mixed thoroughly. As a result, part of the resin never did get hardened and became cloudy in appearance. When Type M plastic is used, do not use Scotch tape to hold the plastic sheet. Otherwise, due to the low modulus, the middle of the sheet may be warped up when pressure is released and resin starts to flow back into the interface. The specimen should be placed on a level table to prevent the plastic sheet from sliding when bonding is getting hardened.

APPENDIX C

Properties of Adiprene Plastic

Adiprene is a photoelastic material, whose characteristics are very much like Hysol 8705 plastic. It contains 100 parts Adiprene L-100 and 8 parts Trimethylolpropane (TMP) curing agent, and is cured at 100° - 105° C for 22 hours. Its properties are as follows:

Elastic modulus = 618 psi

Poisson's ratio = 0.474

Stress Optical Coefficient = 0.9684